



VCU

Virginia Commonwealth University
VCU Scholars Compass

Theses and Dissertations


Graduate School

2020

Epigenetic Regulation of Drug Metabolizing Enzymes in Normal Aging

Mohamad M. Kronfol
Virginia Commonwealth University

Follow this and additional works at: <https://scholarscompass.vcu.edu/etd>

 Part of the [Molecular Genetics Commons](#), [Other Pharmacy and Pharmaceutical Sciences Commons](#), and the [Pharmacology Commons](#)

© The Author

Downloaded from

<https://scholarscompass.vcu.edu/etd/6351>

This Dissertation is brought to you for free and open access by the Graduate School at VCU Scholars Compass. It has been accepted for inclusion in Theses and Dissertations by an authorized administrator of VCU Scholars Compass. For more information, please contact libcompass@vcu.edu.

© Mohamad M. Kronfol 2020
All Rights Reserved

EPIGENETIC REGULATION OF DRUG METABOLIZING ENZYMES IN NORMAL AGING

A dissertation submitted in partial fulfilment of the requirements for the degree of Doctor of
Philosophy at Virginia Commonwealth University.

By

Mohamad Maher Kronfol

PhD Candidate, School of Pharmacy, Virginia Commonwealth University, Virginia, USA

Bachelor of Pharmacy, Beirut Arab University, Lebanon, 2013

Director: Joseph L. McClay, Ph.D.

Assistant Professor, Department of Pharmacotherapy and Outcomes Science

Virginia Commonwealth University

Richmond, Virginia

April 2020

Dedication

This is for you mom

Acknowledgments

This dissertation would not have been achievable without the support of many people.

I am unreservedly thankful to my PhD advisor, **Dr. Joseph McClay** for providing me with his constant support and advice. You are a great mentor whose outstanding intellect and rigor shaped my independence as a scientist.

I want to thank my PhD committee members, **Drs. Patricia Slattum, Mikhail Dozmorov, Elvin Price, Matthew Halquist, and MaryPeace McRae**. I am grateful to and humbled by your advisory that helped me complete my PhD.

Dr. Patricia Slattum for your continuous support and professional advice.

Dr. Elvin Price for your professionalism and career advice.

Dr. Matthew Halquist for your continuous support and feedback.

Dr. Mikhail Dozmorov for your seminal literature, encouragement, and advice.

Dr. MaryPeace McRae for your guidance through the program.

Ms. Fay Jahr for your support in the laboratory.

The Deans Office and the **Department of Pharmacotherapy and Outcomes Science (DPOS)** for the academic, administrative, and financial support.

Ms. Sha-kim Craft for your undying willingness to help in administrative aspects of my PhD.

My friends at DPOS that have kept me motivated to pursue my studies.

Mr. Walid Jamaledine, for being my American father figure.

Finally, my parents **Maher** and **Mona**, for your sacrifice, I am forever in your debt.

Table of Contents

Acknowledgements	iii
Table of Contents	iv
List of Tables	vii
List of Figures	viii
List of Abbreviation	x
Abstract	xii
Chapter 1: The role of epigenomics in personalized medicine: a literature review	1
1.1. Introduction.....	1
1.2. Epigenetics Overview	3
1.2.1. Epigenetic modifications to chromatin.....	5
1.2.2. Epigenetic effects on gene expression and regulation.....	7
1.2.3. Individual differences in epigenetic states and developmental plasticity	8
1.3. Epigenetic Applications in Personalized Medicine	11
1.3.1. Epigenetic biomarkers of disease	11
1.3.2. Epigenetic drugs	15
1.3.3. Epigenetic biomarkers of drug response	24
1.3.4. Epigenetic modification of drug absorption, distribution, metabolism, and excretion (ADME) genes	26
1.4. Aging.....	27
1.4.1. Aging, drug response, and adverse drug reactions	27
1.4.2. Personalized dosing in the elderly population.....	28
1.4.3. Epigenetics of age	28
1.5. Discussion and Conclusions	29
Chapter 2: DNA methylation and histone acetylation changes to cytochrome P450 2E1 regulation in normal aging and impact on rates of drug metabolism in the liver	33
2.1. Abstract	34
2.2. Introduction.....	35
2.3. Methods.....	38
2.3.1. Mice	38
2.3.2. DNA and RNA extraction.....	38
2.3.3. Global 5-MethylCytosine (5mC) and 5-HydroxymethylCytosine (5hmC).....	38
2.3.4. Selection of genomic regions of interest.....	38
2.3.5. Bisulfite conversion of genomic DNA and High-Resolution Melt (HRM) analysis.....	44
2.3.6. Gene expression analysis by reverse transcription – quantitative PCR (RT-qPCR)	45
2.3.7. Western Blots.....	45
2.3.8. Chromatin Immunoprecipitation Quantitative Polymerase Chain Reaction (ChIP- qPCR).....	47

2.3.9. Pyrosequencing	50
2.3.10. CYP2E1 intrinsic clearance	51
2.3.11. Statistics	56
2.4. Results	57
2.4.1. Global epigenetic effects in aged mouse liver	57
2.4.2. Age-associated changes to <i>Cyp2e1</i> 5'UTR methylation and gene and protein expression	61
2.4.3. Base-resolution 5mC analysis of <i>Cyp2e1</i> 5'UTR and upstream regulatory region	63
2.4.4. Histone acetylation analysis of <i>Cyp2e1</i> 5'UTR and upstream regulatory region	66
2.4.5. CYP2E1 pharmacokinetics, chronological age, and epigenetics	68
2.5. Discussion	73

Chapter 3: Histone acetylation at the sulfotransferase 1a1 gene is associated with its hepatic expression in normal aging

3.1. Abstract	78
3.2. Introduction	79
3.3. Methods	84
3.3.1. Mice	84
3.3.2. DNA and RNA extraction	84
3.3.3. Selection of genomic regions of interest	84
3.3.4. Bisulfite conversion of genomic DNA and High-Resolution Melt (HRM) analysis	84
3.3.5. Gene expression analysis by reverse transcription – quantitative PCR (RT-qPCR)	85
3.3.6. Chromatin Immunoprecipitation Quantitative Polymerase Chain Reaction (ChIP-qPCR)	86
3.3.7. Statistics	86
3.4. Results	87
3.4.1. Age-associated changes to <i>Sult1a1</i> and <i>Ugt1a6</i> methylation and gene expression	87
3.4.2. Histone acetylation analysis of <i>Sult1a1</i> regulatory region	87
3.4.3. <i>Sult1a1</i> epigenetics and expression	92
3.5. Discussion	93
3.6. Study Highlights	95

Chapter 4: Cross tissue correlation of *Cyp2e1* and *Sult1a1* methylation levels in mice

4.1. Abstract	96
4.2. Introduction	97
4.3. Methods	98
4.3.1. Sample	98
4.3.2. DNA extraction and bisulfite conversion	98
4.3.3. High-Resolution Melt (HRM) assays	98
4.3.4. Statistics	99
4.4. Results	100

4.4.1. <i>Cyp2e1</i> tissue-specific methylation and cross-tissue correlation.....	100
4.4.2. <i>Sult1a1</i> tissue-specific methylation and cross-tissue correlation.....	100
4.5. Discussion	104
Chapter 5: Method optimization of Reduced Representation Bisulfite Sequencing (RRBS) for genome-wide analysis of mouse liver DNA methylation	106
5.1. Abstract	106
5.2. Introduction.....	107
5.3. Methods.....	111
5.3.1. Sample.....	111
5.3.2. Reduced Representation Bisulfite Sequencing (RRBS)	111
5.3.3. Data Processing.....	113
5.4. Results.....	114
5.4.1. DNA extraction, MspI digestion, and fragment isolation.....	114
5.4.2. RRBS library quality control	114
5.4.3. Next Generation Sequencing (NGS) data	116
5.5. Discussion	119
Chapter 6: Overall Conclusions and Future Directions.....	120
References	122
VITA	138

List of Tables

Table 1.1: Commercially available epigenetic diagnostic tests in the United States.....	13
Table 1.2: Classification of US FDA-approved epigenetic drug classes according to mechanism of action.	17
Table 1.3: Classification of epigenetic drug classes in active clinical trials registered in the US (clinicaltrials.gov) according to mechanism of action.....	20
Table 2.1: Summary of human EWAS findings for phase I drug metabolism genes	39
Table 2.2: High-Resolution Melt (HRM) and Chromatin Immuno-Precipitation (ChIP) primers and qPCR product sequences of phase I genes.....	41
Table 2.3: Pyrosequencing primer sequences	43
Table 2.4: High Performance Liquid Chromatography (HPLC) parameters	52
Table 2.5: Pyrosequencing and HRM 5mC correlation.....	65
Table 2.6: Michaelis-Menten constants per age group	69
Table 2.7: Pearson correlation tests p-values for epigenetic and drug metabolism variables	72
Table 3.1: Summary of human EWAS findings for phase II drug metabolism genes.....	81
Table 3.2: High-Resolution Melt (HRM) and Chromatin Immuno-Precipitation (ChIP) primers and qPCR product sequences of phase II genes.....	83
Table 4.1: <i>Cyp2e1</i> Pearson correlation tests p-values for each pair of tissue types	103
Table 4.2: <i>Sult1a1</i> Pearson correlation tests p-values for each pair of tissue types	103
Table 5.1: Summary table of RRBS samples.....	116
Table 5.2. Summary table reporting average total number of reads and total number of Unique Alignments per age (months).....	116
Table 5.3. Summary table reporting number of unique cytosines captured per replicate after quality control.....	116

List of Figures

Figure 1.1: Representation by Conrad Waddington of the developmental process as a series of “decisions” made by differentiating cells	4
Figure 1.2: Epigenetic regulation of gene expression via chromatin remodeling	10
Figure 1.3: The O-6-methylguanine-DNA methyltransferase (MGMT) enzyme repair mechanism of tumor DNA damage induced by the anticancer drug temozolomide	25
Figure 2.1: Illustration of human CYP2E1 and the mouse homolog <i>Cyp2e1</i> gene TSS with upstream regulatory region	42
Figure 2.2: Chlorzoxazone standard curve	53
Figure 2.3: 6-hydroxychlorzoxazone standard curve	53
Figure 2.4: Metabolite formation against time plot	55
Figure 2.5: Metabolite formation against microsome protein plot	55
Figure 2.6: Box plots with regression line of Age-Associated changes to global 5-MethylCytosine and 5-HydroxymethylCytosine	58
Figure 2.7: LINE 1 methylation percentage per age.....	59
Figure 2.8: Representative melt curves per age	60
Figure 2.9: Box plots with regression line of Age-Associated changes to <i>Cyp2e1</i> 5’UTR percent methylation, gene and protein expression.....	62
Figure 2.10: <i>Cyp1b1</i> 5-MethylCytosine with age.....	63
Figure 2.11: Pyrosequencing data for <i>Cyp2e1</i> showing scatter plot of methylation per CpG investigated and linear regression results	64
Figure 2.12: Chromatin Immunoprecipitation quantitative polymerase chain reaction (ChIP-qPCR) data of both investigated regions on <i>Cyp2e1</i>	67
Figure 2.13: Representative Michaelis-Menten curves of each age group	70
Figure 2.14: Correlation matrix reporting Pearson correlation statistical test result (r) of study variables	71
Figure 3.1: UCSC genome browser tracks showing <i>Sult1a1</i> mouse and human gene structure ..	82
Figure 3.2: Box plots with regression line of Age-Associated changes to <i>Sult1a1</i> promoter percent methylation, histone acetylation, and gene expression	88
Figure 3.3: Boxplot of age-associated change to <i>Ugt1a6</i> methylation, acetylation, and gene expression	90

Figure 4.1: Boxplot of DNA methylation percent of <i>Cyp2e1</i> and <i>Sult1a1</i> across the liver, cortex, hippocampus, and whole blood and corresponding Pearson correlation matrices	101
Figure 4.2: Violin plot showing average expression of <i>SULT1A1</i> and <i>CYP2E1</i> across the liver, whole blood, hippocampus, and cortex.....	102
Figure 5.1: Schematic representation of the seven steps of the optimized RRBS protocol.....	110
Figure 5.2: Representative Bioanalyzer traces showing RRBS library fragment size distribution	115
Figure 5.3: Bar plot of data from Bismark quality report.....	118

List of Abbreviation

5cac	5-CarboxylCytosine
5fc	5-FormylCytosine
5hmc	5-HydroxyMethylCytosine
5mc	5-MethylCytosine
ADME	Absorption, Distribution, Metabolism and Excretion
A-DMR	Age-Differentially Methylated Region
ADR	Adverse Drug Reaction
BET	Bromodomain Extra-Terminal motif
Bp	Base pair
cfDNA	Cell free DNA
ChIP	Chromatin ImmunoPrecipitation
CLIA	Clinical Laboratory Improvement Amendments
Clint	Intrinsic Clearance
CpG	Cytosine-phosphate-Guanine
CTCL	Cutaneous T-cell Lymphoma
CYP2E1	Cytochrome P 450 2 E 1
CYP450	Cytochrome P 450 system
CZ	Chlorzoxazone
DNMT	DNA Methyl Transferase
ENCODE	Encyclopedia of DNA Elements
H3K27ac	Histone 3 Lysine 27 Acetylation
H3K9ac	Histone 3 Lysine 9 Acetylation
HAc	Histone acetylation
HAT	Histone Acetyl Transferase
HDAC	Histone Deacetylase
HDM	Histone Demethylase

HMT	Histone Methyl Transferase
HPLC	High Performance Liquid Chromatography
HRM	High-Resolution Melt
IACUC	Institutional Animal Care and Use Committee
LDT	Laboratory Developed Tests
MLM	Mouse Liver Microsome
NAPQI	N-acetyl-p-benzoquinone imine
ncRNA	noncoding RNA
NGS	Next Generation Sequencing
NIA	National Institute on Aging
NTS	Net Temperature Shift
PD	Pharmacodynamics
PK	Pharmacokinetics
PRMT5	Protein Arginine Methyl Transferase 5
PTCL	Peripheral T-cell Lymphoma
PTM	Post-Translational Modification
RRBS	Reduced Representation Bisulfite Sequencing
RT-qpcr	Reverse Transcription- quantitative polymerase chain reaction
SULT1A1	Sulfotransferase 1a1

Abstract**EPIGENETIC REGULATION OF DRUG METABOLIZING ENZYMES IN
NORMAL AGING**

By Mohamad Maher Kronfol, B. Pharm

A dissertation submitted in partial fulfilment of the requirements for the degree of Doctor of
Philosophy at Virginia Commonwealth University.

Virginia Commonwealth University, 2020.

Major Advisor: Joseph L. McClay, Ph.D.

Assistant Professor, Department of Pharmacotherapy and Outcomes Science

Geriatric populations are at a higher risk for adverse drug reactions (ADRs). This may be partly due to changes in drug metabolism in old age, but the underlying mechanisms are poorly understood. Prior research in humans and mice has shown age-associated changes to the expression of several genes involved in drug metabolism. Furthermore, studies of human blood showed that epigenetic regulation of genes encoding drug metabolizing enzymes change with age. However, it is unknown if genes in the liver are similarly affected. Therefore, we hypothesize that genes encoding drug metabolizing enzymes may show differential epigenetic regulation in the liver with age, and that this will affect rates of drug metabolism.

We selected genes encoding phase I and II drug metabolizing enzymes showing the strongest evidence of age-related epigenetic changes in prior genome-wide studies of human blood DNA. We mapped the homologues of these genes in mice and analyzed DNA methylation and histone acetylation levels in liver samples from aged mice (4, 18, 24 and 32 months) coupled with functional investigations at those genes. We successfully demonstrated a strong relationship between DNA methylation and histone acetylation (H3K9ac) levels at cytochrome P450 2E1

(*Cyp2e1*) and sulfotransferase family 1A member 1 (*Sult1a1*) and their expression levels in liver. Moreover, intrinsic clearance of the CYP2E1 probe drug chlorzoxazone was strongly associated with DNA methylation and histone acetylation at two regulatory regions of *Cyp2e1*. Next, we investigated DNA methylation levels at these genes in peripheral blood and organs like the liver and the brain. We show that DNA methylation levels of *Cyp2e1* and *Sult1a1* are substantially different between blood, liver, and the brain and are correlated to various extents and directions of effects. Finally, we report an optimized method for genome-wide investigation, Reduced Representation Bisulfite Sequencing (RRBS), of methylation levels using the innovative Adaptase technology for utilization in larger aging studies of epigenetics and drug metabolism by our group in the future. Our successful demonstration of epigenetic control of drug metabolism in an aged mouse model could pave the way for future clinical studies to develop epigenetic biomarkers of pharmacokinetic pathways in geriatric patients.

Chapter 1: The role of epigenomics in personalized medicine: a literature review

The majority of this chapter was published in

Kronfol MM, Dozmorov MG, Huang R, Slattum PW, McClay JL. The role of epigenomics in personalized medicine. *Expert Rev Precis Med Drug Dev.* 2017;2(1):33–45. [doi:10.1080/23808993.2017.1284557](https://doi.org/10.1080/23808993.2017.1284557)

Additional excerpts taken from

Kronfol MM, McClay JL (2019) Chapter 14 - Epigenetic biomarkers in personalized medicine. In: Sharma S (ed) *Prognostic Epigenetics*. Academic Press, pp 375–395

1.1. Introduction

Personalized medicine is founded upon the concept that individual differences in therapeutic success are the norm among patients that require pharmacological treatment. This concept is not new. Hippocrates writing in the 5th century BCE is known to have commented, “give different ones [drugs] to different patients, for the sweet ones do not benefit everyone, nor do the astringent ones, nor are all the patients able to drink the same things.” (see Sykiotis et al. 2005). Thus, the concept of variable response to drugs has been discussed for at least two and a half millennia. However, being able to predict who will respond to a given drug has proven an enduring challenge. With the advent of modern genomic technologies, which enable us to read each patient’s genetic make-up, the idea of personalized medicine is becoming a reality.

Pharmacogenetics, the core discipline of personalized medicine, has already delivered some profound and meaningful successes. The effectiveness of Cytochrome P450 (CYP450) genotypes in predicting an individual’s drug metabolizing phenotype is a notable example (Ingelman-Sundberg 2004a). This has led to several of these biomarkers being approved for clinical use by regulatory bodies such as the US Food and Drug Administration (FDA) (www.fda.gov/Drugs/ScienceResearch/ResearchAreas/Pharmacogenetics/ucm083378.htm). Beyond drug metabolism, genetic variants at numerous other loci have shown robust associations

indicative of clinical relevance, with commercial kits and services now available to deliver this information to health providers and consumers (McCarthy et al. 2013).

In the last decade, pharmacogenetics has harnessed the power of genome-wide association studies (GWAS). This has enabled the field to move beyond the study of candidate genes to scanning hundreds of thousands of genetic markers for each subject. Several promising new leads have been discovered. Arguably, however, the success of GWAS in pharmacogenomics has not mirrored that of complex disease studies. Primarily this may be an issue of statistical power, whereby the clinical trials necessary to measure drug response are costly and so sample sizes currently tend to be small. As studies grow in size and number and meta-analyses are conducted across samples, we can expect GWAS to yield additional insight over time (Ritchie 2012). However, GWAS will not yield all the answers for any given drug response phenotype. Beyond the limitation where GWAS focuses on common polymorphisms, even if all the relevant variants for response to a given drug were mapped, we would still be unable to explain all the phenotypic variation in drug response (Manolio et al. 2009). Drug response is complex and, like other complex traits, it likely arises from the interplay of multiple genetic and environmental factors over the life course (Cardon and Harris 2016). DNA sequence is just one component of this complexity.

Most genotype associations in complex traits such as drug response are probabilistic indicators of phenotype, which typically say little of certainty about the state of the organism at the time of sampling. When treating an individual patient with a specific drug, substantial supporting information in addition to genotype information may be required before making a clinical decision. Even phenotypes that are strongly influenced by genetics, such as the CYP450 drug metabolism phenotypes, will be modified by the effects of concurrent medications or

alcohol and tobacco use that may inhibit or interfere with CYP enzyme activity (He et al. 2015; Tracy et al. 2016). This further illustrates the need to consider information beyond genotype alone.

There are two broad complexities to living organisms that are not addressed by genotype information. These are 1) spatial and 2) temporal variation in biological function or phenotypic expression within the same organism. Consider that humans are composed of multiple cell types with a diverse array of functions (spatial, or cell-specific variation) and that we take on very different macroscopic forms in early versus later life (temporal, or developmental variation). Yet essentially the same genome is present in all nucleated cells at all-time points. In this chapter, we will show how the processes that lead to cellular diversity and organismal development, i.e. epigenetics, can be harnessed to provide more nuanced DNA-based biomarkers and novel treatment strategies (Bock 2009). Indeed, epigenetics may also yield an environmental exposure record of the patient that we are just beginning to comprehend (Ladd-Acosta 2015). Epigenetic biomarkers are therefore fundamentally different to studies of gene expression, proteins or metabolites, which provide snapshots of functional state at a single time point. Epigenetics provides layers of regulatory and environmental exposure information on top of each individual's unique genome (Feinberg 2007). Thus, it indicates what happened to you and you alone, and from this we may be able to determine your truly personal drug regimen design and success, disease susceptibility and cure.

1.2. Epigenetics Overview

The term “epigenetics” was first described by the British developmental biologist Conrad Waddington in the 1940s as “the branch of biology which studies the causal interactions between genes and their products, which bring the phenotype into being” (Goldberg et al. 2007; Noble

2015). Waddington's definition therefore predates the discovery of DNA and so the term "epigenetics" has developed over time. Waddington was focused on organismal development, whereby cells starting with the fertilized egg follow trajectories of increasing specialization until terminal differentiation, which cannot be reversed. One of Waddington's visual metaphors for this process, where the cell is conceptualized as a marble rolling down a rolling hillside with ravines and valleys, has an enduring intuitive appeal and is explained in **Figure 1.1**.

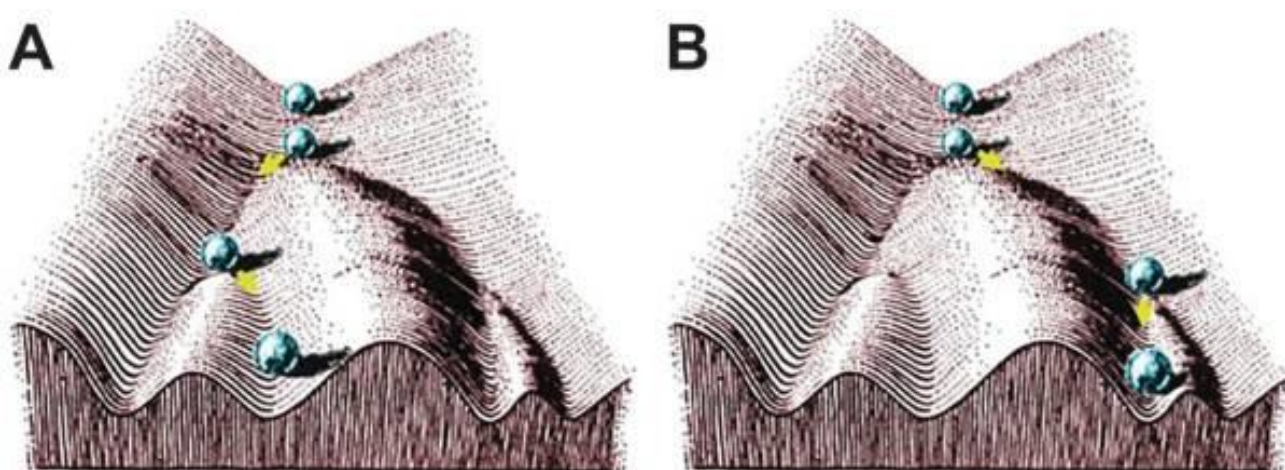


Figure 1.1. Waddington represented the developmental process as a series of “decisions” made by differentiating cells that could be represented as forks in the valleys of the “developmental landscape”. Panels A and B represent the alternate fates of the cell, or ball by analogy. As the pluripotent stem cell of the egg (ball at the top), begins to specialize, the differentiation “decisions” made are irreversible. Its pattern of epigenetic regulation is established by the point of terminal differentiation at the bottom of the landscape. With epigenetic drugs and therapies, the aim is to artificially reverse maladaptive epigenetic states and essentially “push the ball back up the hill”. Figure from Noble (2015) (Noble 2015) reproduced with permission.

Today, backed by knowledge of the genome and some core molecular processes, epigenetics can be defined as the study of mitotically stable changes in genetic regulation that do not involve changes to nucleotide sequence (Russo et al. 1996). Mitotic stability, in this sense, means that the epigenetic state of the parent cell is written to the daughter cell after mitosis, thereby continuing the developmental trajectory of the parent. This regulation is enacted via epigenetic marks, which are reversible regulatory modifications to chromatin.

1.2.1. Epigenetic modifications to chromatin

The most intensively studied epigenetic mark is the methylation of DNA cytosine residues at the carbon 5 position (5mC). This mark is made via the DNA N-methyl transferase (DNMT) enzymes and is most often found in the sequence context CpG (Irizarry et al. 2009). DNA methylation is one of the core epigenetic marks essential for regulating gene expression in normal cell development and differentiation (Reik et al. 2001). While 5mC is the most well-characterized, other cytosine modifications have now been discovered, such as 5-hydroxymethylcytosine (5hmC), 5-formylcytosine (5fC) and 5-carboxylcytosine (5caC) (Ito et al. 2011; Bachman et al. 2015). The functions of these exotic marks are still being elucidated, but 5hmC may play an important role in the central nervous system, where it is prevalent, and in the regulation of pluripotency in stem cells (Kriaucionis and Heintz 2009; Pastor et al. 2011).

Another major class of epigenetic mark involves the post-translational modification of histones, the proteins that package DNA into nucleosomes (Jenuwein and Allis 2001). Histones are the chief protein components of chromatin, whereby 146 bp of DNA is wound around each histone octamer (Luger et al. 1997). There are five major classes of canonical histones, where each octamer is typically formed of two H2A-H2B dimers and a H3-H4 tetramer while H1 serves as a linker protein between nucleosomes. H3 and H4 have long tails that protrude from the

nucleosome that can be covalently modified in several places, while other histones can also be modified to a lesser degree. The best characterized modifications include mono-, di- and trimethylation, acetylation and phosphorylation, although a growing number continue to be reported (Bannister and Kouzarides 2011). Standard nomenclature abbreviates the histone, the modified residue and the type of modification, such that histone 3 lysine 27 acetylation is written as “H3K27Ac”. These modifications are written and erased by specific enzyme families, such as histone acetyltransferases (HATs) and histone deacetylases (HDACs) in the case of acetylation marks, or histone methyl transferases (HMTs) and demethylases (HDMs) in the case of methylation marks (Bannister and Kouzarides 2011).

In addition to histone modifications, histone variants can have significant transcriptional regulatory roles. Histone variants replace canonical histones to alter nucleosome structure and ultimately DNA accessibility (Weber and Henikoff 2014). An example histone variant is H2A.Z, which replaces nucleosomal H2A to perform several complex regulatory roles in gene expression and development (Marques et al. 2010). Finally, for the purposes of this chapter, we also mention polycomb epigenetic repressors and bromodomain-containing proteins. Polycomb proteins can remodel chromatin and typically function as epigenetic gene silencers (Entrevan et al. 2016), while bromodomain proteins are transducers of the acetylation signal on histones (Filippakopoulos and Knapp 2014). These chromatin-interacting proteins are relevant for epigenetic personalized medicine because they are targets for epigenetic drugs that we mention below in Section 1.3.2. Other putatively epigenetic regulatory mechanisms exist, most notably the non-coding RNAs (ncRNAs). NcRNAs primarily function as post-transcriptional regulators of gene expression, but also play roles in regulating chromatin accessibility. They have been extensively reviewed elsewhere (<http://www.cell.com/cell/collections/noncoding-rna>).

1.2.2. Epigenetic effects on gene expression and regulation

The “textbook”, or classic, view of epigenetic regulation is focused on DNA methylation at gene promoters. In this view, hypomethylated CpGs are typically associated with active, expressed genes, while hypermethylated CpGs are typically associated with silenced genes. This effect arises because methylation of cytosine inhibits transcription factor binding (Jaenisch and Bird 2003). Subsequent research has indicated that methylated cytosine, in addition to methylated histone H3K9, and deacetylated H3 combine to form a repressive epigenetic signature, while unmethylated DNA, methylated H3K4, and acetylated H3 combine to form an activating epigenetic signature (Ivanov et al. 2014), although not all histone modifications are coupled with DNA methylation (Hansen and Helin 2009). An overview is provided in **Figure 1.2**. During development, epigenetic patterns change and differentiated cells develop a stable and unique epigenetic pattern that regulates tissue-specific gene transcription. While this view is broadly consistent with current findings, waves of new genomic data have yielded a more nuanced view.

Massive studies such as ENCODE (ENCODE Project Consortium 2012) and Roadmap Epigenomics (Roadmap Epigenomics Consortium et al. 2015) have significantly advanced our understanding of genetic and epigenetic regulation. The ENCODE project aims to identify all functional elements in the genome, while RoadMap Epigenomics aims to elucidate epigenetic processes that contribute to human biology and disease. Both projects make extensive use of next-generation sequencing (NGS) to profile reference epigenomes and genome-wide protein-DNA binding patterns, including binding patterns for specific modified histones. The most recent culmination of these efforts was the publication of 111 reference epigenomes by RoadMap Epigenomics (Roadmap Epigenomics Consortium et al. 2015). This study revealed epigenetic

regulatory modules of coordinated activity, which are specific combinations of DNA methylation, histone modifications and other proteins that shape chromatin structure, which in turn determine transcriptional activity. These multi-layer data were used to classify genomic regions according to functional state (Ernst et al. 2011). The working models produced by RoadMap Epigenomics include a core 15 chromatin state model (Roadmap Epigenomics Consortium et al. 2015) and an expanded 18 chromatin state model (http://egg2.wustl.edu/roadmap/web_portal/chr_state_learning.html), the latter including twelve active and six inactive states. Active states include transcribed regions, active transcription start sites and their flanking regions, active enhancers and zinc finger protein binding sites. Inactive states include heterochromatin and repressed polycomb regions. This model, although complex, has already proven powerful for understanding regulation of gene expression. (Consortium 2015; Aguet et al. 2017)

1.2.3. Individual differences in epigenetic states and developmental plasticity

Epigenetic modifications to chromatin are affected by exposure to environmental factors, and any changes so induced are inherited mitotically in somatic cells (Feinberg 2007). Studies in human twins have shown that, while their epigenomes are very similar in early life, they diverge as the twins become older as a result of differing environmental exposures across the life course, in addition to stochastic effects (Fraga et al. 2005). Epigenetic changes in response to environmental factors may have evolved to provide plasticity in adaptation to environmental cues (Feinberg 2007). Through the phenomena of de novo epigenetic writing and mitotic stability, the effects of environmental factors can become embedded in the genome and persist to produce long-term phenotypic changes (Feil and Fraga 2012). Example environmental factors with demonstrated developmental consequences include diet, toxins and stress. There is

increasing recognition of the importance of this phenomenon for epigenetic translational research, because it provides concrete biological pathways that are involved in the persistence of environmental effects (Rutter 2016).

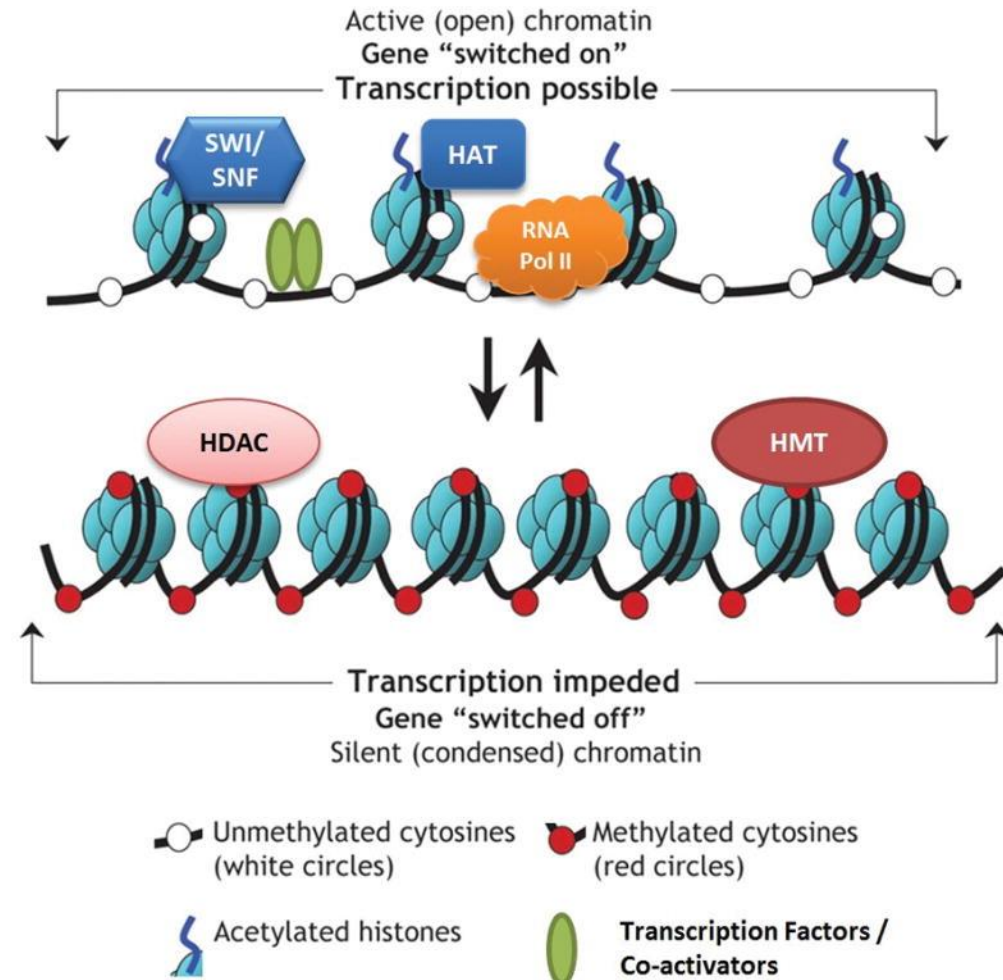


Figure 1.2. Epigenetic regulation of gene expression via chromatin remodeling. The diagram shows two generic chromatin activity states. At the top, active chromatin is open and accessible to transcription factors and polymerases, with nucleosomes spread apart, DNA typically in an unmethylated state and acetylation marks on histones. HAT is histone acetyltransferase, SWI/SNF is a nucleosome remodeling complex, RNA Pol II is RNA polymerase II. The lower panel shows the opposite inactive chromatin scenario, where the nucleosomes are tightly packed, the DNA is methylated and inaccessible to transcription factors, while histones have their acetylation marks removed. HDAC is histone deacetylase, HMT is histone methyltransferase. Figure is adapted from Luong, P. Basic Principles of Genetics, Connexions Web site. [http://cnx.org/content/m26565/1.1/] (2009) under a Creative Commons Attribution License ([http://creativecommons.org/licenses/by/3.0/CC-BY 3.0]).

Epigenetic states can also vary between individuals because of genetic differences. In the case of methylation, one of the simplest examples involves polymorphic CpG sites (Zhi et al. 2013). If a nucleotide substitution ablates a CpG in some individuals, those individuals cannot be methylated at that locus. There are several examples of disease-associated polymorphic CpGs, suggesting that this is a significant contributor to individual differences in disease risk (Cazaly et al. 2015; Zhou et al. 2015). In addition to polymorphic CpGs, DNA sequence variation may also affect the binding of chromatin-interacting proteins and thus influence epigenetic states (McClay et al. 2015). Thus, individual differences in epigenetic states, whether arising via genotype or maladaptive responses to environmental factors, can lead to disease.

1.3. Epigenetic Applications in Personalized Medicine

Epigenetic disease associations provide not only mechanistic clues to disease etiology but can also function as diagnostic biomarkers. The developmental stage- and tissue-specificity of epigenetic marks has led to considerable interest in developing biomarkers that capitalize on these unique properties (García-Giménez 2015). Furthermore, the fact that epigenetic marks are reversible has led to significant interest in the development of drugs with epigenetic modes of action (Szyf 2009; Hunter 2015).

1.3.1. Epigenetic biomarkers of disease

The largest body of work in disease epigenetics to date is on cancer. Since the first links between DNA methylation and cancer were established in the early 1980s, a number of epigenetic findings have been described, implicating several aspects of the epigenetic machinery. Some excellent reviews of cancer epigenetics have been published recently (Suvà et al. 2013;

Feinberg et al. 2016), so here we limit ourselves to epigenetic marks in cancer showing evidence or potential as diagnostic or prognostic biomarkers.

Current epigenetic biomarker applications predominantly involve DNA methylation (Amacher 2016). In the United States, nucleic acid-based tests intended for general clinical use are regulated by the Food and Drug Administration (FDA) as medical devices. Currently there are no FDA-approved tests that rely exclusively on epigenetic biomarkers. However, one commercially available test with an epigenetic component has received full FDA approval. This is ColoGuard®, a screening test for colorectal cancer in adults over 50. The test uses DNA methylation levels at *BMP3* and *NDRG4*, in combination of mutated *KRAS* and an immunochemical assay for hemoglobin (**Table 1.1**). This test was reported to have superior sensitivity but slightly lower specificity for colorectal cancer compared to the traditional screening method, fecal immunochemical testing (FIT) (Imperiale et al. 2014). However, more recent results suggest FIT may be more effective and less costly than ColoGuard®, the latter necessitating either very high patient uptake or a 60% reduction in cost per test to become the preferred testing method (Ladabaum and Mannalithara 2016). This illustrates the economic barriers that diagnostic tests must overcome, beyond the demonstration of efficacy and reproducibility, in order to become widespread.

Two other epigenetic tests are currently available in the US, classified as Laboratory Developed Tests (LDTs) and regulated under the Clinical Laboratory Improvement Amendments (CLIA) program. This means that the test may only be conducted “in house” in the laboratory where it was developed, once the lab meets CLIA performance standards. The two tests are ConfirmMDx and AssureMDx, for prostate cancer and bladder cancer respectively.

Hypermethylation of the glutathione S-transferase gene (*GSTP1*) promoter in prostate cancer

was first shown in the 1990s (Lee et al. 1994). This marker, plus *APC* and *RASSF1*, are now components of the ConfirmMDx test (**Table 1.1**), which is used to address false-negative prostate biopsy concerns (Partin et al. 2014). The AssureMDx test for bladder cancer involves the analysis of DNA methylation levels of three genes (*TWIST1*, *ONECUT2* and *OTX1*) in combination with mutation analysis of three others (van Kessel et al. 2016).

In lung cancer, the DNA methylation of the *SHOX2* gene was reported to be an accurate marker for identifying lung cancer based on analysis of bronchial aspirates (Schmidt et al. 2010). In Europe, this biomarker is now commercially available as the Epi proLungVR BL Reflex Assay (Dietrich et al. 2012). However, this test has not yet received regulatory approval for use in the USA.

Product	Proprietor/ Launch year	Disease	Specimen	Epigenetic Targets	Regulation
Cologuard	Exact sciences/2014	Colorectal cancer	Stool	DNA methylation of <i>NDRG4</i> and <i>BMP3</i> (plus other genetic markers)	FDA
ConfirmMDx	MDxHealth/2012	Prostate cancer	Tissue	DNA methylation of <i>GSTP1</i> , <i>RASSF1</i> and <i>APC</i> .	LDT/CLIA
AssureMDx	MDxHealth/2016	Bladder cancer	Urine	DNA methylation of <i>TWIST</i> , <i>ONECUT2</i> and <i>OTX1</i> (plus other genetic markers)	LDT/CLIA

Table 1.1. Commercially available epigenetic diagnostic tests in the United States.

In breast and ovarian cancer, hypermethylation of the *BRCA1* promoter region has been observed repeatedly (Cancer Genome Atlas Research Network 2011; Stefansson and Esteller 2013). *BRCA1* is also thought to epigenetically repress expression of the oncogenic microRNA miR-155 via a mechanism involving histone deacetylase 2 (HDAC2) (Chang et al. 2011). A recent study by Anjum et al. (2014) identified a blood cell DNA methylation signature at *BRCA1* that was able to predict breast cancer risk several years prior to diagnosis (Anjum et al. 2014). However, this biomarker is not yet available in a commercial kit or test.

The biomarker potential of circulating cell-free DNA (cfDNA) has been investigated in breast cancer and other cancers. Circulating cfDNA is extracted from plasma or serum and is derived from dying tumor cells that release their DNA into the bloodstream. Kloten et al (2013) used a panel of three genes (*ITIH5*, *DKK3* and *RASSF1A*) that showed hypermethylation in serum cfDNA from breast cancer patients and found these could discriminate between patients and controls with a sensitivity of 67% and specificity of 69% (Kloten et al. 2013). Fackler et al. (2014) followed this with a panel of 10 genes and cancer-specific DNA was detected in sera with a sensitivity of 91% and specificity of 96% in the test samples (Fackler et al. 2014). The researchers of the latter study are reportedly working with the diagnostics company Cepheid to bring this test to market (Butkus).

While epigenetic studies of cancer are arguably the most advanced relative to other areas, several diseases have shown promising findings, particularly with respect to DNA methylation. These include neurological disorders such as Alzheimer's Disease (De Jager et al. 2014; Lunnon et al. 2014) and Parkinson's Disease (Jowaed et al. 2010), autoimmune disorders such as systemic lupus erythematosus (Absher et al. 2013), and psychiatric disorders such as schizophrenia (Pidsley et al. 2014; Aberg et al. 2014) and autism (Ladd-Acosta 2015). Despite

these advances, there are no currently available diagnostic kits for these diseases that employ epigenetic markers. Nevertheless, it is hoped that the clinical value of epigenomics already seen in oncology will be replicated in these areas (Heyn and Esteller 2012).

1.3.2. Epigenetic drugs

The dynamic and reversible nature of epigenetic modifications is of particular relevance to drug development, as it implies that specific disease-associated epigenetic states may be reversible with pharmacological treatment (DeWoskin and Million 2013). This segment will summarize current and potential “epidrugs”, or drugs with epigenetic modes of action. Epidrugs are classified according to their respective target enzymes, and include the following: DNA N-methyl transferase inhibitors (DNMTi), histone acetyltransferase inhibitors (HATi/KATi), histone methyltransferase inhibitors (HMTi/KMTi), histone N-methyl lysine demethylase inhibitors (HDMi/KDMi), histone deacetylase inhibitors (HDACi/KDACi), and bromodomain inhibitors. As of 2019, there are two classes of epigenetic drugs that have been approved by FDA for clinical use in the United States: DNMTi and HDACi (see **Table 1.2**).

The first approved epidrug in the US was azacitidine (Vidaza, Azadine), a DNMTi indicated to treat chronic myelomonocytic leukemia and myelodysplastic syndrome. Azacitidine was approved in 2004 and quickly followed by decitabine (Dacogen) with same indication two years later. Both drugs cause broad hypomethylation that leads to cellular dysregulation that most seriously affects rapidly dividing cells. It is important to note that these drugs are not highly locus-specific and these agents can cause hypomethylation at many genomic sites. Even though current drugs are designed to favorably induce genes that have been silenced in cancer (Liang et al. 2002), they may also activate the expression of prometastatic genes as well as oncogenes

(Cheishvili et al. 2015). There remains a need to develop more selective DNMTi to improve the efficacy and reduce side effects for this class of drug.

The potential application of DNMTi to other diseases is also under investigation and examples include multiple sclerosis (Peedicayil 2016), HIV (Abdel-Hameed et al. 2016), pain (Sun et al. 2015) and memory (Singh et al. 2015). For example, DNMT activity was observed in HIV-1 infection of CD4(+) T-cells in vitro and induced hypermethylation of distinct cellular promoters (Abdel-Hameed et al. 2016). Studies from Rajasethupathy et al. suggested that DNA methylation is necessary for serotonin-dependent long-term facilitation in memory formation (Rajasethupathy et al. 2012). For a curative therapy of AIDS patients, a combination of antiretroviral drugs and epidrugs has been suggested for the reactivation of latent HIV-1 genomes. These epidrugs include DNMTi, HDACi, histone methyltransferase inhibitors (HMTi) and histone demethylase inhibitors (Abdel-Hameed et al. 2016).

The HDAC inhibitors suberoylanilide hydroxamic acid (SAHA, vorinostat, in 2006) and romidepsin (depsipeptide, in 2009) have proven to be successful in cancer therapeutics (Lane and Chabner 2009). These agents cause the accumulation of acetylated histones and prevent progression of tumor cells. Vorinostat was the first HDACi to be approved by the FDA, indicated for cutaneous manifestations in patients with cutaneous T-cell lymphoma (CTCL). Panobinostat is the latest HDACi approved by the FDA in 2015 and is indicated for the treatment of multiple myeloma in combination with bortezomib and dexamethasone. Outside the US, HDACi approvals vary.

Mechanism of Action	Active Ingredient (Trade name®, Proprietor)	Date of Approval	Indication(s)
DNA N-Methyltransferase Inhibitor (DNMTi)	Azacitidine (Vidaza®, Celgene)	May 19, 2004	Chronic Myelomonocytic Leukemia. Myelodysplastic Syndrome ⁱ .
	Decitabine (Dacogen®, Otsuka)	May 2, 2006	Chronic Myelomonocytic Leukemia. Myelodysplastic Syndromes ⁱⁱ .
Histone Deacetylase inhibitors (HDACi)	Vorinostat (Zolinza®, Merck)	October 6, 2006	Cutaneous manifestations in patients with cutaneous T-Cell Lymphoma (CTCL) who have progressive, persistent or recurrent disease on or following two systemic therapies.
	Romidepsin (Istodax®, Celgene)	November 5, 2009	Cutaneous T-cell Lymphoma (CTCL) ⁱⁱⁱ , Peripheral T-cell Lymphoma (PTCL) ⁱⁱⁱ
	Belinostat (Beleodaq®, Spectrum Pharmaceuticals)	July 3, 2014	Relapsed or Refractory Peripheral T-cell Lymphoma (PTCL)
	Panobinostat (Farydak®, Novartis)	February 23, 2015	Multiple Myeloma after receiving at least 2 prior regimens, including bortezomib and an immunomodulatory agent ^{iv}

Table 1.2. Classification of US FDA-approved epigenetic drug classes according to mechanism of action.

ⁱ Subtypes: refractory anemia or refractory anemia with ringed sideroblasts (if accompanied by neutropenia or thrombocytopenia or requiring transfusions), refractory anemia with excess blasts, refractory anemia with excess blasts in transformation. ⁱⁱ Including 90 previously treated and untreated, de novo and secondary MDS of all French-American-British subtypes 91 (refractory anemia, refractory anemia with ringed sideroblasts, refractory anemia with excess blasts, 92 refractory anemia with excess blasts in transformation, and 93 intermediate-1, intermediate-2, and high-risk International Prognostic Scoring System groups). ⁱⁱⁱ In patients who have received at least one prior systemic therapy. ^{iv} In combination with bortezomib and dexamethasone.

In Europe, for example, only panobinostat has been approved for general clinical use (to treat multiple myeloma), while belinostat received orphan designation for peripheral T-cell lymphoma (PTCL). In China, an additional HDACi known as chidamide (Epidaza®), was approved for treatment of PTCL by the Chinese FDA in 2015. Although most HDACi are approved for cancer type indications, studies have suggested potential roles in schizophrenia (Kurita et al. 2012) and Type2 diabetes (Sharma and Taliyan 2016). However, similar to the DNMTi drugs, current HDACi have broad effects across the genome and lack locus-specificity. These drugs can have serious side effects (Hunter 2015) and use of currently approved HDACi in cancer is often indicated only after other treatments have failed, or as combination therapies (**Table 1.2**).

Besides these two approved epidrug classes, HMTi and bromodomain inhibitors are other emerging epidrug classes under development. Pinometostat is a small molecule inhibitor of the histone methyltransferase DOT1L for the treatment of MLL-r leukemia (Daigle et al. 2013). Tazemetostat is an orally administered, first-in-class small molecule HMTi that targets the EZH2 transcriptional repressor to treat multiple types of hematological malignancies and genetically defined solid tumors (Kurmasheva et al. 2017). GSK3326595, an inhibitor of the transcriptional regulator protein arginine methyltransferase 5 (PRMT5), is also in phase 1 clinical trial. Bromodomain proteins are readers that recognize acetylated lysine and transduce the gene activation signal (Filippakopoulos and Knapp 2014). OTX-015 and CPI-0610 are bromodomain protein inhibitors both in phase I trials for cancers. These drugs target a specific family of bromodomain proteins, known as Bromodomain Extra-Terminal motif (BET) proteins (Chung et al. 2011). Another BET inhibitor, Apabetalone (RVX-208), is in Phase III clinical trials for cardiovascular events in Type 2 diabetes subjects with coronary artery disease. These example

epidrugs, and several more are advancing through the clinical trial pipeline, are summarized in **Table 1.3**. In this table, we focus only on epidrugs in active or planned clinical trials registered in the US (clinicaltrials.gov) and show the latest phase trial for each drug, plus any trials for indications outside oncology. We restrict our listing of early phase cancer indications because these are too numerous to list concisely.

Mechanism of action	Active ingredient (Proprietor)	Indication	Clinical Trial Phase	Trial Ref ID
BET Bromodomain Inhibitors	Apabetalone/ RVX-208 (Resverlogix)	High-risk type 2 diabetes mellitus with coronary artery disease	Phase III	NCT02586155
	CPI-0610 (Constellation Pharmaceuticals)	Malignant Peripheral Nerve Sheath Tumor	Phase II	NCT02986919
	INCB054329 (Incyte)	Advanced malignancies	Phase I/II	NCT02431260
	GSK525762 (GlaxoSmithKline)	Carcinoma and hematological malignancies	Phase I	NCT01587703, NCT01943851
	GSK2820151 (GlaxoSmithKline)	Advanced or recurrent solid tumors	Phase I	NCT02630251
	ZEN-3694 (Zenith Epigenetics)	Metastatic castration-resistant prostate cancer (mCRPC) ⁱ	Phase I	NCT02711956 ⁱ , NCT02705469
	OTX015/MK-8628 (Merck)	Selected advanced solid tumors	Phase I	NCT02698176
	TEN-010/ RO6870810 (Hoffmann-La Roche)	Advanced Solid Tumors; Acute Myeloid Leukemia	Phase I	NCT01987362, NCT02308761
	FT-1101 (Forma therapeutics)	Relapsed/Refractory Acute Leukemia	Phase I	NCT02543879
	BMS-986158 (Bristol-Myers Squibb)	Advanced Solid Tumors	Phase I	NCT02419417
	Mivebresib/ABBV-075 (AbbVie)	Advanced cancers	Phase I	NCT02391480

DNA N-Methyltransferase Inhibitor (DNMTi)		Guadecitabine (Astex)	Acute Myeloid Leukemia	Phase III	NCT02920008
		TdCyd (NCI)	Advanced Solid Tumors	Phase I	NCT02423057
Histone Deacetylase inhibitors (HDACi)	Non-Selective	Entinostat (Syndax)	Advanced Hormone Receptor positive (HR+) Breast Cancer ⁱⁱ	Phase III	NCT02115282
		Givinostat/ITF2357 (Italfarmaco)	Chronic Myeloproliferative Neoplasms	Phase II	NCT01761968
		Resminostat (4SC AG)	Advanced Stage Mycosis Fungoides or Sézary Syndrome	Phase II	NCT02953301
		Quisinostat/JNJ-26481585 (Janssen)	Ovarian cancer ⁱⁱⁱ	Phase II	NCT02948075
		Pracinostat/SB939 (NCIC Clinical Trials Group)	Acute Myeloid Leukemia ^{iv} , Myelofibrosis ^v	Phase II	NCT01912274 ^{iv} NCT02267278 ^v
		Tefinostat (Chroma)	Hepatocellular Carcinoma	Phase I/II	NCT02759601
		AR-42 (Celgene)	Relapsed multiple myeloma ^{vi}	Phase I	NCT02569320
		CUDC-907 (Curis)	Multiple Myeloma	Phase I	NCT01742988
	HDAC 1&4 Selective	Mocetinostat (Mirati)	Non-Small Cell Lung Cancer ^{vii}	Phase II	NCT02954991
	HDAC 6 Selective	ACY 241 (Acetylon)	Non-Small Cell Lung Cancer ^{vii}	Phase I	NCT02635061

		KA2507 (Karus)	Solid tumor	Phase I	NCT03008018
Histone Lysine De- methylases (KDM/HDM)	LSD1 inhibitors	GSK2879552 (GlaxoSmithKline)	Myelodysplastic Syndrome	Phase II	NCT02929498
		Tranlycypromine (Martin Luther Universität)	Relapsed/Refractory Acute Myeloid Leukemia ^{viii}	Phase I/II	NCT02261779
		INCB059872 (Incyte)	Advanced Malignancies	Phase I/II	NCT02712905
		IMG-7289 (Imago BioSciences)	Acute Myeloid Leukemia	Phase I	NCT02842827
Histone Lysine Methyl Transferase (KMT/HMT)	DOT1L inhibitor	Pinometostat/ EPZ-5676 (Epizyme)	Relapsed/Refractory Leukemias ^{ix}	Phase I	NCT01684150
	EZH1/2 inhibitor	DS-3201b (Daiichi Sankyo)	Lymphomas	Phase I	NCT02732275
	EZH2 inhibitor	Tazemetostat/ EPZ-6438 (Epizyme)	Advanced Solid Tumors or B-cell lymphomas	Phase I/II	NCT01897571
		MAK683 (Novartis)	Diffuse Large B-cell Lymphoma	Phase I/II	NCT02900651
		GSK2816126 (GlaxoSmithKline)	Lymphomas, Multiple Myeloma, Solid Tumors	Phase I	NCT02082977
	PRMT5 inhibitor	GSK3326595 (GlaxoSmithKline)	Solid Tumors and Non- Hodgkin's Lymphoma	Phase I	NCT02783300

Table 1.3. Classification of epigenetic drug classes in active clinical trials registered in the US (clinicaltrials.gov) according to mechanism of action.

ⁱ In combination with Enzalutamide.

- ii In combination with Aromasin (Exemestene).
- iii In combination with Paclitaxel and Carboplatin chemotherapy.
- iv In combination with Azacitidine.
- v In combination with Ruxolitinib.
- vi In combination with Pomalidomide.
- vii In Combination with Nivolumab.
- viii In combination with all-trans-retinoic acid (ATRA) chemotherapy.
- ix Only patients with rearrangements involving the MLL gene.

LSD1: Lysine (K)-specific demethylase 1A, DOT1L: Disruptor of telomeric silencing 1-like, EZH1 or EZH2: Enhancer Of Zeste Homolog 1 or 2 Polycomb Repressive Complex 2 Subunit, PRMT5: Protein Arginine Methyl Transferase 5.

Finally, several HATi are in preclinical studies at time of writing. Aberrant function of HATs, also called lysine acetyltransferases (KATs), is correlated with cancer and other diseases (Khan and Khan 2010). HATi are great candidates with potential therapeutic utility, but current HATi only have moderate potency and specificity and none are in clinical trial at time of writing. Nevertheless, some HATi have shown efficacy in preclinical studies. Compound C646 is a pyrazolone-containing small molecule inhibitor of the p300/CBP HAT subfamily (Bowers et al. 2010). It has been shown to cause growth arrest in melanoma cell lines and inhibit cancer cell growth in prostate and lung cancer cell lines. PU139 is a pyridoisothiazolone that inhibits several HAT subfamilies and was shown to block neuroblastoma xenograft growth in mice (Gajer et al. 2015). These agents and others in development are indicative that HATi are still in infancy relative to other epigenetic drugs, but they show enormous promise and need further investment to reach their potential as therapeutic compounds.

1.3.3. Epigenetic biomarkers of drug response

As a natural extension of pharmacogenetics, it is possible to use epigenetic biomarkers to predict drug response. While none have yet achieved regulatory approval for clinical use, a small number of examples are established in the literature. Among the best known is DNA methylation of the *MGMT* promoter. This gene encodes a DNA repair enzyme (O6-alkylguanine DNA alkyltransferase). Methylation in the promoter region of *MGMT* is associated with better response to alkylating neoplastic agents like temozolomide, as first shown in glioblastoma by Esteller et al. (2000) (Esteller et al. 2000) and later by Hegi et al. (2005) (Hegi et al. 2005). The mechanism of effect is as follows. Temozolamide alkylates or methylates DNA at the N-7 or O-6 positions of guanine residues and the resulting DNA damage triggers tumor cell death. Hypomethylation of *MGMT* leads to expression of O6-alkylguanine DNA alkyltransferase,

which can repair the DNA damage, whereas hypermethylation leads to silencing of the gene and thus greater susceptibility to the drug (**Figure 1.3**). In addition to glioma, a role for *MGMT* in predicting response to metastatic colorectal cancer (mCRC) treatment has also been suggested (Fornaro et al. 2016).

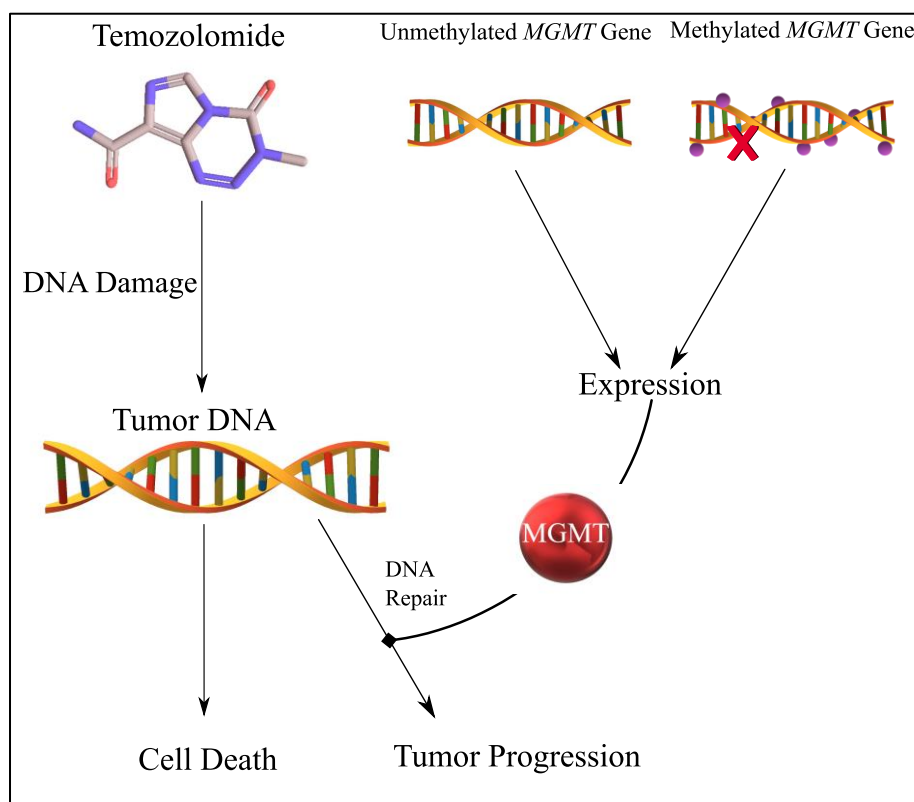


Figure 1.3. MGMT: O-6-methylguanine-DNA methyltransferase. The MGMT enzyme repairs tumor DNA damage induced by the anticancer drug temozolomide. However, if the MGMT gene is methylated and not expressed, the DNA damage cannot be adequately repaired leading to greater tumor sensitivity to temozolomide and a better clinical response. Adapted from (Kronfol and McClay 2019).

Other published epigenetic biomarker examples include *GSTP1* and *BRCA1*. Methylation of the promoter of *GSTP1* is correlated with survival in breast cancer patients and may be

predictive of treatment efficacy with doxorubicin (Chiam et al. 2011) or DNA methyltransferase (DNMT) inhibitors (Dejeux et al. 2010). The *BRCA1* gene plays a role in DNA damage response and hypermethylation of the *BRCA1* promoter region may be predictive of enhanced sensitivity to platinum-derived drugs in cancer cell lines and xenografted tumors; it also may be predictive of increased time to relapse and survival in ovarian cancer patients under cisplatin treatment (Stefansson et al. 2012).

The impact of epigenetics in drug response has been investigated beyond oncology. For example, methylation of the P2 promoter of the *IGF1* gene affects transcriptional response to growth hormone (GH) (Ouni et al. 2016). GH is mainly used to treat children with short stature due to growth hormone deficiency. Ouni et al. (Ouni et al. 2016) measured P2-driven and total *IGF1* transcripts before and 12 h after the GH injection and found an increase in P2-driven transcripts with a very strong inverse correlation with CG-137 methylation. This correlation accounted for ~ 25% of the variability in the response to GH.

1.3.4. Epigenetic modification of drug absorption, distribution, metabolism and excretion (ADME) genes

ADME genes encode transporters, plasma proteins, and drug metabolizing enzymes that are responsible for absorption, distribution, metabolism and excretion of xenobiotics. Genetic variation at ADME genes has proven extremely successful in predicting individual differences in pharmacokinetics, particularly in the case of drug metabolizing phenotypes associated with the CYP450s, as mentioned above. However, there remain large individual differences in drug metabolism unexplained by genetic variation that have led to the suggestion that epigenetics may substantially influence these phenotypes (Ivanov et al. 2012). Unfortunately, research to date has not yet directly addressed this question, but individual variation in epigenetic states of ADME

genes has been correlated with a range of outcomes. For example, Parkinson's disease has been associated with hypomethylation of the *CYP2E1* gene promoter in the brain (Kaut et al. 2012). Methylation levels at *CYP1B1* (Tokizane et al. 2005) and *CYP1A1* (Okino et al. 2006) have been associated with prostate cancer, and *CYP2W1* with colon cancer (Gomez et al. 2007). Methylation levels at the drug transporter genes *OCT1* (Schaeffeler et al. 2011) and *OCT2* (Liu et al. 2016), responsible for the renal excretion of drugs, have been associated with renal carcinoma. These findings demonstrate the existence of inter-patient variability in ADME gene epigenetic states, some of which have functional effects on gene expression. However, the extent of normal epigenetic variation at these loci in the population and the extent to which it will affect pharmacokinetic phenotypes remains to be determined.

1.4. Aging

1.4.1. Aging, drug response, and adverse drug reactions

The elderly population in the U.S comprises 15% of the total population, which translates to 49 million Americans aged 65 or older in 2016. This number is projected to increase to 56 million in 2020. The older adult population has a higher mean healthcare expenditure per annum (\$5,994) than that of the rest of the population (\$4,612). It is estimated that 40% of persons 65 years of age or older take five to nine medications concurrently, while almost one fifth (18%) take 10 or more. Ultimately, older adults are almost seven times as likely as younger persons to have adverse drug reactions (ADRs) that require hospitalization (Budnitz et al. 2006). The high level of drug intake associated with older age makes older adults particularly vulnerable to ADRs, but there is strong potential to improve this situation because 80 percent of ADRs in this population are dose-related and thus preventable (Routledge et al. 2004). Alleviation of dose

related ADRs for the aging population would be advantageous for managing this population's pharmacological interventions and improve their health.

1.4.2. Personalized dosing in the elderly population

Age-related changes to drug response are multifactorial in origin (McLachlan et al. 2009). First, aging effects on renal and hepatic function alter drug pharmacokinetics (PK) and pharmacodynamics (PD), but these functions are considered too coarse to guide dosing because they do not capture specific changes to drug metabolizing enzymes (Butler and Begg 2008; McLachlan and Pont 2012; Tan et al. 2015). Second, despite significant successes in several areas, particularly in oncology, genetic tools are insufficient to bring about optimal drug therapy in all instances (Roses 2000). Genotype-based markers are of limited utility to explain intra-individual changes in drug response with age because they are invariant across lifespan. Therefore, to enable personalization of dosing in older adults, new markers of determinants of drug metabolism are needed (McLachlan and Pont 2012)

1.4.3. Epigenetics of Aging

The most well studied epigenetic modification is the methylation of carbon 5 of cytosines at cytosine-guanine dinucleotide (CpG) positions, termed 5-methylcytosine (5mC). A haploid human genome has around 28 million CpGs, or 1% of total sequence (Jabbari and Bernardi 2004; Babenko et al. 2017). Global 5mC, or the aggregate measure of all the 5mC in the genome, has been consistently reported to decrease with age in humans (Gonzalo 2010; Unnikrishnan et al. 2018). However, studies with the ability to measure site-specific methylation revealed hypermethylation at some gene promoters in older persons indicating that some loci gain methylation while others either lose methylation or remain unchanged with age

(Unnikrishnan et al.; Fraga and Esteller 2007; Fraga 2009). Those genomic regions displaying changes with age, regardless of the direction of effect, subsequently came to be known as age-associated differentially methylated regions (a-DMRs) (Bjornsson et al. 2008; Christensen et al. 2009; Teschendorff et al. 2010; Bocklandt et al. 2011). a-DMRs have implications for gene activity. Several large-scale studies of aging in humans examined gene expression, DNA methylation, or both (**Table 2.1**) and found that not only do DNA methylation marks correlate with age but are also predictive of gene expression levels (Steegenga et al. 2014). As we show in our preliminary data (**Table 2.1**), human genome-wide studies of blood DNA have shown that genes involved in the Absorption, Distribution, Metabolism, and Excretion (ADME) of drugs are differentially methylated with age. However, it has not yet been established if these changes also occur in the liver and affect expression levels of genes involved in drug metabolism. Furthermore, we do not know if these changes exert any functional effect on rates of drug clearance *in vivo*. Therefore, further studies are needed to determine if a-DMRs at ADME genes affect drug metabolism.

1.5. Discussion and Conclusions

Epigenomic medicine is already here, with numerous epigenetic disease associations reported, six epidrugs and a handful of epigenetic biomarker tests available the US, plus a small number of other products available worldwide. The largest number of findings and applications to date is in the field of oncology. However, the field of epigenetics is only a few decades old and epigenomic medicine is a very recent arrival, so we are still in early days. The perceived benefits that epigenomics will bring to healthcare are emphatically illustrated by the large number of epidrugs currently in development and the large sums of research dollars spent on large-scale discovery efforts such as RoadMap Epigenomics. To drive the field forward,

epigenomic medicine needs to expand beyond cancer. Also, while significant efforts are being devoted to bringing new epidrugs to market, more efforts must be devoted to developing new epigenetic biomarkers, of which there are few.

Several factors are currently driving innovation in epigenomic medicine. First is the general level of interest in the field, which is high. Second is the ongoing characterization of reference epigenomes to enrich and accelerate research efforts. Third is the availability of powerful methods such as next-generation sequencing (NGS) to characterize epigenomes. Discussion of technical methods is largely outside the scope of this chapter and reviews have been published elsewhere (Laird 2010; Krueger et al. 2012). However, with NGS approaches already in use to characterize genome-wide DNA methylation and protein-DNA binding patterns, we would argue that technology is not a bottleneck for the advancement of epigenomic medicine.

Considering epigenomic biomarker research, among the most significant difficulties are data complexity and the clean interpretation of findings (Ledford 2015). Unlike studies of genotype, epigenomics has a direction of causality problem. While epigenetic biomarkers may be predictive of disease state or drug response, epigenetic changes are also inducible by pharmacological treatments (Feinberg 2007; Wang et al. 2007). As a result, there is the risk that epigenetic differences between cases and controls in an epigenome-wide association study could be the result of drug treatment in cases, rather than causal variation. Furthermore, evidence from genome-wide studies suggests that not all epigenetic changes are functional or cause identifiable changes to gene expression (Stricker et al. 2017). Targeting specific populations, such as drug-naïve patients, may go some way to solving issues related to the direction of causality, but it is certain that experimental model systems will be needed to adequately disentangle causality and establish functionality of epigenetic changes.

Another complexity is that epigenetic modifications are cell specific. While this is in many ways an advantage and can give precise insight into the workings of the cell of origin, it also leads to some challenges in sample collection, particularly with respect to clinical studies. Blood DNA is the most readily-accessible source from humans, but the extent to which blood DNA methylation is reflective of methylation changes in other tissues is debated and it seems there may not be a hard and fast rule with respect to which changes are reflected in blood as compared to which are not. Aging epigenetic signatures, also known as the “epigenetic clock”, appear to transcend tissue barriers (Horvath 2013), but the extent to which a blood DNA methylation mark is informative about a disease of, for example, the lung or heart remains an open question. Circulating cfDNA is an exception, since it is sourced from the diseased tissue of interest and is merely liberated into the bloodstream.

While these considerations apply to the discovery of novel epigenetic biomarkers, a separate set of considerations apply to novel epigenetic drugs. Paramount among priorities for future epidrugs development is improving target specificity. This can be viewed in two ways. First, as mentioned above, current drugs lack genomic locus specificity and affect DNA methylation or histone modifications somewhat indiscriminately. To truly enable precision correction of aberrant changes, some sort of nucleic acid targeting adjunct is likely to be required. While antisense RNA (MG98) has already been used to modulate DNMT activity with some success (Reid et al. 2002), it is difficult to speculate how this could be used to target epigenetic modifications at specific target loci. On the other hand, it may be possible to capitalize on the locus targeting abilities of CRISPR/Cas9 systems to deliver epigenetic modifying agents to specific loci. Indeed, epigenome editing has already been demonstrated using this broad approach (Thakore et al. 2016). A second consideration involves the specificity

of epidrugs to specific members of families of chromatin modifying enzymes. For example, there are numerous human DNMTs and HDAC enzymes with somewhat different functions and substrate specificities but currently available DNMTi and HDACi are non-selective and inhibit many isozymes. However, some drugs currently in clinical trials appear to be more selective, e.g. mocetinostat that inhibits only HDAC 1 and 4 (see **Table 1.3**). Thus, the problem of specificity does not appear to be insurmountable. To conclude, we mention two areas, one technological and one clinical, that we consider to be of significant interest going forward.

In the clinical arena, aging is an area where epigenomic medicine may make an impact. Older adults are at increased risk for adverse drug events and this may be partly because aging is associated with changes in physiology that can affect drug pharmacokinetics and pharmacodynamics (Fillit et al. 2017). The clinical challenge is to identify those patients who are more likely to experience an adverse drug event or altered drug response among the older adult population when weighing the risk versus the benefit of a drug therapy. Chronologic age alone is insufficient as an indicator that dosage adjustment or avoidance of a particular therapeutic agent is warranted. Pharmacogenetic information alone is also insufficient, as altered drug response and risk of adverse drug events changes across the lifespan while genotype remains constant (Brunet and Berger 2014; Pal and Tyler 2016). Epigenetic alterations may be a better indicator than chronological age for personalizing drug therapy for the older population. For example, it has been proposed that epigenetic regulation of cytochrome P450 (CYP) enzymes responsible for drug metabolism through DNA methylation may result in altered drug exposure in geriatric patients (Seripa et al. 2015). More research is needed to elucidate the relationships between epigenetics and drug exposure and response during senescence but is a promising alternative to chronologic age for adjusting pharmacotherapy in older adults.

Chapter 2: DNA methylation and histone acetylation changes to cytochrome P450 2E1 regulation in normal aging and impact on rates of drug metabolism in the liver.

This chapter has been accepted for publication in *GeroScience*
(Official Journal of the American Aging Association (AGE))

The formatting has been modified from its original version to improve readability.

Mohamad M. Kronfol¹, Fay M. Jahr¹, Mikhail G. Dozmorov², Palak S. Phansalkar³, Lin Y. Xie⁴, Karolina A. Aberg⁴, MaryPeace McRae¹, Elvin T. Price¹, Patricia W. Slattum¹, Philip M. Gerk³, Joseph L. McClay¹. *GeroScience* 2020 Mar 27 [Epub ahead of print] [doi: 10.1007/s11357-020-00181-5](https://doi.org/10.1007/s11357-020-00181-5)

¹Department of Pharmacotherapy and Outcomes Science, School of Pharmacy, Virginia Commonwealth University, Richmond, Virginia.

²Department of Biostatistics, School of Medicine, Virginia Commonwealth University, Richmond, Virginia.

³Department of Pharmaceutics, School of Pharmacy, Virginia Commonwealth University, Richmond, Virginia.

⁴Center of Biomarker Research and Precision Medicine, School of Pharmacy, Virginia Commonwealth University, Richmond, Virginia.

Keywords: DNA methylation, Histone acetylation, Aging, *Cyp2e1*, Pharmacokinetics, Drug metabolism

2.1. Abstract

Aging is associated with reduced liver function that may increase the risk for adverse drug reactions in older adults. We hypothesized that age-related changes to epigenetic regulation of genes involved in drug metabolism may contribute to this effect. We reviewed published epigenome-wide studies of human blood and identified the cytochrome P450 2E1 (*CYP2E1*) gene as a top locus exhibiting epigenetic changes with age. To investigate potential functional changes with age in the liver, the primary organ of drug metabolism, we obtained liver tissue from mice aged 4-32 months from the National Institute on Aging. We assayed global DNA methylation (5mC), hydroxymethylation (5hmC) and locus-specific 5mC and histone acetylation changes around mouse *Cyp2e1*. The mouse livers exhibit significant global decreases in 5mC and 5hmC with age. Furthermore, 5mC significantly increased with age at two regulatory regions of *Cyp2e1* in tandem with decreases in its gene and protein expression. H3K9ac levels also changed with age at both regulatory regions of *Cyp2e1* investigated, while H3K27ac did not. To test if these epigenetic changes are associated with varying rates of drug metabolism, we assayed clearance of the CYP2E1-specific probe drug chlorzoxazone in microsome extracts from the same livers. CYP2E1 intrinsic clearance is associated with DNA methylation and H3K9ac levels at the *Cyp2e1* locus but not with chronological age. This suggests that age-related epigenetic changes may influence rates of hepatic drug metabolism. In the future, epigenetic biomarkers could prove useful to guide dosing regimens in older adults.

2.2. Introduction

Adverse drug reactions (ADRs) are estimated to be between the fourth and sixth leading cause of death in the United States (Lazarou et al. 1998). The impact and management of ADRs are complex and has been estimated to cost up to \$30.1 billion annually (Sultana et al. 2013). Previous research suggests that rates of ADRs increase as people age, have more chronic health conditions, and take more medications (McLean and Le Couteur 2004; ElDesoky 2007; Budnitz et al. 2011). Human life expectancy has more than doubled in the last two centuries, and while mortality has been delayed, aging is still accompanied by a significantly elevated risks for many diseases (Issa 2002; Duron and Hanon 2008; Barzilai et al. 2012). Comorbid chronic conditions in individuals older than 65 years cause high degree of polypharmacy in this population. According to a 2006 survey, 40% of persons 65 years of age or older were taking five to nine medications, while almost one fifth (18%) were taking 10 or more (Slone Epidemiology Center 2006). Ultimately, older adults are almost seven times more likely than younger persons to have ADRs that require hospitalization (Budnitz et al. 2006). While ADRs are a serious problem in the aging population, up to 80% of ADRs in older patients are dose related and therefore, are potentially avoidable (Routledge et al. 2004). This implies that effective methods for predicting the correct dose for the individual patient could make a significant impact in geriatric healthcare.

Age-associated changes to hepatic metabolism of drugs increase risk for ADRs in older adults (McLachlan et al. 2009; McLachlan and Pont 2012) but the determinants of these changes are not fully understood. One possible mechanism that may influence rates of drug metabolism in older adults is epigenetics (Seripa et al. 2015; Fisel et al. 2016; Kronfol et al. 2017). Aging is associated with substantial changes to the epigenome (Benayoun et al. 2015; Pal and Tyler 2016; Horvath and Raj 2018) and genes encoding drug metabolizing enzymes in human liver are under

epigenetic control (Bonder et al. 2014, Park et al. 2015). Furthermore, treatment with epigenetic drugs affects the metabolic capacity of cultured cells (Ruoß et al. 2019). These considerations led us to hypothesize that age-associated epigenetic changes at genes encoding drug metabolizing enzymes could affect rates of drug metabolism. Epigenome-wide association studies (EWAS) in human blood have found significant changes to DNA methylation at several genes encoding phase I (oxidative) drug metabolism enzymes with age (Heyn et al. 2012; Hannum et al. 2013; Horvath 2013; Steegenga et al. 2014; Reynolds et al. 2014; Marttila et al. 2015; Peters et al. 2015). However, the extent to which these age-related changes are present and affect enzymatic activity in the liver, the primary site of drug metabolism, is unclear. Therefore, the goal of this study is to identify age-related epigenetic changes at phase I genes encoding drug metabolizing enzymes in the liver and test if these epigenetic changes are associated with rates of drug metabolism. Due to the experimental control afforded and availability of the relevant tissue, we chose to conduct the experiments in mice.

To date, the number of published studies on epigenetics and drug metabolism in aging is limited. As a starting point to identify potential genes of interest, we reviewed published EWAS and genome-wide gene expression studies in human blood and chose the phase I drug metabolism genes showing the best empirical evidence of change with age. The rationale for using human blood studies to guide gene selection is because 1) the largest number of aging EWAS have been conducted in this tissue, 2) epigenetic aging effects are significantly correlated across tissues and species (Horvath 2013) and 3) consistent patterns of gene expression changes with age have been observed across several species (McCarroll et al. 2004). We identified two phase I drug metabolism genes, *CYP2E1* and *CYP1B1*, showing strong evidence for age-associated epigenetic changes in human blood. We mapped the associated regions in the human

genome to their homologous mouse regions and tested for epigenetic changes in mouse liver. Only *Cyp2e1* showed differential methylation with age. Based on these results, we focused on *Cyp2e1* and conducted a detailed analysis of regulation at this locus including assays for DNA methylation and histone post-translational modifications (PTMs) with reported associations with age (McClay et al. 2014; Dozmorov 2015). Finally, we investigated if these effects were associated with CYP2E1 metabolic function by isolating liver microsomes and applying Michaelis–Menten kinetics to determine the intrinsic clearance (CL_{int}) of the probe drug chlorzoxazone (CZ), which is predominantly metabolized by CYP2E1 (Lucas et al. 1999).

2.3. Methods

2.3.1. Mice: Liver tissue samples from 20 male CB6F1 mice (5 subjects in each of four age groups 4, 18, 24, and 32 months) were obtained from the National Institute on Aging (NIA) tissue bank.

2.3.2. DNA and RNA extraction: Genomic DNA was extracted using the AllPrep DNA/RNA kit (80204, Qiagen, Hilden, Germany) according to manufacturer's protocol. DNA and RNA purity and quantity were measured using a Nanodrop spectrometer (ThermoFisher, Waltham, MA).

2.3.3. Global 5-MethylCytosine (5mC) and 5-HydroxymethylCytosine (5hmC): Global 5mC and 5hmC levels were measured using ELISA colorimetric assays by MethylFlash kits (1030-96, 1032-96, Epigentek, Farmingdale, NY). 5mC- or 5hmC-specific antibodies, provided in the kit, were incubated with 100ng genomic DNA. Optical density at 450 nm was measured on a Synergy HT plate reader (BioTek Instruments, Winooski, VT). Known standards provided in the kit consisting of 0.1, 0.2, 0.5, 1, 2, and 5% for 5mC and 0.02, 0.04, 0.1, 0.2, 0.4, and 1% for 5hmC were also assayed. The optical density of liver samples was used to determine the percentage of 5mC and 5hmC of each sample by interpolation on respective standard curves. Each unknown and standard was run in duplicate.

2.3.4. Selection of genomic regions of interest: Aging EWAS findings for human blood were obtained from published studies (see Dozmorov 2015) and genes encoding drug metabolizing enzymes were obtained from the ADME (absorption, distribution, metabolism, and excretion) gene list from the pharmaADME consortium (pharmaADME.org), see **Table 2.1**. Significant findings by ADME gene were summed across studies and the top two phase I drug metabolism genes showing the most significant findings were selected for study.

Reference	Longevity Map (Human Ageing Genomic Resources)	Peters et al. 2015	Heyn et al. 2012	Hannum et al. 2013	Horvath 2013	Reynolds et al. 2014	Marttila et al. 2015	Steegenga et al. 2014	Total
	Exp	Exp	Meth	Meth	Meth	Meth	Both	Both	
Phase I genes									
CYP2E1	X	X			X			X	4
CYP1B1	X	X	X				X		4
CYP2J2		X		X					2
CYP1A1	X							X	2
ADHFE1		X			X				2
PDE3B		X				X			2
DHRS9		X					X		2
CYP2D6	X								1
CYP3A4									0

Table 2.1. Summary of human EWAS findings for phase I drug metabolism genes. Human ADME genes list from pharmaADME (www.pharmaadme.org) was contrasted on the top findings from EWAS and gene expression studies of normal aging in human blood DNA. Genes encoding phase I drug metabolizing enzymes that showed significant association in the top findings of these studies is marked with an “X”. The total number of studies were a specific gene is a top association in the reported results is shown as a total in the last column of the table. Exp: Expression, Meth: Methylation.

Genomic location of human age-associated Cytosine-phosphate-Guanine (CpG) positions were used to extract the homologous regions in mouse using the “convert” function in the University of California Santa Cruz (UCSC) genome browser (Kent et al. 2002). A complete list of the genomic coordinates of all investigated regions in mouse can be found in **Table 2.2**. An additional regulatory region around human *CYP2E1* was identified using the GeneHancer track (Fishilevich et al. 2017) on the UCSC genome browser (**Figure 2.1**). Data from the mouse Encyclopedia of DNA Elements (ENCODE) (Stamatoyannopoulos et al. 2012) and Ludwig Institute for Cancer Research (LICR) (Barrera et al. 2008) chromatin immunoprecipitation (ChIP) sequencing runs on young (8 weeks) male mouse liver tissue were used to identify two regions with high levels of histone 3 lysine 9 acetylation (H3K9ac) and histone 3 lysine 27 acetylation (H3K27ac) PTMs (GSM1000153, GSM1000140).

Gene	Primers (5' → 3')		Product size/coordinates/assembly	CpG count
	Forward Primer	Reverse Primer		
	High-Resolution Melt			
<i>Cyp2e1</i>	AATTAGTATTTTAGGTTAAGGGAGATGAGTGG	TCCCTTACCTTAATTAATAAACTTAAAAATATCCTTC	319/chr7:147,949,616-147,949,934/mm9	7
<i>Cyp1b1</i>	TGTTTTGTTGTATTAGGGTTTGGTGGATGG	CCTTTATATCCCAACATAACCACCAAC	350/chr17:80,113,318-80,113,667/mm9	21
	Chromatin Immunoprecipitation Quantitative Polymerase Chain Reaction			
<i>Cyp2e1</i>				
<i>Region 1</i>	ATGCTGAGCCAGCTGTGA	CCACATGCAAAGACAATCCT	145/ chr7:147,950,223-147,950,367/mm9	
<i>Region 2</i>	ATTTGCTGCCTAGCTGCTTC	CAGCACTCTGAGACCCAGT	119/ chr7:147,942,350-147,942,468/mm9	
<i>Gapdh</i>				
Positive control	AGAGAGGGAGGAGGGGAAATG	AACAGGGAGGAGCAGAGAGCAC	200/ chr6:125,115,604-125,115,803/mm9 ^a	
Negative control	CTCCAGATGCTGAGAGAAAAAC	AGGCATACCAAGCACAGAAA	100/ chr17:95,049,080-95,049,179/mm9	

Table 2.2. HRM and ChIP primers and qPCR product sequences. Primers used in the High-Resolution Melt and Chromatin Immunoprecipitation Quantitative Polymerase Chain Reaction assays with size of PCR product, genomic coordinates, and assembly with CpG count when appropriate. ^ablasted from Pace et al., 2018 to obtain coordinates

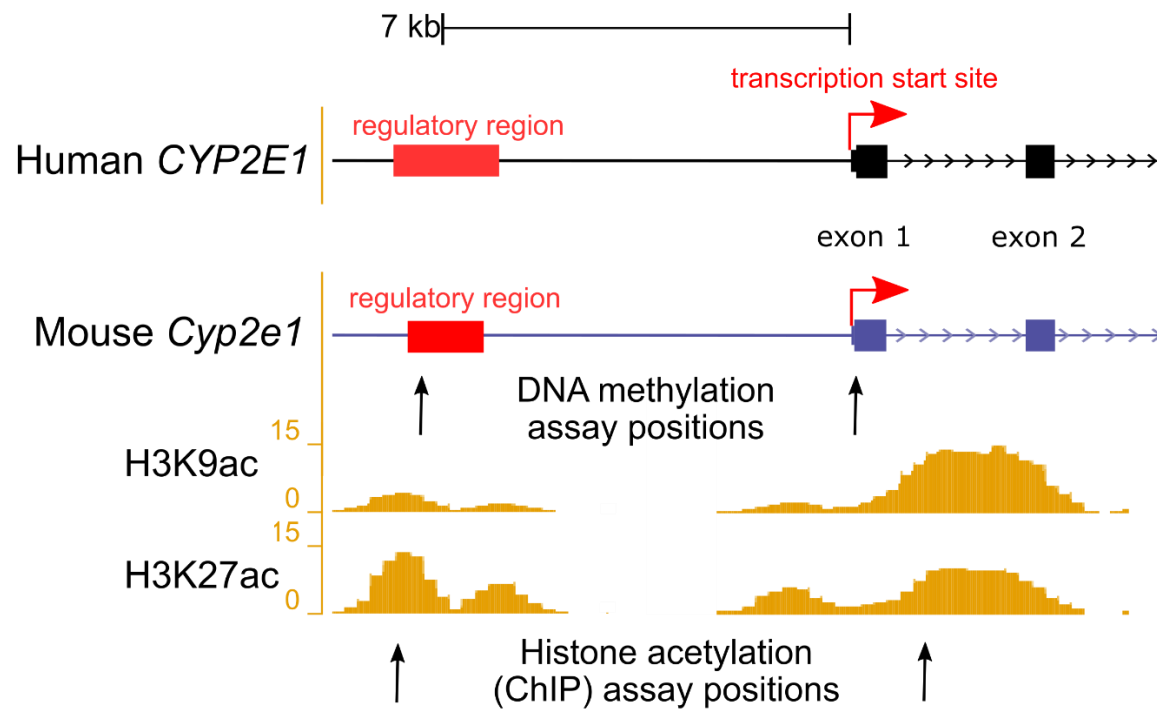


Figure 2.1 Illustration showing the transcription start site (TSS) and upstream regulatory regions of the human CYP2E1 and the homologous mouse Cyp2e1 gene. Upstream regulatory element positions were obtained from GeneHancer (Fishilevich et al. 2017) and ORegAnno (Lesurf et al. 2016). DNA methylation assays were conducted in the current study at both the TSS and upstream regulatory region in mouse at positions marked by the arrows. Reference histone 3 lysine 9 acetylation (H3K9ac) and histone 3 lysine 27 acetylation (H3K27ac) in 8-week-old mouse livers are from the ENCODE/LICR track in UCSC Genome Browser. Two loci with high liver histone acetylation levels were chosen for analysis using ChIP-qPCR in the current study, at positions marked by the arrows. For exact assay coordinates see **Table 2.2** and **Table 2.3**.

Region	<i>Cyp2e1</i> Region 1	<i>Cyp2e1</i> Region 2
Product size/coordinates/assembly	275/chr7:147,949,576-147,949,850/mm9	157/ chr7:147,942,437-147,942,593/mm9
Forward primer	5'GGGGGTAGGTTTTAATTTTTATAGAT3'	5'TTAGTATTTTTATTGGGGTTTTAGAGTG3'
Reverse primer	5'CGCCAGGGTTTTCCCAGTCACGAC ATCAACCTTTAAAATAATAACCAACTACA3'	5'CGCCAGGGTTTTCCCAGTCACGAC ATAACCTCCAAATCTAAACTTCTATTTAAC3'
Sequencing primer	5'ATTTTTATAGATTTGTTTTTAGATG3'	5'GTTGGAGTTAATGGGA3'
M13 primer ^a	5'biotin-CGCCAGGGTTTTCCCAGTCACGAC3'	
CpG count	7	1

Table 2.3. Pyrosequencing primer sequences. Primers used in the Pyrosequencing assays of region 1 and 2 with size of pyrosequenced PCR product, coordinates, and assembly with CpG count. ^aM13 primer sequence published in Royo et al. 2007.

2.3.5. Bisulfite conversion of genomic DNA and High-Resolution Melt (HRM) analysis:

200ng of liver genomic DNA was treated with sodium bisulfite according to the EZ DNA Methylation kit protocol (D5002, Zymo Research, Irvine, CA). Mouse genomic DNA of 5 and 85% methylation were used as standards (808063, 808064, EpigenDx, Hopkinton, MA). Ratios of the standard DNA were mixed at 5, 25, 45, 65, and 85% to create a standard curve. A negative (no template) control was also used per plate. High-Resolution Melt (HRM) assays using MeltDoctor HRM MasterMix (4409535, Applied Biosystems, Foster City, CA) on a Quantstudio 3 instrument were used to measure 5mC levels at LINE1 elements using the method of Newman et al. (2012) with minor modifications and at a 319 base pair region on the 5'UTR of mouse *Cyp2e1* (chr7:147,949,616-147,949,934, mouse genome assembly mm9 NCBI37/ build 9, July 2007) encompassing 7 CpGs (**Table 2.2**). For *Cyp2e1*, samples were amplified by qPCR as follows 10min hold at 95°C followed by 40 cycles of: 15sec at 95°C, 30sec at 57°C and 30 sec at 72°C, followed by a final extension at 72°C for 7 min and a melt curve stage with temperature range of 57°C to 95°C with fluorescence capture at 0.025 degrees per second increment. Each reaction included 20ng bisulfite-converted DNA and final concentration of 1X MeltDoctor HRM MasterMix (Applied Biosystems), 0.2μM forward and 0.2μM reverse primer (**Table 2.2**).

HRM LINE1 assay was performed as described previously (Newman et al. 2012) with slight adjustments. MeltDoctor HRM MasterMix (Applied Biosystems, Foster City, CA) on a Quantstudio 3 instrument was used to measure 5mC levels at the 193 base pair LINE1 region reported in Newman et al encompassing 11 CpGs. Samples were amplified by qPCR as follows 10min hold at 95°C followed by 45 cycles of: 15sec at 95°C, 60sec at 60°C, followed by a melt curve stage with temperature range of 60°C to 95°C. Each reaction included 20ng bisulfite-converted DNA and 0.75μM each of unmethylated forward and reverse primer (Newman et al.

2012) in 1X MeltDoctor HRM MasterMix. Standards of 0, 25, 50, 75, 100% methylation (EpigenDx, Hopkinton, MA) were run in duplicate while the liver samples were run in triplicate. The NTS values (Newman et al. 2012) of the liver samples were interpolated on the standard curve to yield their 5mC percentage.

2.3.6. Gene expression analysis by reverse transcription – quantitative PCR (RT-qPCR):

For each sample, 1µg of total liver mRNA was reverse transcribed to cDNA by iScript kit according to manufacturer's protocol (1708891, Bio-Rad, Hercules, CA). Aliquots of cDNA were amplified in triplicate using final concentration of 1X TaqMan master mix (4369016, Applied Biosystems) and 1X TaqMan *Cyp2e1* Mouse Gene Expression Assay (Mm00491127_m1, ThermoFisher) (Martinez et al. 2010; Koh et al. 2011). qPCR conditions were as follows 40 cycles of 15 sec at 95°C and 60 sec at 60°C. Mouse *Gapdh* endogenous control was also assayed in triplicate (Mm99999915_g1, ThermoFisher) (Scarzello et al. 2016; Wilhelm et al. 2016; Jia et al. 2018). A 1:2 serial dilution of control cDNA was used to generate a 5-point standard curve. Quantification cycles (C_q) were determined using the Relative Quantification application on the ThermoFisher Cloud. Normalized quantification cycles (ΔC_q) were obtained by subtracting the mean *Gapdh* C_q from the mean *Cyp2e1* C_q . $\Delta\Delta C_q$ was calculated for each age group by subtracting the ΔC_q of the 4 months (youngest age group as reference) from each of the other age group's ΔC_q to calculate fold differences.

2.3.7. Western Blots: Cell protein lysates were created from homogenization of 20mg liver tissues in 200µL Pierce RIPA buffer (89900, Thermo Fisher, Waltham, MA) with final concentration of 1% v/v (2 µL) Halt Protease Inhibitor buffer (78430, Thermo Fisher, Waltham, MA). The Pierce BCA assay (23227, Thermo Fisher, Waltham, MA) was used to measure protein concentrations using manufacturer's standard protocol. Absorbance at 562nm was

measured on a Synergy HT plate reader and the unknown protein concentration was determined by interpolating absorbance of unknown samples on an 8-point standard curve created from diluted albumin standards.

10 μ g of total protein in 30 μ L β -Mercaptoethanol (β ME)-Laemmli buffer (1610710, 1610747, Bio-Rad) were separated on 10% Mini-PROTEAN precast SDS-PAGE gels (4568033, Bio-Rad) at constant 200V for 35min and transferred onto PVDF membrane using a TransBlot Turbo (1704150, Bio-Rad) at 1.3A for 5 min. Membranes were blocked for 30 min in 5% milk in 1X TBST (Tris Buffered Saline, Tween20). Blots were probed using anti-CYP2E1 primary antibody (1:2500, ab28146, Abcam) in 10mL 5% Milk in 1X TBST at 4°C overnight and washed three times with 1X TBST the next day. The blots were incubated with HRP-coupled rabbit IgG secondary antibody (1:10000, Cell Signaling, Danvers, MA) and 0.5 μ L Precision Protein StrepTactin-HRP conjugate (Bio-Rad) for 1hour at RT in 10mL 5% Milk in 1X TBST. Membranes were washed five times with 1X TBST. Blots were treated with 2mL Clarity Western ECL (1705060, Bio-Rad) at 1:1 clarity western luminol enhancer: peroxide solution ratio to start chemiluminescence and imaged 2min afterwards on the ChemiDoc Touch (Bio-Rad). Blots were washed with 1X TBST and stripped for 30min using Restore stripping buffer (21059, Thermo Fisher). After stripping, the membrane was incubated with GAPDH primary antibody (1:5000, MA5-15738, Thermo Fisher) and then mouse IgG secondary antibody (1:20000, 7076S, Cell Signaling, Danvers, MA). The bands were visualized at 49 and 37 kDa for CYP2E1 and GAPDH respectively using Image Lab software v 6.0 (Bio-Rad, Hercules, CA). For each sample, CYP2E1 band intensity were normalized to GAPDH.

2.3.8. Chromatin Immunoprecipitation Quantitative Polymerase Chain Reaction (ChIP-qPCR): 80 mg of mouse liver was minced into 1 mm³ fragments with -20 C precooled scalpel and transferred to 2mL Eppendorf tube. TruChIP tissue shearing kit (520237, Covaris, Woburn, MA) was used to prepare sheared chromatin. Centrifugations were at 200g for 5 min at 4°C unless otherwise noted. The minced tissue was washed with 1 mL 1X cold PBS and centrifuged at 200g for 5min at 4°C. The supernatant was discarded and 1mL of fixing buffer A was used to resuspend the pellet. 100µL of freshly prepared 11.1% methanol-free formaldehyde (1% final concentration) was added and the fixation was quenched after 2 min with 58µL quenching buffer E. The suspension was centrifuged, and the supernatant discarded. Pellet was washed twice with 1mL 1X cold PBS and centrifuged. Pellet was transferred to tissueTUBE (TT05M XT) provided in the kit and flash frozen in liquid nitrogen for 45sec and pulverized into powder by a precooled pestle. Pulverized tissue was transferred by inverting to a screwed-on milliTUBE-2mL and stored at -80°C until nuclei separation and shearing step the next day. Pulverized tissue was transferred to a 2mL Eppendorf tube using two successive transfers by 500µL lysis buffer B. The 2mL tube was incubated on a rotor at 4°C for 20min to complete lysis. Nuclei were pelleted by centrifugation at 1700g for 5min at 4°C. Supernatant was discarded and pellet was resuspended in 1mL wash buffer C and incubated on a rocker for 10min at 4°C. Nuclei were pelleted again at 1700g for 5min at 4°C and supernatant discarded. Pellet was resuspended with 1mL wash buffer C and centrifuged at 1700g for 5min at 4°C. Pellet was resuspended with 1mL shearing buffer D2 and sheared on M220 (Covaris, Woburn, MA) for 8min at 75 PIP, 10% duty factor, 200CPB, 7C set point temperature (4/10 Min/Max), and no degassing. Time course trials were conducted to determine optimal shearing (2-20 min) and fixation times (2 and 5 min) of 8 and 2 min respectively which yielded the highest percentage (>75%) of fragment sizes between 150 and

700 bp and the lowest percentages (<25%) of fragment sizes less than 150 and higher than 701 bp combined. Shearing and fixation time course trials were analyzed on the Agilent 2100 Bioanalyzer using the Agilent DNA 12000 chip on Agilent 2100 expert software. 25 μ L of sheared chromatin was incubated with 1 μ L 10mg/ml RNase (EN0531, Thermo Fisher, Waltham, MA) at 37°C for 30min, then it was treated with 4 μ L 10mg/ml Proteinase K (17916, Thermo Fisher, Waltham, MA) at 65°C overnight (16 hours). DNA was purified using QIAquick PCR purification Kit (Qiagen, Hilden, Germany). The concentration of eluted DNA was measured on Qubit 4.0 fluorometer and used to calculate the volume required to have 2 μ g sheared chromatin as starting material for the Chromatin immunoprecipitation (ChIP) step (1:1 ratio of DNA to chromatin was used to calculate chromatin concentration). The sheared chromatin was diluted 1:2 with 3X Covaris IP dilution buffer in order to decrease final SDS concentration to 0.083% and prevent SDS interference with epitope and antibody binding.

Each ChIP had 2 μ g of sheared chromatin. 2% of the volumes of sheared chromatin per IP was set aside at 4°C as input control and was not processed through ChIP step. ChIP was carried out by incubating 5 μ L of H3K9ac (39137, Active Motif, Carlsbad, CA), or 5 μ L of H3K27ac (39133, Active Motif, Carlsbad, CA), or 5 μ L of Rabbit IgG (ab171870, Abcam) with 2 μ g sheared chromatin from each sample overnight (16 hours) at 4°C. Hence, three worth of ChIP volumes were used from each sample. The formed complex was incubated with 50 μ L Dynabeads Protein G (10003D, Thermo Fisher, Waltham, MA) for 4 hours at 4°C. The bead linked complex was inserted on the DynaMag (Thermo Fisher, Waltham, MA) magnet rack for 2 min and the supernatant discarded. The bead coupled complex was removed from the magnet and washed 3 times with 500 μ L with cold 0.05X Tween 20 in PBS PH7.4 (10010023, Thermo Fisher, Waltham, MA) for 3 min each at room temperature on HulaMixer (Thermo Fisher,

Waltham, MA). Finally, 50 μL of IP elution buffer (Aq. 1% SDS, 0.1 M NaHCO_3 , pH 9.0) was added to the bead coupled complex and incubated on a heat block for 1 hour at 65°C with 15sec vortexing every 15 min. The samples were then inserted back on the DynaMag for 2 min and 50 μL of the supernatant was transferred to a 96 well PCR plate. The input control was diluted 1:2 with 3X Covaris IP dilution buffer to mimic the dilution done to the samples and preserve its percentage (2%). The ChIP'ed samples and their input controls were incubated each with 2 μL RNase for 30 min at 37°C and then 8 μL of Proteinase K was added and incubated overnight (16 hours) at 65°C . The next day, DNA was purified using QIAquick PCR purification kit (Qiagen, Hilden, Germany) to final elution volume of 50 μL . 2 μL of each DNA elution (H3K9ac, H3K27ac, IgG, and input control) per sample was used per qPCR reaction.

Each ChIP'ed DNA was amplified in triplicate using PowerUp SYBR Green (A25742, Applied Biosystems), with 0.2 μM of forward and reverse primers (**Table 2.2**) as follows: 2min at 50°C , 2min at 95°C followed by 40 cycles of: 15sec at 95°C , 30sec at 59°C and 1min at 72°C , followed by melt curve stage. This stage is as follows: 15sec hold at 95°C followed by 1min hold at 59°C and then the continuous fluorescence acquisition starts while increasing the temp by $0.15^\circ\text{C}/\text{s}$ to end at 95°C followed by a 15sec hold at 95°C . Primer specificity and efficiency were tested on 2% agarose gel and a 5-point 1:2 serial dilution standard curve respectively. No secondary amplification or primer dimers were detected indicating primer specificity. A singular melt peak was shown by the qPCR melt curves indicating formation of a single product. Primer efficiency outside of accepted ranges [90-110] were discarded until reaction conditions were optimized. Cq values for each plate were downloaded and the mean threshold cycle (Cq) obtained for each sample and normalized to the dilution factor ($2\%=1/50$) corrected Cq value ($\text{Log}_2(50)=5.6438$) of the input control to obtain ΔC_q . The percentage of input was calculated

by multiplying 100 with 2 raised to the exponent of Delta Cq. For each sample, three “percentage of input” values were obtained and are H3K9ac, H3K7ac, and IgG.

2.3.9. Pyrosequencing: Quantitative methylation measures of individual CpGs were assessed with Pyrosequencing of bisulfite converted DNA (Tost et al. 2003). Primers targeting the loci of interest were designed with PyroMark Assay Design version 2.0.1.15 (Qiagen) (see **Table 2.3** for details). The first pyrosequencing assay amplified a 257 base pair product at *Cyp2e1* 5'UTR (chr7:147,949,576-147,949,850/mm9) that encompasses 7 CpGs (Position 2-8) chr7: 147,949,679 - 147,949,684 - 147,949,743 - 147,949,754 - 147,949,770 - 147,949,791 - 147,949,806, mm9. The second assay amplified a 157 base pair product at *Cyp2e1* promoter (chr7:147,942,437-147,942,593, mm9) that encompass 1 CpG (Position 1) chr7: 147,942,492, mm9. Amplification was performed using the PyroMark PCR Kit (978703, Qiagen) and the vendor specified program for bisulfite converted DNA. The final concentrations in the PCR reaction mixture as follows: 1x PyroMark PCR Master Mix, 1x CoralLoad Concentrate, 1.5mM MgCl₂, 1x Q-Solution, 10 ng of bisulfite modified genomic DNA, and 0.2μM of Forward, 0.2μM Reverse, and 0.2μM biotinylated M13 (Royo et al. 2007) primers (**Table 2.3**). 2μL of the PCR product was separated by 2% agarose gel electrophoresis to confirm correct product size and absence of primer dimers and secondary amplification. The 2% agarose gel was made with the following ratio to obtain 0.75mm thickness in the Owl EasyCast B2 Mini Gel Electrophoresis System cast (Thermo Fisher Scientific, Waltham, MA): 2.52 g of agarose powder (BP2410-100, Fisher Scientific, Hampton, NH) and 1.89 μL ethidium bromide (BP1302-10, Fisher Scientific, Hampton, NH) in 126 mL 0.5X Tris-Borate-EDTA (TBE) buffer (95:5, H₂O:10XTBE (BP1333-4, Fisher Scientific, Hampton, NH)) mixed until complete gelling of agarose. The gel was poured onto cast and let to solidify for 30 min at RT. The cast was filled with 400 μL 0.5X TBE buffer.

Each gel had 2 μ L of 100 bp DNA ladder in the first and last well of the gel. The gel was run on constant voltage of 100V for 1 hour. The gel was imaged on ChemiDoc Touch (Bio-Rad, Hercules, CA) using default settings of auto optimal exposure for ethidium bromide stained gels.

Next, 5 μ L of PCR amplicon were bound with 2 μ L to Streptavidin Sepharose beads (45-000-279, Fisher, Hampton, NH) by shaking for 5 min in 40 μ L Binding buffer (979006, Qiagen, Hilden, Germany) and 33 μ L of molecular biology grade water. The complex was transferred to a 96-well HS plate (979101, Qiagen, Hilden, Germany) containing 12 μ L per well of final concentration of 0.3 μ M of sequencing primer in Annealing buffer (979009, Qiagen, Hilden, Germany) on the PyroMark Q96 vacuum preparation station. The HS plate was inserted on the PyroMark Q96 MD and the PyroMark Gold Q96 reagents (972804, Qiagen, Hilden, Germany) were used for each assay to sequence the PCR product. Each pyrosequencing assay was run duplicate for each sample. A standard consisting of 0, 5, 10, 25, 50, 75, and 100% methylated mouse genomic DNA was included on each plate (808060M, EpigenDx, Hopkinton, MA). Both the standard and the liver test samples were pyrosequenced in duplicates.

2.3.10. CYP2E1 intrinsic clearance: Mouse Liver Microsomes (MLM) were prepared as described previously (Knights et al. 2016). 500 mg of liver tissue was homogenized using the Fisher 150 homogenizer (15340167, Fisher Scientific) on high speed in cold 10 mL microsome preparation buffer (10 mM potassium phosphate, pH 7.4, 1.15% (w/v) potassium chloride) 5 times for 30 sec each with 30 sec breaks in between on ice and centrifuged at 700g for 10 min and 10,000g for 10min at 4°C on the Optima I-90K ultracentrifuge using the SW41 rotor. The supernatant was ultracentrifuged at 100,000g for 75min at 4°C and the microsome pellet transferred to a precooled 5mL Potter-Elvehjem grinder, ground for 1 min at low speed with 10 strokes, transferred back into microsome preparation buffer, and the ultracentrifugation and

grinding steps repeated. The suspension containing the microsomes was stored at -80°C . $10\mu\text{L}$ of the microsome suspension was used to measure microsomal protein concentration by the microplate procedure of the BCA assay (23227, Thermo Fisher).

Standards for CZ and 6-OH-CZ (18869, 10009029, Cayman Chemical, Ann Arbor, MI) were purchased. Chromatographic separation was achieved using an Agilent 1100 series HPLC (Agilent Technologies, Santa Clara, CA) system equipped with PerkinElmer series 200 degasser and auto injector (PerkinElmer, Waltham, MA) and C18 BDS hypersil 50 mm x 4.6 with $5\mu\text{m}$ particle size (28105-054630, ThermoFisher) column. Diode array detector was used to monitor the depletion of CZ and the formation of 6-OH-CZ at the wavelengths 280 and 299 nm for CZ and 6-OH-CZ respectively. Isocratic gradient elution was used with the initial mobile phase being 85% aqueous (2% acetic acid (BDH20108.292, VWR, Radnor, PA) and 1% triethylamine (A12646 Alfa Aesar, Tewksbury, MA), v/v) and 15% methanol (A452-4, Fisher Scientific) (Table 2.4).

Chromatographic conditions		
Column	BDS Hypersil C18 (50 x 4.6 mm, $5\mu\text{m}$)	
Column temperature	35 $^{\circ}\text{C}$	
Flow rate	1.0 mL/min	
Wavelength	CZ at 280 nm, 6-OH-CZ at 299 nm	
Injection volume	80 μL	
Run time	6.5 min	
Time (minute)	A (%)	B (%)
0	85	15
1.5	85	15
1.6	75	25
5	75	25
5.1	85	15

Table 2.4. HPLC parameters. Chromatography parameters of the isocratic gradient co-elution and detection method of Chlorzoxazone and 6-hydroxychlorzoxazone. A is the aqueous mobile phase (2% acetic acid and 1% trimethylamine v/v). B is organic mobile phase (HPLC grade methanol).

Total run time was 6.5 min with retention times of 1.86 and 5.17 min for 6-OH-CZ and CZ respectively. Linear standard curves with $R^2 \geq 0.999$ were obtained from 0.47-240 μM for 6-OH-CZ and 2.34-1200 μM for CZ (Figure 2.2 and 2.3).

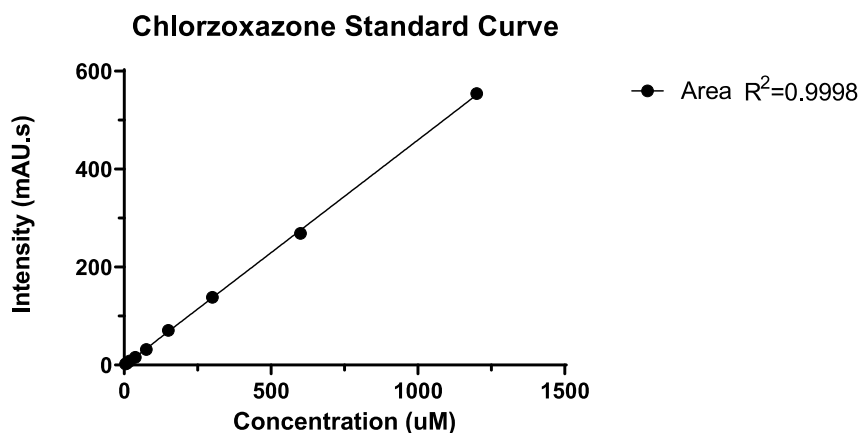


Figure 2.2 Chlorzoxazone standard curve. High performance liquid chromatography coupled with Ultraviolet detection method linearity for parent probe drug Chlorzoxazone. Linear range established at 2.34-1200 μM . Scatter plot with linear regression line of peak area intensity (mAU.s) against chlorzoxazone concentration (μM).

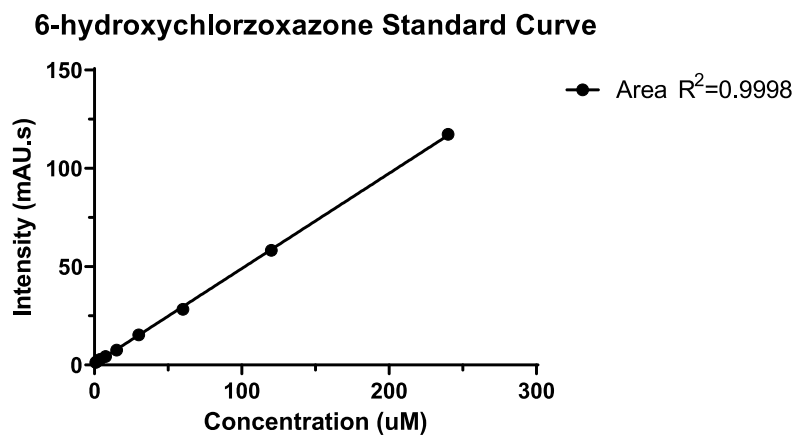


Figure 2.3 6-hydroxychlorzoxazone standard curve. High performance liquid chromatography coupled with Ultraviolet detection method linearity for metabolite 6-hydroxychlorzoxazone. Linear range established at 0.47-240 μM . Scatter plot with linear regression line of peak area intensity (mAU.s) against 6-hydroxychlorzoxazone concentration (μM).

Hydroxylation of chlorzoxazone (CZ) to 6-hydroxychlorzoxazone (6-OH-CZ) was measured to determine the catalytic activity of CYP2E1. Linearity of metabolite formation with time and MLM protein concentration established (**Figure 2.4** and **2.5**). The final concentrations in the metabolic reactions were 50 mM potassium phosphate buffer pH 7.4, 10 mM MgCl₂, 1 mg/ml MLM protein, 1 mM EDTA (E4884, Sigma, St. Louis, MO), 1mM NADPH (AK1395, AkronBiotech, Boca Raton, FL), 0.5% DMSO (16785, Acros Organics), with incubation time of 25 min at 37 °C. The final concentration of DMSO in each reaction was maintained at 0.5%. Each MLM sample was run in 8 MLM reactions that vary by the final concentration (10, 20, 40, 80, 160, 320, 640, 1000 μM) of the parent probe drug (CZ) to determine Michaelis-Menten kinetic constants. The reaction was stopped with equal volume (150μL) of HPLC grade methanol (A452-4, Fisher Scientific, Hampton, NH) and centrifuged for 10 min at 20,000g at room temperature. The supernatant was transferred to 96-well plate and 80 μL was injected into the High-Performance Liquid Chromatography (HPLC) system.

Reaction rates (pmol/min/mg protein) of 6-OH-CZ formation were plotted against CZ concentration (μM), and K_m and V_{max} values were estimated by GraphPad Prism using equation 1 (Eq1), where Y is the reaction rate (pmol/min/mg protein), X is CZ concentration (μM), V_{max} is the maximal reaction rate of 6-OH-CZ formation (pmol/min/mg protein), and K_m is CZ concentration at half maximal rate (μM). Eq1. $Y = V_{max} * X \div (K_m + X)$

Intrinsic clearance (CL_{int}) is the enzyme-mediated activity toward a drug that would occur at concentration below K_m without physiological limitations such as hepatic blood flow (Houston 1994). CL_{int} by CYP2E1 for the hydroxylation reaction was calculated according to equation 2 (Eq2). Eq2. $CL_{int} = V_{max} \div K_m$

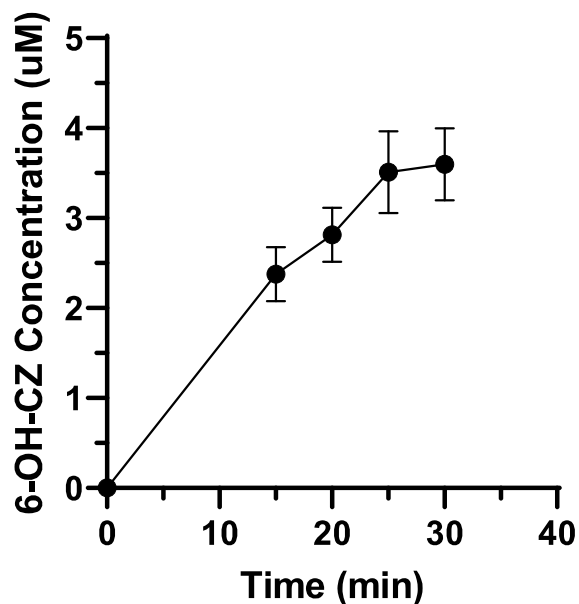


Figure 2.4 Metabolite formation against time plot. Line plot of 6-hydroxychlorzoxazone (6OH-CZ) concentration (μM) against tested total microsomes reaction time (min). $n=3$ for each time point.

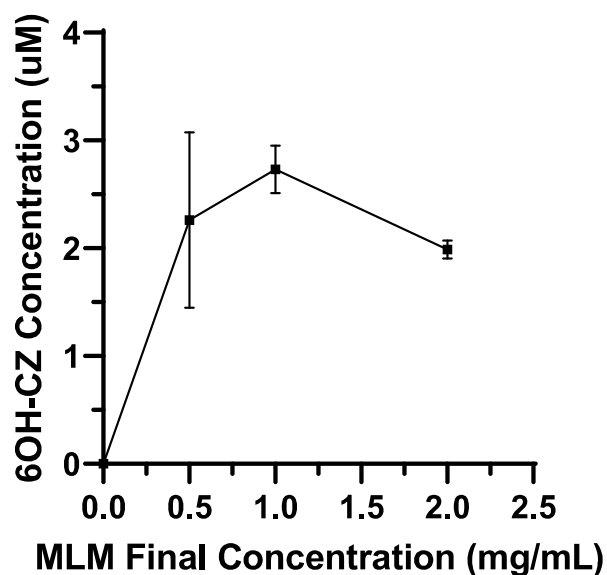


Figure 2.5 Metabolite formation against microsomes protein plot. Line plot of 6-hydroxychlorzoxazone (6OH-CZ) concentration (μM) against tested final Mouse Liver Microsomes (MLM) total protein concentration (mg/mL). $n=3$ for each concentration.

2.3.11. Statistics: Linear regression and Pearson correlation tests were conducted in R version 3.6.1 (www.r-project.org) with $\alpha=0.05$. Beta values (β) and Pearson correlation coefficients (r), are reported. β indicates the degree of change in the outcome variable for every unit change in the predictor variable, while r indicates the degree of association found in the correlation test. Replicates beyond 2 standard deviations from the mean of any of the assays were discarded.

2.4. Results

2.4.1. Global epigenetic effects in aged mouse liver

DNA and RNA extractions from the mouse liver samples were successful with an average 260/280 value of 1.94 [1.8-2.1] for DNA and 2.05 [1.94-2.1] for RNA. Prior to locus-specific analysis, we first assayed age-associated changes to the global abundance of epigenetic marks in mouse liver. Using ELISA assays, we observed a significant decrease in global abundance of 5mC ($\beta=-0.011$, $SE=0.004$, $p=0.024$) and 5hmC ($\beta=-0.001$, $SE=0.0004$, $p=0.002$) (**Figure 2.6** a, b). This translates to approximately 50% reduction in the 32months age group compared to the 4 months group for both modifications (0.6% v 0.32% for 5mC and 0.1% v 0.06% for 5hmC). We also measured 5mC at LINE1 elements using High-Resolution Melt (HRM) analysis of bisulfite converted DNA (**Figure 2.7** and **2.8**). We observed a significant decrease in abundance of 5mC at LINE1 elements with increasing age in our sample ($\beta= -2.062$, $p= 1 \times 10^{-8}$), with an average reduction of 2% methylation per month of age. These results demonstrated that, in a broad sense, epigenetic changes were occurring with age in this study's liver samples.

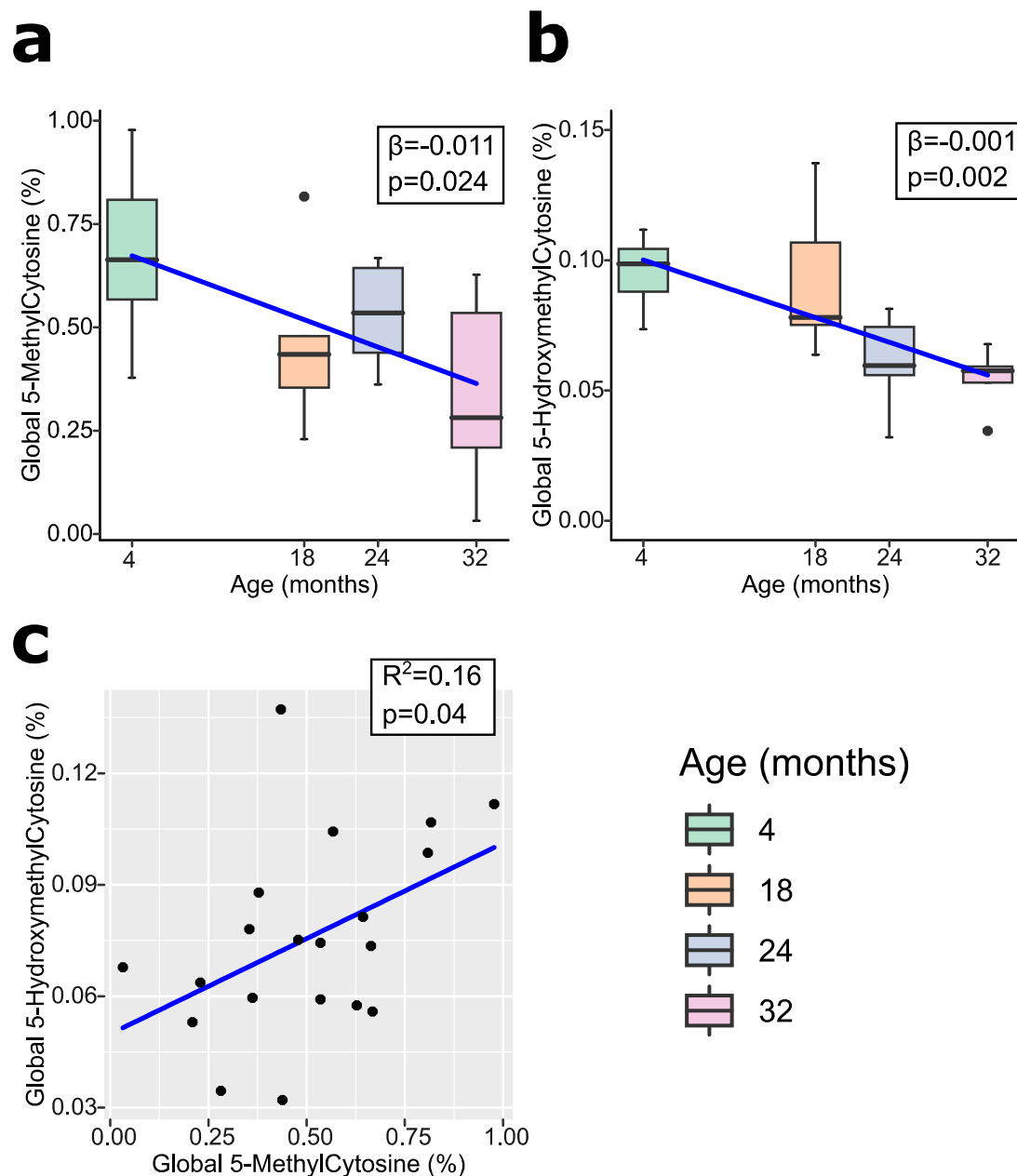


Figure 2.6 Box plots with regression line (blue) of Age-Associated changes to global (a) 5-MethylCytosine (n=20), (b) 5-HydroxymethylCytosine (n=20). Data represent median (middle hinge), 25% (lower hinge) and 75% (upper hinge) quantile. Data points beyond upper or lower $1.5 \times$ Inter Quantile Range are represented as individual black dots. (c) Scatter plot of 5-MethylCytosine and 5-HydroxymethylCytosine with regression line (blue) (n=20)

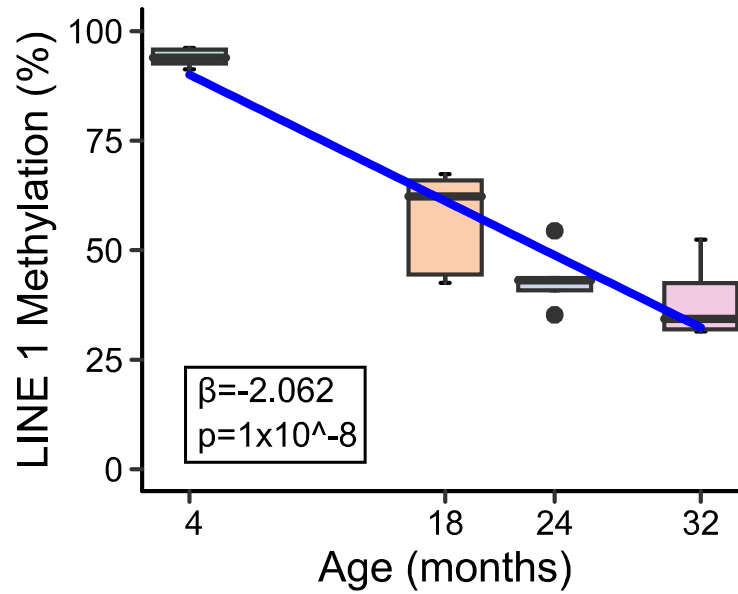


Figure 2.7 LINE 1 methylation percentage per age. Box plots with regression line (blue) of age-associated changes to LINE 1 methylation percentage (n=20). Data represent median (middle hinge), 25% (lower hinge) and 75% (upper hinge) quantile. Data points beyond upper or lower 1.5 * Inter Quantile Range are represented as individual black dots.

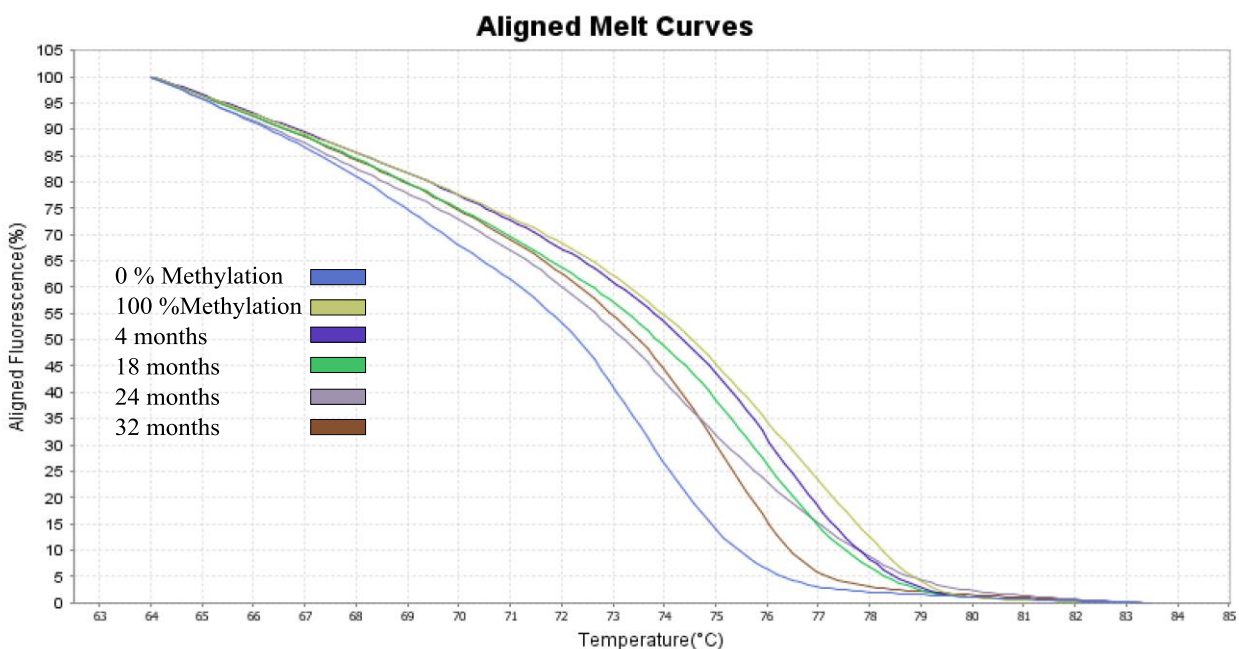


Figure 2.8 Representative melt curves per age. Aligned melt curve from the LINE-1 High-Resolution Melt assay showing representative curves for ages 4, 18, 24, and 32 months. Melt curves of the 0 and 100 % methylation standard are shown for reference.

2.4.2. Age-associated changes to *Cyp2e1* 5'UTR methylation and gene and protein expression

We reviewed published EWAS and genome-wide gene expression studies of aging in human blood (**Table 2.1**) and identified *CYP2E1* and *CYP1B1* as the phase I drug metabolism genes showing most evidence for age-associated changes. We mapped the human age-associated differentially methylated regions from EWAS to their homologous mouse regions and tested for epigenetic changes at these loci in our aged mouse liver samples. The human *CYP2E1* region mapped to the mouse *Cyp2e1* 5'UTR (**Figure 2.1**) and HRM analysis revealed that methylation at this locus increased significantly with age in mouse liver DNA ($\beta=1.3$, $SE=0.0038$, $p=0.002$) (**Figure 2.9 a**). However, no changes to *Cyp1b1* methylation were observed with age (**Figure 2.10**) so we focused on *Cyp2e1*.

The observed *Cyp2e1* 5'UTR methylation increase with age corresponds to a 1.3% increase in methylation per month of increased age. In tandem, *Cyp2e1* gene expression decreased significantly with age in the same samples ($\beta= -0.03$, $SE=0.011$, $p=0.01$) (**Figure 2.9 b**). Using the 4 months group as reference, we observed a 2.15% reduction in expression of *Cyp2e1* per month of increased age. Furthermore, we observed a significant decrease of CYP2E1 protein expression with age, as measured by change in chemiluminescence detected in Western blot ($\beta=-4.0e+5$, $SE=0.01$, $p=0.02$) (**Figure 2.9 c**).

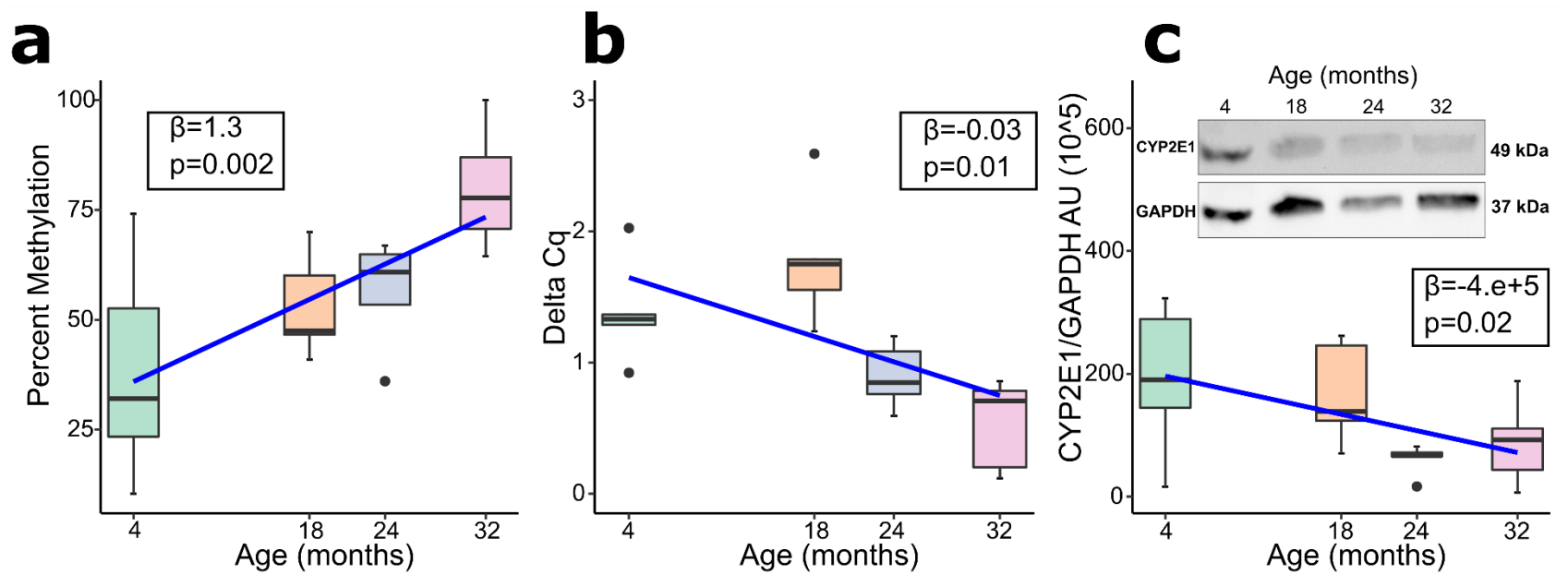


Figure 2.9 Box plots with regression line (blue) of Age-Associated changes to *Cyp2e1* (a) 5'UTR percent methylation (n=19), (b) gene expression (n=20). (c) Box plot of Age-Associated changes to *Cyp2e1* protein expression with representative western blot (n=20). Data represent median (middle hinge), 25% (lower hinge) and 75% (upper hinge) quantile. Data points beyond upper or lower 1.5 * Inter Quantile Range are represented as individual black dots

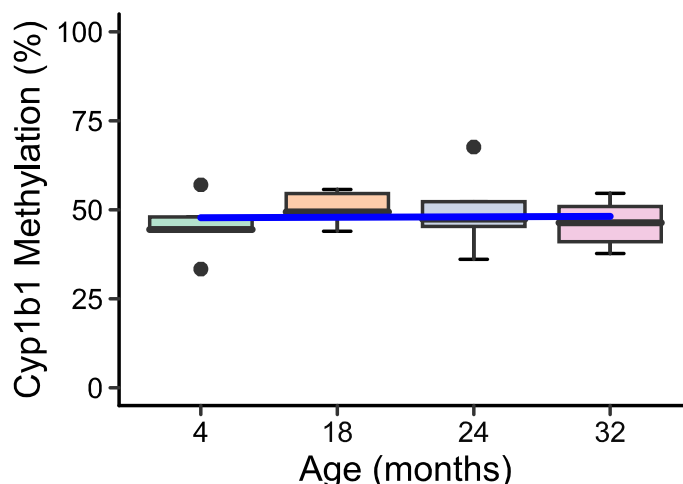


Figure 2.10 *Cyp1b1* 5mC with age. Boxplot showing no changes to methylation at *Cyp1b1* as age increases from 4 to 32 months.

2.4.3. Base-resolution 5mC analysis of *Cyp2e1* 5'UTR and upstream regulatory region

Having established that DNA methylation changes were occurring with age at the *Cyp2e1* 5'UTR, we aimed to obtain a fuller picture of *Cyp2e1* epigenetic regulation. Our first priority was to assay 5mC levels at each of the seven CpGs in the 5'UTR region individually, in contrast to the aggregate measure obtained via HRM. We also identified an upstream regulatory region in human *CYP2E1* (**Figure 2.1**) that we used to obtain the homologous region in mouse that harbored a single CpG. Therefore, we subjected both regions to bisulfite pyrosequencing that allows highly quantitative methylation measurements at single-base resolution. This revealed that the single CpG in the upstream regulatory region (position 1, chr7: 147,942,492, mm9) was significantly hypermethylated with age ($p=0.023$, **Figure 2.11** a & b, position 1). Pyrosequencing further confirmed the methylation increases at the 5'UTR with age observed via HRM (**Table 2.5**), with all individual CpGs showing significant increase in methylation with age (**Figure 2.11** a & b, positions 2 through 8). The CpG at position 5 (chr7: 147,949,754, mm9) was

the most significantly hypermethylated ($p=0.007$) with the largest beta value of 0.84% increase per month of age (**Figure 2.11 b**).

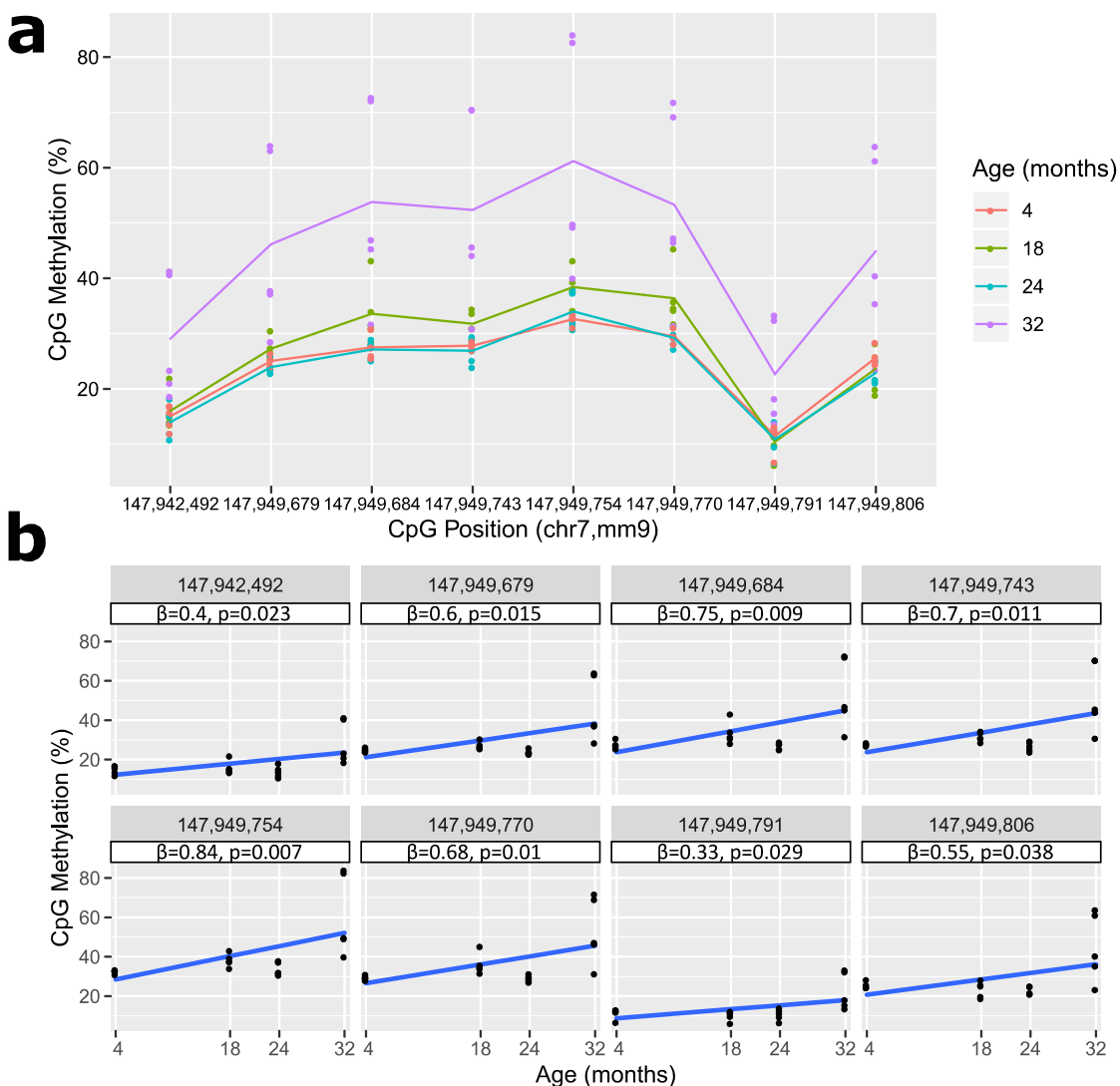


Figure 2.11 Pyrosequencing data for *Cyp2e1*. (a) Scatter plot of percent methylation of Cytosine-phosphate-Guanine (CpG) and all investigated CpG positions with superimposed line plot for each age group connecting the average methylation percentage at each CpG ($n=20$ per CpG, $N=80$ total). X-axis not drawn to scale. chr 7 = chromosome 7; mm9 = mouse genome assembly NCBI37/ build 9, July 2007. (b) Scatter plot of CpG methylation and age of individual CpG positions with regression line and statistics under each location. A simple linear regression

was performed on all 20 data points for each CpG (n=20) against each age 4, 18, 24, and 32 months (N=80). Position 1-8: chr7: 147,942,492-147,949,679 - 147,949,684 - 147,949,743 - 147,949,754 - 147,949,770 - 147,949-791 - 147,949,806, mm9.

Pyrosequencing Methylation	High Resolution Melt Methylation	
	Pearson r	p-value
Pos1	0.5106	0.0013
Pos2	0.4909	0.0003
Pos3	0.5122	0.0015
Pos4	0.4859	0.0002
Pos5	0.5224	0.0007
Pos6	0.5185	0.0011
Pos7	0.3985	8.58E-08
Pos8	0.4035	6.49E-06

Table 2.5. Pyrosequencing and HRM 5mC correlation. Pearson correlation test result rho (r) and p-value of each CpG methylation values investigated by Pyrosequencing and the High-Resolution Melt (HRM) methylation result of the 5'UTR region of *Cyp2e1*. The pyrosequencing assays confirmed the HRM data with all CpG positions positively correlated with HRM methylation. Pos 1-8: Position 1-8 chr7: 147,942,492-147,949,679 - 147,949,684 - 147,949,743 - 147,949,754 - 147,949,770 - 147,949-791 - 147,949,806, mm9.

2.4.4. Histone acetylation analysis of *Cyp2e1* 5'UTR and upstream regulatory region

We viewed publicly available mouse ChIP-Seq data (GSM1000153, GSM1000140) in UCSC genome browser to identify two regions neighboring and/or overlapping the 5' UTR and the upstream regulatory region that showed high histone 3 lysine 9 acetylation (H3K9ac) and histone 3 lysine 27 acetylation (H3K27ac) occupancy rates in young mouse liver (**Figure 2.1**). To assay histone acetylation levels in these regions, we used chromatin immunoprecipitation coupled to quantitative PCR (ChIP-qPCR). We observed a significant increase in H3K9ac at *Cyp2e1* intron 1, adjacent to the 5'UTR (Region 1, chr7:147,950,223-147,950,367, mm9) ($\beta=0.133$, SE=0.06, p=0.044) and at the upstream regulatory region (Region 2, chr7:147,942,350-147,942,468, mm9) ($\beta= 0.194$, SE=0.08, p=0.041) when regressing ChIP-qPCR percentage of input on age (**Figure 2.12**). This corresponds to a 0.133% and 0.194% increase in H3K9ac per month of increased age at each site, respectively. However, H3K27ac levels were stable with age at both regions of *Cyp2e1* in this sample.

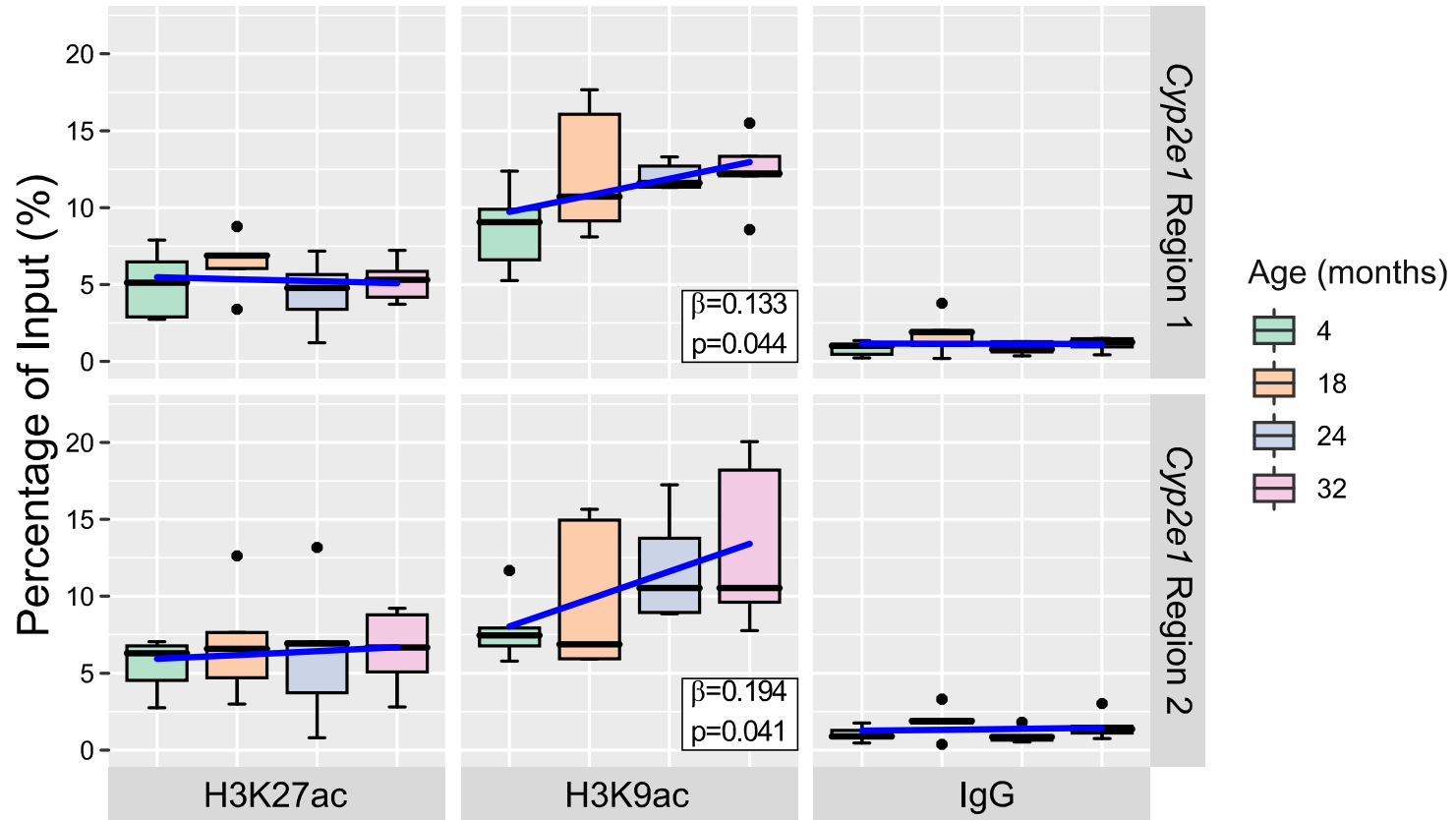


Figure 2.12 Chromatin Immunoprecipitation quantitative polymerase chain reaction (ChIP-qPCR) data. Box plots with regression line (blue) of Age-Associated changes to percentage of input occupancy of Histone 3 Lysine 9 acetylation (H3K9ac) (n=20 per region), Histone 3 Lysine 27 acetylation (H3K27ac) (n=20 per region) at *Cyp2e1* intron 1 (Region1, chr7:147,950,223-147,950,367, mm9) and promoter (Region 2, chr7:147,942,350-147,942,468, mm9). IgG percentage of input shows a low background noise signal for each of the sample's age groups (n=20 per region). Data represent median (middle hinge), 25% (lower hinge) and 75% (upper hinge) quantile. Data points beyond upper or lower 1.5 * Inter Quantile Range are represented as individual black dots.

2.4.5. CYP2E1 pharmacokinetics, chronological age, and epigenetics

As shown above, 5mC and H3K9ac levels at *Cyp2e1* changed with age in tandem with reduced gene and protein expression in our sample. To determine if these effects impacted CYP2E1 metabolic activity, we assayed metabolism of the CYP2E1-specific probe drug chlorzoxazone (CZ) in microsome extracts from the same livers. The average microsome yield was 1.07% w/w [0.55-1.69], which was within expected range (Knights et al. 2016). Linearity of the HPLC assays of $R^2 \geq 0.999$ were established for 2.34-1200 μM CZ and 0.46-240 μM 6-OH-CZ (**Figure 2.2** and **2.3**). Linearity of 6-OH-CZ formation with reaction time and MLM final concentration was established and the final reaction time and MLM concentration was 25 min and 1 mg/ml respectively (**Figure 2.4** and **2.5**). V_{max} and K_m values were estimated and used to calculate intrinsic clearance (CL_{int}) according to Eq2. Initial analyses established that chronological age was not significantly associated with CL_{int} of CYP2E1 despite a relatively large correlation coefficient ($r=0.31$, $p=0.8$). Average Michealis-Menten constants and CL_{int} per age group are reported in **Table 2.6**. Representative Michaelis-Menten curves of each age group can be found in **Figure 2.13**. This result suggests that chronological age is not a robust independent predictor of CL_{int} , corroborating prior research (Schmucker et al. 1990; Hunt et al. 1990; Mach et al. 2016).

Age (months)	Vmax (pmol/min/mg protein) Mean (+-SD)	Km (uM) Mean (+-SD)	CL _{int} (uL/min/mg protein) Mean (+-SD)
4	626.05 (297.1)	391.44 (196.7)	1.59 (1.51)
18	602.96 (493.9)	1009.54 (1662.1)	0.59 (0.29)
24	915.07 (774.7)	377.59 (405.2)	2.42 (1.91)
32	604.8 (434.3)	732.24 (891.9)	0.82 (0.48)

Table 2.6 Michaelis-Menten Constants per age group. Table reporting mean (+-SD) of the pharmacokinetics constants Vmax (pmol/min/mg protein), Km (uM), and CL_{int} (uL/min/mg protein) per age group (months).

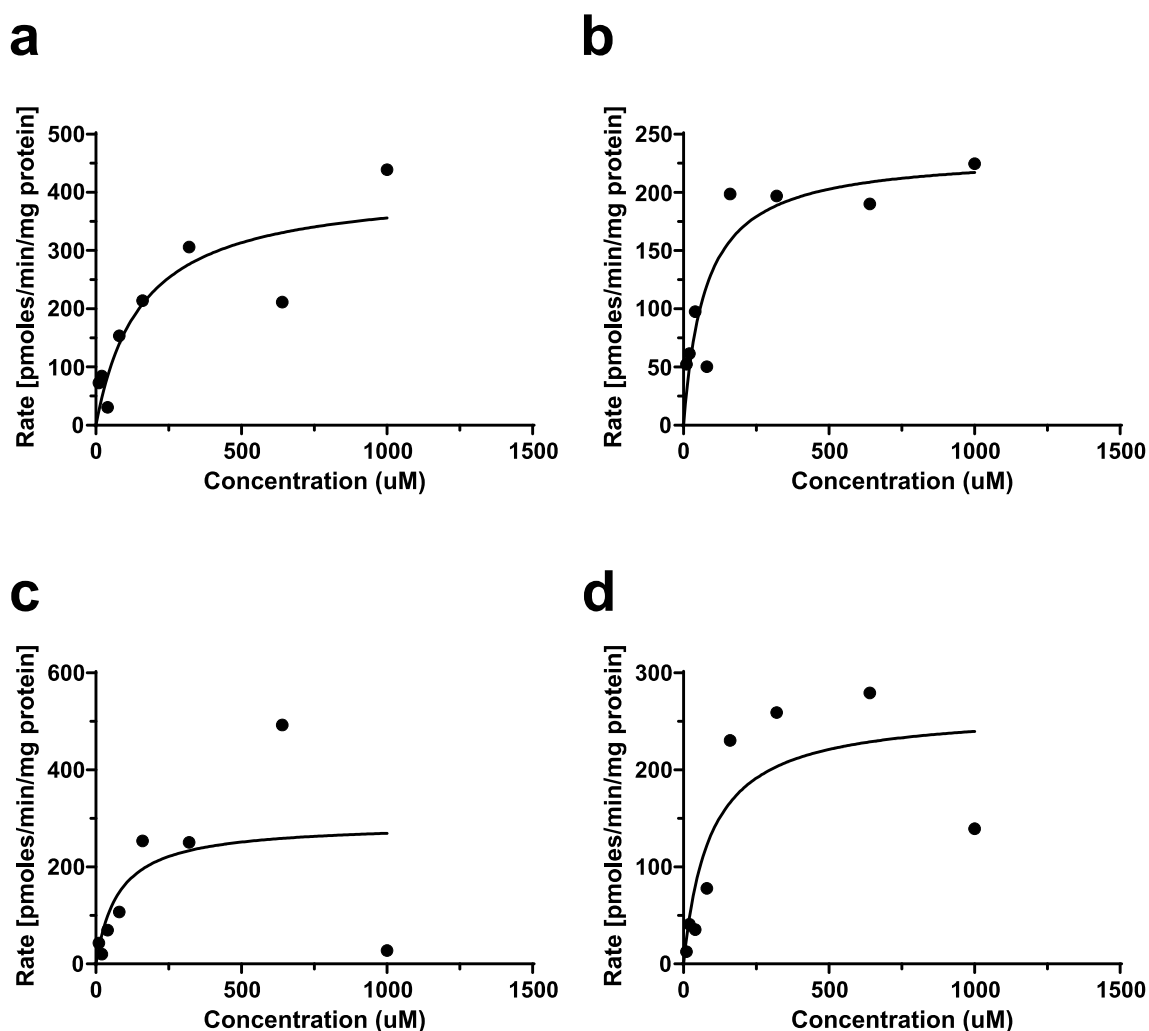


Figure 2.13 Representative Michaelis-Menten curves of each age group. Representative Michaelis-Menten curves for (a) 4 months, (b) 18 months, (c) 24 months, and (d) 32 months ages. X-axis is parent drug chlorzoxazone concentration (μM). Y-axis is reaction rate (pmol/min/mg protein).

We then tested *Cyp2e1* epigenetic measures for association with the pharmacokinetic variables. All CpGs were associated with CL_{int} (**Figure 2.14**) and the most significant was with CpG at position 8 (chr7: 147,949,806, mm9) ($r=-0.29$, $p=0.0008$). Furthermore, H3K9ac levels at the upstream regulatory region, but not intron 1, of *Cyp2e1* were positively correlated with CL_{int} ($r=0.49$, $p=0.005$). All p-values are provided in **Table 2.7**.

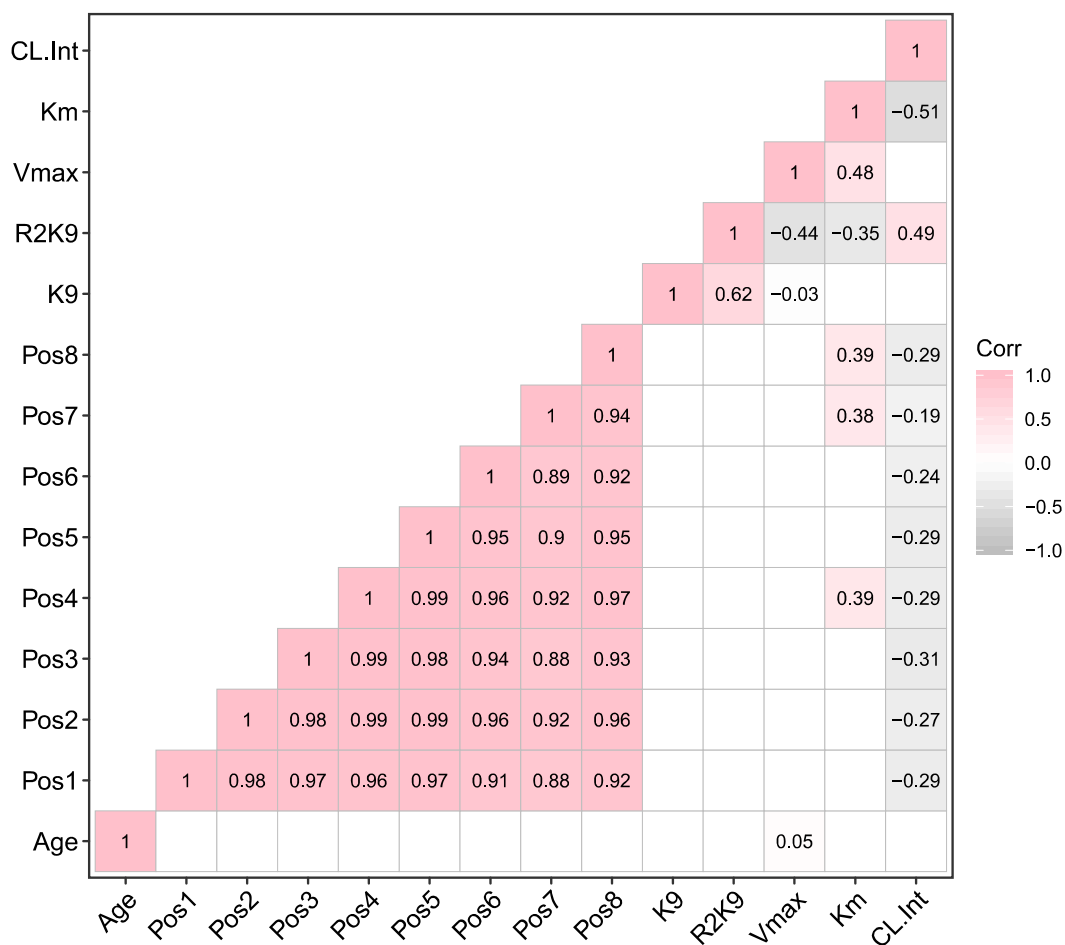


Figure 2.14 Correlation matrix reporting Pearson correlation statistical test result (r). White blank cells indicate non-significant association ($p > 0.05$). Refer to **Table 2.7** for individual p -values of each Pearson correlation test of a given pair. Color gradient indicates the direction of effect of the association with dark pink representing the strongest positive association of 1 while dark gray representing the strongest negative association of -1. Only lower half of the plot is shown to prevent redundancy in reporting the results. Age: chronological age, Pos 1-8: Position 1-8 chr7: 147,942,492-147,949,679 - 147,949,684 - 147,949,743 - 147,949,754 - 147,949,770 - 147,949-791 - 147,949,806, mm9. Vmax: maximal rate of hydroxylation reaction of chlorzoxazone by Cyp2e1, Km: chlorzoxazone concentration at half maximal rate, CL.Int: intrinsic clearance, K9: Histone 3 Lysine 9 acetylation in *Cyp2e1* intron 1 (chr7:147,950,223-147,950,367, mm9), R2K9 Histone 3 Lysine 9 acetylation in *Cyp2e1* promoter (chr7:147,942,350-147942468, mm9).

	Age	Pos1	Pos2	Pos3	Pos4	Pos5	Pos6	Pos7	Pos8	K9	R2K9	Vmax	Km	CL.Int
Age	0													
Pos1	0.0653	0												
Pos2	0.0818	7.70E-14	0											
Pos3	0.0716	3.97E-14	3.56E-15	0										
Pos4	0.0922	3.79E-12	1.55E-17	9.63E-15	0									
Pos5	0.0705	9.53E-14	2.54E-17	8.87E-19	1.48E-16	0								
Pos6	0.0820	5.76E-11	9.50E-15	1.47E-12	1.25E-15	1.01E-13	0							
Pos7	0.1827	6.65E-08	1.19E-09	1.08E-08	2.97E-10	3.22E-09	2.62E-10	0						
Pos8	0.1568	1.93E-09	5.77E-12	2.06E-10	4.16E-13	3.93E-11	1.94E-12	2.02E-13	0					
K9	0.0808	0.8220	0.9914	0.8680	0.9338	0.9260	0.8881	0.6116	0.6991	0				
R2K9	0.1326	0.3089	0.1978	0.2274	0.1581	0.2115	0.1536	0.0556	0.0843	0.0023	0			
Vmax	0.0315	0.3860	0.5458	0.5289	0.6336	0.5521	0.6367	0.9921	0.8266	0.0250	0.0007	0		
Km	0.3677	0.1023	0.0681	0.0670	0.0491	0.0668	0.0566	0.0255	0.0298	0.0629	5.46E-05	0.0214	0	
CL.Int	0.8085	0.0030	0.0020	0.0015	0.0012	0.0017	0.0020	0.0008	0.0008	0.5186	0.0050	0.2682	1.79E-05	0

Table 2.7. Pearson correlation tests p-values for epigenetic and drug metabolism variables. Table reporting Pearson correlation test p-value for each pair of variables. Age: Chronological age, Pos1-8, Position 1-8: chr7: 147,942,492-147,949,679 - 147,949,684 - 147,949,743 - 147,949,754 - 147,949,770 - 147,949,791 - 147,949,806, mm9. Vmax: maximal rate of 6-hydroxylation reaction of chlorzoxazone by CYP2E1, Km: chlorzoxazone concentration at half maximal rate, CL.Int: intrinsic clearance, K9: Histone 3 Lysine 9 acetylation in *Cyp2e1* intron 1 (chr7:147,950,223-147,950,367, mm9), R2K9 Histone 3 Lysine 9 acetylation in *Cyp2e1* promoter (chr7:147,942,350-147942468, mm9).

2.5. Discussion

In this study, we demonstrated that 5mC and H3K9ac levels change with age at *Cyp2e1* in mouse liver. Furthermore, we showed that these epigenetic changes were significantly associated with rates of CYP2E1-mediated drug metabolism in microsome extracts from the same livers, while chronological age was not. This finding suggests that epigenetic marks may be better predictors of drug metabolism in advanced age than chronological age itself.

Considering our findings in the context of published work, we found that global 5mC levels diminished with increasing age and this effect has been shown before in studies of different tissues (Booth and Brunet 2016), including the liver (Wilson et al. 1987). Previous reports have also shown reduced global 5hmC in mouse liver with age, as we observed here (Tammen et al. 2014). However, recent genome-wide bisulfite sequencing studies in mouse liver have shown either a modest excess of hypermethylated sites (Hahn et al. 2017), or no overall excess in either direction with age (Gravina et al. 2016). One possible reason for this discrepancy is that “genome-wide” approaches such as next-generation sequencing (NGS) are not truly representative of the whole genome. For example, NGS approaches typically underrepresent repetitive elements because reads in these regions may not align unambiguously to the reference genome and so are discarded. This may diminish the influence of repeats on the cumulative abundance of methylation in bisulfite sequencing studies. Several classes of repetitive elements reportedly lose methylation with age (Cardelli 2018). Therefore, underrepresentation of these elements could lead to underestimation of age-related hypomethylation in genome wide NGS studies of aging. In our sample, we observed significant hypomethylation of LINE1 elements, with an average reduction of 2% per month of age. As LINE1 elements are the dominant repeat class in mouse and human, comprising almost 20% of the genome (Mouse Genome Sequencing

Consortium et al. 2002), this result could partly explain the discrepancy between global 5mC studies and genome-wide bisulfite sequencing studies of aging in liver DNA.

Considering our locus-specific results, we found that DNA methylation of the *Cyp2e1* 5'UTR and upstream regulatory region increased significantly with age, while its gene expression declined with age. This supports and extends prior observations in human blood studies. For example, Peters et al. (2015) reported a hypermethylated CpG at human *CYP2E1* and decreased gene expression with age. Reduced *Cyp2e1* expression was also reported in mouse liver tissue aged 28 months compared to 4 months, as detected via RNA sequencing (White et al. 2015). To date, prior studies of histone PTM changes in the context of aging are limited and we are not aware of available published data for the liver. Park et al. (2015) found that histone deacetylase inhibitors influenced transcription of cytochrome P450s in cultured hepatocytes, suggesting histone acetylation affects expression, but this study did not examine the effect of aging nor specific histone acetylation marks. Further work is needed in this area, in particular genome-wide analysis of H3K9ac with age, given our findings with respect to H3K9ac in this study.

We observed a significant negative correlation between CL_{int} and *Cyp2e1* methylation and a significant positive correlation between CL_{int} and *Cyp2e1* histone acetylation. The effect sizes are substantial, with a maximum correlation of -0.31 for 5mC and 0.49 for H3K9ac, suggesting that epigenetics plays a significant role in regulating CYP2E1 hepatic activity. This finding may have clinical relevance because CYP2E1 is responsible for the metabolism of hepatotoxic substrates such as ethanol, acetaminophen, chlorzoxazone (CZ), pro-carcinogens (benzene, chloroform, and N-nitroso-nicotine), and endogenous compounds such as estrogen, acetone, and linoleic acid (Lieber 1997; Caro and Cederbaum 2004; Porubsky et al. 2008).

Unlike other cytochrome P450s, human *CYP2E1* is not functionally polymorphic and its reported variants to date have no clinical or functional effects (Ingelman-Sundberg 2004b; Zanger and Schwab 2013). *CYP2E1* comprises 5.5–16.5% of the hepatic P450 pool (Zanger and Schwab 2013) and its substrate profile makes it relevant to older adults due to the detrimental and unpredictable ADRs of these substrates. For example, *CYP2E1* is inducible at heavy ethanol intake which is responsible, along with Alcohol dehydrogenases (ADH), for the majority of alcohol-mediated liver toxicity hospitalizations (Caro and Cederbaum 2004). In addition, acetaminophen related liver injury is the primary over-the-counter drug-related hospitalization (Lee 2017). Acetaminophen hepatotoxicity is mediated by the excessive formation of the toxic byproduct N-acetyl-p-benzoquinone imine (NAPQI) and subsequent thiol residue depletion upon acetaminophen overdose. *CYP2E1* is responsible for NAPQI formation at high acetaminophen doses, which highlights its importance in acetaminophen-induced liver damage (French 2013). Finally, CZ is a high-risk drug listed on the 2019 American Geriatrics Society Beers criteria for potentially inappropriate use in older adults. CZ is a centrally acting skeletal muscle relaxant that is strongly recommended to avoid in the elderly due to moderate evidence of poor toleration by this population according to these criteria. Taken together, these examples provide evidence for clinical significance of the metabolism of drugs that are *CYP2E1* substrates.

A limitation of the study as presented is that we could not manipulate epigenetic levels in our post-mortem samples, so the association between epigenetics and drug metabolism is correlational, rather than causal. Nevertheless, the use of the probe drug CZ renders the association highly specific to the action of *CYP2E1*. In addition, sex differences in drug metabolism have been described, however, our sample was comprised of only male mice. Hence, female-specific effects should be investigated in future studies. Age-related changes to

pharmacokinetic attributes such as plasma protein binding and hepatic blood flow should be the subject of future in vivo investigations that pertain to drugs that are highly protein bound or have high hepatic extraction ratio due to the possible changes to these attributes that affect the overall disposition of drugs with advanced age (McLachlan and Pont 2012). Looking to the future, this work may have clinical applications if extended to human populations. Age-related epigenetic changes at human CYP2E1 and other drug metabolizing genes should be studied, and if these changes are linked to altered clearance clinically, epigenetic biomarkers of altered drug metabolism could be potentially used to guide dosing decisions in older adults. One potential issue is that epigenetic modifications vary by cell and tissue type. Therefore, age-related effects mapped in the liver will need to be tested for equivalency in peripheral cells or tissues (e.g. blood) that are more readily accessible for the purposes of biomarker testing. However, prior work by Horvath (2013) and others (Spiers et al. 2016; Zhu et al. 2018) suggests that many age-related epigenetic changes are consistent across tissues and indeed in this study we demonstrated continuity across mouse and human. Future work should investigate genome-wide epigenetic changes with age in the liver and blood concurrently, for the same organism.

Chapter 3: Histone acetylation at the sulfotransferase 1a1 gene is associated with its hepatic expression in normal aging

In Preparation for submission

Mohamad M. Kronfol¹, Mikhail G. Dozmorov², Fay M. Jahr¹, Matthew Halquist³, MaryPeace McRae¹, Dayanjan S. Wijesinghe¹, Elvin T. Price¹, Patricia W. Slattum¹, Joseph L. McClay¹

¹Department of Pharmacotherapy and Outcomes Science, School of Pharmacy, Virginia Commonwealth University, Richmond, Virginia.

²Department of Biostatistics, School of Medicine, Virginia Commonwealth University, Richmond, Virginia.

³Department of Pharmaceutics, School of Pharmacy, Virginia Commonwealth University, Richmond, Virginia.

Keywords: DNA methylation, Histone acetylation, Aging, *Sult1a1*, *Ugt1a6*, Pharmacokinetics, Drug metabolism

3.1. Abstract

Phase II drug metabolism is poorly studied with advanced age and older adults may exhibit significant variability in their expression of phase II enzymes. We hypothesized that age-related changes to epigenetic regulation of genes involved in phase II drug metabolism may contribute to these effects. We examined published epigenome-wide studies of human blood and identified the *SULT1A1* and *UGT1A6* genes as the top loci exhibiting epigenetic changes with age. To assess possible functional alterations with age in the liver, we assayed DNA methylation (5mC) and histone acetylation (HAc) changes around the mouse homologs *Sult1a1* and *Ugt1a6* in liver tissue from mice aged 4-32 months obtained from the National Institute on Aging tissue bank. Our liver sample shows significant changes to 5mC and histone 3 lysine 9 acetylation (H3K9ac) around *Sult1a1* but not at *Ugt1a6* with age. Histone 3 lysine 27 acetylation (H3K27ac) did not change with age at either locus. *Sult1a1* gene expression is positively associated with its H3K9ac levels but not with 5mC or chronological age. Our findings indicate that *Sult1a1* expression is under epigenetic influence in normal aging, and that this influence is more pronounced for histone acetylation than DNA methylation in this sample. In the future, epigenetic biomarkers could prove useful to inform dosing regimens in older adults.

3.2. Introduction

Age-associated changes to hepatic phase II drug metabolism is poorly understood. Recently, it has been suggested that epigenetic mechanisms could regulate genes encoding drug metabolizing enzymes in older adults (Fisel et al. 2016). Aging is known to be associated with extensive changes to epigenetic marks such as 5-methylCytosine (5mC) (Horvath and Raj 2018) and, crucially, these changes are not purely stochastic. Several hundred loci in the genome exhibit consistent 5mC changes in normal aging and these are known as age-associated differentially methylated regions (a-DMRs). Many a-DMRs have functional consequences (McClay et al. 2014; Horvath and Raj 2018), leading us to seek out a-DMRs at genes encoding drug metabolizing enzymes to determine if they affect regulation of these genes. Previously, we showed that a-DMRs at the cytochrome P450 2E1 gene, which encodes a phase I drug metabolizing enzyme, showed significant changes with age that were associated with CYP2E1 function (Kronfol et al. 2020). In the current study, we extend this work to consider genes encoding phase II (conjugation) drug metabolizing enzymes.

Data from epigenome-wide association studies (EWAS) in human blood have shown significant changes to 5mC at several phase II genes with age (Heyn et al. 2012; Steegenga et al. 2014; Reynolds et al. 2014; Peters et al. 2015). However, the degree to which these a-DMRs are present and affect gene expression in the liver, the primary site of drug metabolism, is unclear. Therefore, the aim of this study is to identify age-related changes to 5mC and histone acetylation at genes encoding phase II drug metabolizing enzymes in the liver and test if these epigenetic changes are associated with gene expression. This study used liver tissue from mice aged under controlled conditions, obtained from the National Institute on Aging tissue bank.

We identified two phase II drug metabolism genes, *SULT1A1* and *UGT1A6*, showing strong evidence for a-DMRs in human blood studies (**Table 3.1**). We mapped the associated sites in the human genome to their homologous mouse regions and tested for epigenetic changes at these regions in mouse liver (**Figure 3.1**). High-Resolution Melt analysis of bisulfite-converted DNA and chromatin immunoprecipitation assays was used to measure 5mC and histone post-translational modifications respectively (Dozmorov 2015). We observed significant age-related epigenetic change at the *Sult1a1* gene and confirmed that this change was strongly associated with its gene expression.

Reference	Longevity Map (Human Ageing Genomic Resources)	Peters et al. 2015	Heyn et al. 2012	Hannum et al. 2013	Horvath 2013	Reynolds et al. 2014	Marttila et al. 2015	Steegenga et al. 2014	
	Exp	Exp	Meth	Meth	Meth	Meth	Both	Both	Total
Phase II genes									
SULT1A1	X					X		X	3
UGT1A6			X				X		2
UGT2B15								X	1
GSTT1	X								1
SULT2B1								X	1
UGT1A4							X		1
UGT1A5							X		1
UGT1A1									0
SULT1A3									0

Table 3.1. Summary of human EWAS findings for phase II drug metabolism genes. Human ADME genes list from pharmaADME (www.pharmaadme.org) was contrasted on the top findings from EWAS and gene expression studies of normal aging in human blood DNA. Genes encoding phase II drug metabolizing enzymes that showed significant association in the top findings of these studies is marked with an “X”. The total number of studies were a specific gene is a top association in the reported results is shown as a total in the last column of the table. Exp: Expression, Meth: Methylation.

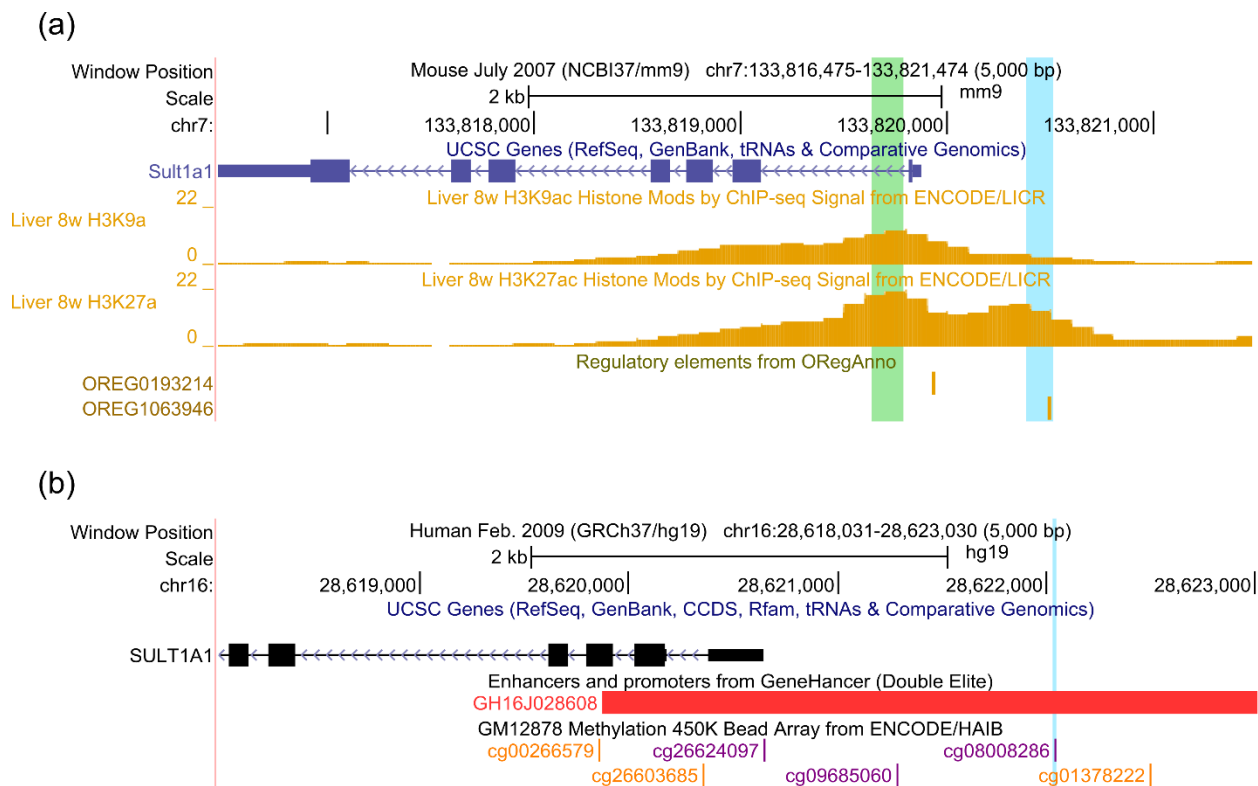


Figure 3.1 UCSC genome browser tracks showing (a) Mouse *Sult1a1* gene location, H3K9ac, H3K27ac occupancy, and ORegAnno regulatory elements. ORegAnno track shows identification (ID) and transcription factor binding site (orange). Vertical bars highlighted in blue and green represent the investigated regions in the High Resolution Melting, and Chromatin Immunoprecipitation Quantitative Polymerase Chain Reaction assays respectively (full coordinates in **Table 3.2**), and (b) The homologous genomic region in human showing *SULT1A1* gene location, GeneHancer regulatory elements location and ID, and the identifier of the significant CpG found in humans (blue bar).

Gene	Primers (5' → 3')		Product size/coordinates/assembly	CpG count
	Forward Primer	Reverse Primer		
	High-Resolution Melt			
<i>Sult1a1</i>	GGAAGGTGTTTTGTTTTATG	CTAAAAATATATCTCTCCCAACT	134/chr7:133,820,382-133,820,515/mm9	1
<i>Ugt1a6</i>	AGTATGAAGGAGATAGTAGAATAT	AAAAAACCATCAAAAAACAC	206/chr1:90,035,169-90,035,374/mm9	4
	Chromatin Immunoprecipitation Quantitative Polymerase Chain Reaction			
<i>Sult1a1</i>	GGGGAAC TCAGACAAACCAC	TCCTGCC CAGATACTGGTTC	154/ chr7:133,819,634-133,819,787/mm9	
<i>Ugt1a6</i>	GCCACTCAGGAAGGACAGAG	GTGAGGC ACTGGTCTGGTTT	153/ chr1:90,030,630- 90,030,782/mm9	

Table 3.2. HRM and ChIP primers and qPCR product sequences. Primers used in the High-Resolution Melt and Chromatin Immunoprecipitation Quantitative Polymerase Chain Reaction assays with size of PCR product, genomic coordinates, and assembly with CpG count when appropriate.

3.3. Methods

3.3.1. Mice: Liver tissue samples from 20 male CB6F1 mice (5 subjects in each of four age groups 4, 18, 24, and 32 months) were obtained from the National Institute on Aging (NIA) tissue bank.

3.3.2. DNA and RNA extraction: Genomic DNA was extracted using the AllPrep DNA/RNA kit (80204, Qiagen, Hilden, Germany) according to manufacturer's protocol. DNA and RNA purity and quantity were measured using a Nanodrop spectrometer (ThermoFisher, Waltham, MA).

3.3.3. Selection of genomic regions of interest: Aging EWAS findings for human blood were obtained from published studies (see Dozmorov 2015) and genes encoding drug metabolizing enzymes were obtained from the ADME (absorption, distribution, metabolism, and excretion) gene list from the pharmaADME consortium (pharmaADME.org), see **Table 3.1**. A complete list of the genomic coordinates of all investigated regions in mouse can be found in **Table 3.2**. Publicly available data from the mouse Encyclopedia of DNA Elements (ENCODE) and Ludwig Institute for Cancer Research (LICR) chromatin immunoprecipitation (ChIP) sequencing runs on young (8 weeks) male mouse liver tissue were used to identify two regions with high levels of histone 3 lysine 9 acetylation (H3K9ac) and histone 3 lysine 27 acetylation (H3K27ac) PTMs (GSM1000153, GSM1000140) (**Figure 3.1**).

3.3.4. Bisulfite conversion of genomic DNA and High-Resolution Melt (HRM) analysis: 200ng of liver genomic DNA was treated with sodium bisulfite according to the EZ DNA Methylation kit protocol (Zymo Research, Irvine, CA). Mouse genomic DNA of 0, 5, 25, 50, 75, and 100% methylation were used as standards (808060M, EpigenDx, Hopkinton, MA). High-

Resolution Melt (HRM) assays using MeltDoctor reagents (Applied Biosystems, Foster City, CA) on a Quantstudio 3 instrument were used to measure 5mC levels on the promoter and exon 2 of *Sult1a1* and *Ugt1a6* (**Table 3.2**). Samples were amplified by qPCR as follows 10min hold at 95°C followed by 45 cycles of: 15sec at 95°C, 60sec at 60°C or 55°C for *Sult1a1* or *Ugt1a6* respectively, followed by a melt curve stage. Each reaction included 20ng bisulfite-converted DNA and final concentration of 1X MeltDoctor HRM MasterMix (Applied Biosystems), 0.2μM forward and 0.2μM reverse primer (**Table 3.2**). The liver samples and the standards were run in triplicate. The Net Temperature Shift values (Newman et al. 2012) of the liver samples were interpolated on the standard curve to yield their 5mC percentage.

3.3.5. Gene expression analysis by reverse transcription – quantitative PCR (RT-qPCR):

Gene expression was measured for *Sult1a1*, *Ugt1a6a* and *Ugt1a6b*. We opted to measure the gene expression of both isoforms of *Ugt1a6* present in mouse liver because they are both expressed from the same locus and the 5mC region investigated is shared among them. Hence, allowing us to test for whether either isoform is affected by epigenetic changes if present. For each sample, 1μg of total liver mRNA was reverse transcribed to cDNA by iScript kit according to manufacturer's protocol (Bio-Rad, Hercules, CA). Aliquots of cDNA were amplified in triplicate using final concentration of 1X TaqMan master mix (Applied Biosystems) and 1X TaqMan *Sult1a1* or *Ugt1a6a/b* Mouse Gene Expression Assay (Mm01132072_m1, Mm01967851_s1, Mm03032310_s1 ThermoFisher). qPCR conditions were as follows 2 min hold at 50 °C then 10min at 95 °C, followed by 40 cycles of 15 sec at 95°C and 60 sec at 60°C. Mouse *Gapdh* endogenous control was also assayed in triplicate (Mm99999915_g1, ThermoFisher). Quantification cycles (C_q) were determined using the Relative Quantification

application on the ThermoFisher Cloud. Normalized quantification cycles (ΔC_q) were obtained by subtracting the mean *Gapdh* C_q from the mean C_q of any of the genes.

3.3.6. Chromatin Immunoprecipitation Quantitative Polymerase Chain Reaction (ChIP-qPCR): 80 mg of mouse liver per sample was processed using the TruChIP tissue shearing kit (520237, Covaris, Woburn, MA). Minced tissue was fixed in 1% formaldehyde for 2 min, washed, transferred to a tissueTUBE (Covaris), flash frozen in liquid N₂ and pulverized. After cell lysis, chromatin was sheared on a Covaris M220 for 8min. 2% of sheared chromatin per IP was set aside as input control. ChIP used 5 μ L of anti-H3K9ac (39137, Active Motif, Carlsbad, CA), or 5 μ g of anti-H3K27ac (39133, Active Motif), or 5 μ g of Rabbit IgG isotype control (ab171870, Abcam) incubated with 2 μ g sheared chromatin from each sample overnight (16 hours) at 4°C. This mixture was added to Dynabeads Protein G (10004D, ThermoFisher) for 4 hours at 4°C before washing and elution of ChIP DNA by heating to 65°C for 1 hour. After elution, samples were treated with RNase and Proteinase K and DNA was purified using QIAquick (28104, Qiagen).

Each ChIP'ed DNA was amplified in triplicate using PowerUp SYBR Green (Applied Biosystems), with 0.2 μ M of forward and reverse primers (**Table 3.2**) as follows: 2min at 50°C, 2min at 95°C followed by 45 cycles of: 15sec at 95°C, 30sec at 58 °C or 60°C for *Sult1a1* or *Ugt1a6* respectively and 1min at 72°C, followed by melt curve stage. C_q values for each plate were downloaded and the mean threshold cycle (C_q) obtained for each sample and normalized to the dilution factor (2%=1/50) corrected C_q value ($\text{Log}_2(50) = 5.6438$) of the input control to obtain ΔC_q . The percentage of input was calculated by multiplying 100 by $2^{\Delta C_q}$.

3.3.7. Statistics: Linear regression tests were conducted in R version 3.6.1 (www.r-project.org) with $\alpha=0.05$.

3.4. Results

3.4.1. Age-associated changes to *Sult1a1* and *Ugt1a6* methylation and gene expression

DNA and RNA extractions from the mouse liver samples were successful with an average 260/280 value of 1.94 [1.8-2.1] for DNA and 2.05 [1.94-2.1] for RNA. We tested for epigenetic changes in mouse liver DNA using HRM. HRM analysis revealed that 5mC at *Sult1a1* decreases significantly with age ($\beta=-1.08$, 95%CI [-1.8, -0.2], SE=0.38, $p=0.011$) (**Figure 3.2 a**) but did not change at *Ugt1a6* (**Figure 3.3 a**).

The observed *Sult1a1* promoter 5mC decrease with age translates to a 24% decrease in the 32 months group versus 4 months groups. On the other hand, neither of *Sult1a1* or *Ugt1a6a/b* gene expression changed in a consistent manner with chronological age in this sample ($p>0.05$) (**Figure 3.2 b**, **Figure 3.3 c/d**).

3.4.2. Histone acetylation analysis of *Sult1a1* regulatory region

To assay histone acetylation levels in these regions, we used chromatin immunoprecipitation coupled to quantitative PCR (ChIP-qPCR). We observed a significant increase in H3K9ac at *Sult1a1* ($\beta= 0.11$, 95%CI [0.002,0.22], SE=0.05, $p=0.04$) (**Figure 3.2 c**) but not at *Ugt1a6* when regressing ChIP-qPCR percentage of input on age (**Figure 3.3 b**). This corresponds to a 0.11% increase in H3K9ac per month of increased age at *Sult1a1*. Furthermore, H3K27ac levels were stable with age at both genes in this sample (**Figure 3.2 c**, **Figure 3.3 b**)

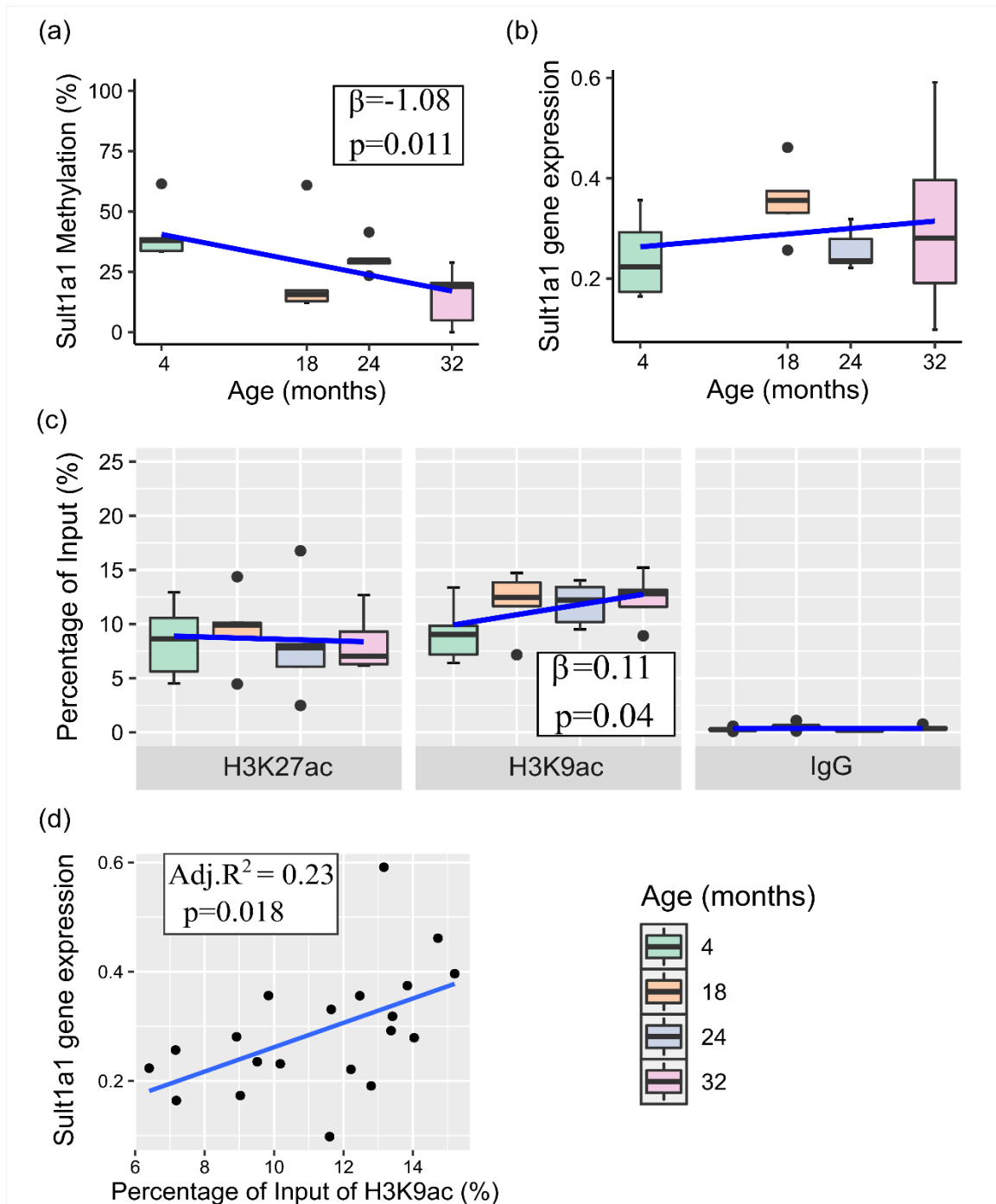


Figure 3.2 Box plots with superimposed regression line (blue) of Age-Associated changes to *Sult1a1* (a) methylation (n=20), (b) gene expression (n=20), and (c) Histone 3 Lysine 27 and Lysine 9 acetylation (H3K27ac and H3K9ac), chromatin Immunoprecipitation quantitative polymerase chain reaction (ChIP-qPCR) data (n=20 per target), IgG percentage of input shows a low background noise signal for each of the sample's age groups. Data represent median (middle

hinge), 25% (lower hinge) and 75% (upper hinge) quantile. Data points beyond upper or lower 1.5 * Inter Quantile Range are represented as individual black dots. (d) linear regression plot of percentage of input of H3K9ac and *Sut1a1* gene expression. (n=20 per locus) with reported Adjusted R² and p-value.

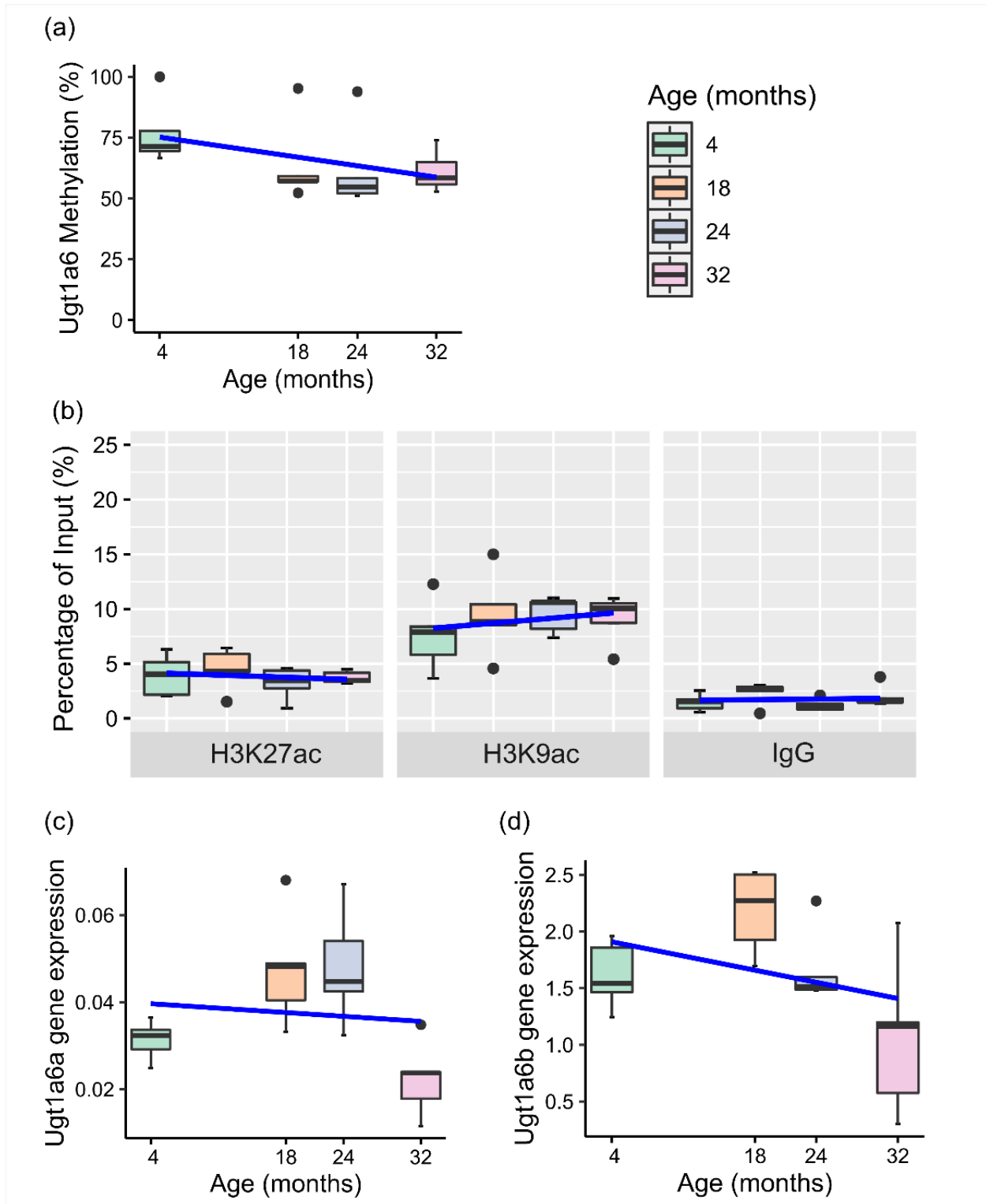


Figure 3.3 (a) Box plot with superimposed regression line (blue) of age-associated changes to *Ugt1a6* methylation (n=20) ($p>0.05$). (b) Histone 3 Lysine 27 and Lysine 9 acetylation (H3K27ac and H3K9ac), Chromatin Immunoprecipitation quantitative polymerase chain reaction

(ChIP-qPCR) data (n=20 per target) ($p>0.05$), IgG percentage of input shows a low background noise signal for each of the sample's age groups. Data represent median (middle hinge), 25% (lower hinge) and 75% (upper hinge) quantile. Data points beyond upper or lower 1.5 * Inter Quantile Range are represented as individual black dots. Box plot with superimposed regression line (blue) of age-associated changes to gene expression of (c) *Ugt1a6a* isoform and (d) *Ugt1a6b* isoform (n=20 per locus) ($p>0.05$).

3.4.3. *Sult1a1* epigenetics and expression

As shown above, 5mC and H3K9ac levels at *Sult1a1* changed with age. However, *Sult1a1* gene expression was not associated with chronological age. To determine if epigenetic effects impacted *Sult1a1* gene expression, we tested the degree of association between 5mC and H3K9ac on *Sult1a1* with its gene expression. H3K9ac changes on *Sult1a1* intron1 are associated with its gene expression ($\beta=0.02$, 95%CI [0.004,0.04], SE=0.008, $p=0.018$), explaining 23% of the variability of the latter (Adj.R²=0.23, $p=0.018$) (**Figure 3.2 d**). However, 5mC at the *Sult1a1* promoter did not associate with its gene expression ($p>0.05$, data not shown). This result suggests that H3K9ac is a more robust independent predictor of gene expression of *Sult1a1* than 5mC or chronological age.

3.5. Discussion

This study demonstrates that 5mC and H3K9ac levels change with age at *Sult1a1* in mouse liver. Furthermore, we showed that H3K9ac was significantly associated with *Sult1a1* gene expression, while chronological age was not. This finding suggests that histone acetylation levels may be a better predictor of drug sulfonation by *Sult1a1* in advanced age than chronological age itself.

Comparing our findings to published work, we found that *Sult1a1* 5mC levels diminished with increasing age and this direction of effect supports prior observations in human blood studies. For example, Reynolds et al. (2014) reported a hypomethylated CpG with age at human *SULT1A1* (Reynolds et al. 2014) overlapping the homologous mouse region investigated in this study. Furthermore, Fu et al. (2012) reported increased *Sult1a1* expression in mouse liver tissue aged 27 months compared to 3 months, as detected via RT-qPCR (Fu et al. 2012). This suggests that increases to *Sult1a1* gene expression could occur with age but require more power through larger sample sizes to be reliably detectable. On the other hand, age-related changes to 5mC and H3K9ac were detectable at *Sult1a1* in this study's sample and H3K9ac is associated with its gene expression to a substantial degree of 23%. Prior studies of histone PTM changes in the context of aging are limited and we are not aware of existing data for *Sult1a1* in the liver. Schroeder et al. (2013) found that histone deacetylase inhibitors influenced gene expression of *Sult1a1* in specific brain regions, prefrontal cortex and nucleus accumbens, of mice suggesting that histone acetylation affects expression, but this study did not examine the effect of aging nor changes in the liver (Schroeder et al. 2013).

This finding may have clinical relevance because the *SULT1A1* enzyme is involved in the sulfonation of drugs including tamoxifen and estrogen replacement therapies (Glatt et al.

2001). *SULT1A1* comprises the majority, 53%, of the total hepatic sulfotransferase (Riches et al. 2009) and its substrate profile makes it relevant to older adults because these substrates are indicated for the treatment of age-related disease or have detrimental and unpredictable toxicities. For example, *SULT1A1* activates the prodrug tamoxifen which is essential for its anti-estrogen activity in the treatment of breast cancer (Brauch et al. 2009). In addition, prior studies have implicated genetic sequence variants at *SULT1A1* in response to estrogen-replacement therapy (Rebbeck et al. 2006; Hildebrandt et al. 2009). Therefore, it is conceivable that age-related functional epigenetic changes at *SULT1A1*, as shown here, may similarly affect response to estrogen-replacement therapy. This suggests an area of future clinical study in humans.

A limitation of the study is that we could not directly manipulate epigenetic levels in our post-mortem samples, so the relationship between epigenetics and gene expression is correlational, not causal. Also, sex differences in metabolism have been reported, but our sample was comprised of only male mice. Hence, female-specific effects should be inspected in forthcoming studies. Age-related epigenetic changes at human *SULT1A1* should be studied, and if these changes are connected to altered clearance clinically, epigenetic biomarkers of altered drug metabolism could be potentially used to guide dosing decisions in older adults.

3.6. Study Highlights

What is the current knowledge on the topic?

The determinants of age-related changes of drug response due to phase II metabolism is poorly understood. The study of epigenetic regulation of ADME genes is in its infancy and no reports correlate age-related changes to epigenetic regulation of genes controlling phase II metabolism.

What question did this study address?

What is the extent of age-related change of DNA methylation and histone acetylation at the *Sult1a1* and *Ugt1a6* genes? What is the extent of association of these epigenetic marks with gene expression?

What does this study add to our knowledge?

Determine the extent of change to DNA methylation and histone acetylation on sulfonation gene, *Sult1a1*, and its degree of association with its gene expression in advanced age. This study reports a lack of change to age-related epigenetic regulation on glucuronidation gene, *Ugt1a6*, in mouse liver.

How might this change clinical pharmacology or translational science?

This might stimulate clinical work that determines how we dose older patients based on epigenetic levels at genes controlling phase II metabolism to optimize drug response and decrease adverse events.

Chapter 4: Cross tissue correlation of *Cyp2e1* and *Sult1a1* methylation levels in mice

4.1 Abstract

Epigenetic levels vary by tissue type, yet the degree of variation shared between tissues is less established. The relationship between blood methylation and methylation in organs that express phase I and II metabolism genes is not well characterized. We hypothesized that blood DNA methylation (5mC) levels of genes involved in drug metabolism are correlated with those of the liver and the brain. We recently identified the cytochrome P450 2E1 (*Cyp2e1*) and sulfotransferase (*Sult1a1*) genes as top mouse ADME loci exhibiting epigenetic changes with age. To investigate the extent of association between methylation levels of *Cyp2e1* and *Sult1a1* in blood and organs that express those genes, we obtained liver, blood, hippocampus, and cortex from mice aged 5 months from the Jackson Laboratory. We then assayed 5mC using High-Resolution Melt assays, around mouse *Cyp2e1* and *Sult1a1* from these tissues. 5mC of mouse livers exhibit significant negative correlation with that of blood at both genes. However, blood 5mC of neither gene was significantly associated with 5mC in the cortex nor hippocampus brain regions. This suggests that epigenetic levels in blood 5mC may inversely reflect those in the liver for *Cyp2e1* and *Sult1a1* genes. This study could serve as the starting point of future in depth studies that explicitly looks at blood based 5mC as a proxy to infer the status of methylation on *Cyp2e1* and *Sult1a1* in the liver.

4.2 Introduction

Tissue-specific patterns of DNA methylation are recognized to be highly discordant (Bird 2002; Zhang et al. 2013; Dmitrijeva et al. 2018). Although significant differences in mean levels of 5mC between tissues exist, they should not be used to imply a lack of relationship between these marks. Studies have shown that cross-tissue patterns of 5mC can be used to predict a singular outcome such as mortality, disease risk, or longevity (Horvath and Raj 2018), indicating a mutual underlying process influencing 5mC levels across tissues, however with different nuances. We aimed to test this cross-tissue correlation around two genes encoding drug metabolizing phase I and II enzymes, *Cyp2e1* and *Sult1a1* respectively, which have been previously shown to be influenced by epigenetic regulation with age (see Chapters 2, 3 and Kronfol et al 2020).

Changes to hepatic 5mC at *Cyp2e1* are associated with changes to gene expression levels (Kronfol et al 2020). Furthermore, the regions that we tested were known a-DMRs in human blood. However, the degree to which these changes, or lack thereof, in 5mC are present in other tissues is unknown. These considerations led us to hypothesize that the variability of hepatic 5mC could be associated with that of 5mC from whole blood or other tissue that show high expression of these genes such as the brain, specifically the cortex and hippocampus. In this study, we aimed to test for the degree of association between 5mC levels in the liver, whole blood, hippocampus, cortex, and whole brain in young male C57BL6J mice. Through this investigation we set out to measure the extent and nature of association between 5mC levels on *Cyp2e1* and *Sult1a1* in organs that exhibit high expression of those genes and whole blood.

4.3. Method

4.3.1. Sample

All procedures were conducted according to the Institutional Animal Care and Use Committee (IACUC) protocol (AD10002047) approved by Virginia Commonwealth University. 8 male C57BL/6J were purchased from the Jackson Laboratory. Animals were housed in groups of 4 and maintained in controlled conditions of 21°C and a 12-h light/dark cycle in microbe free environment. Animals were fed standard chow as needed. Animals were healthy and showed no signs of aggression or harm. Blood samples were obtained from the submandibular vein prior to sacrifice. Animals were sacrificed by decapitation without anesthesia, because this could interfere with epigenetic marks. The age of the animals was 5 months at the day of sacrifice. The hippocampus and the cortex were dissected from the brain and the remainder was kept as a whole and analyzed as “rest of brain”. The hippocampus, cortex, rest of brain, liver, and 100µL whole blood mixed with 1% EDTA were collected from each animal and flash frozen in liquid N₂ and stored in -80°C until day of analysis.

4.3.2. DNA extraction and bisulfite conversion

Genomic DNA (gDNA) was extracted using DNeasy Blood and Tissue kit (69506, Qiagen) according to manufacturer’s recommendations. Bisulfite conversion was performed on 250 ng of gDNA using the EZ DNA methylation kit (D5001, Zymo Research). Single stranded DNA quantity and quality were measured by Nanodrop spectrophotometer.

4.3.3. High-Resolution Melt (HRM) assays

HRM assays were performed as previously described for *Cyp2e1* and *Sult1a1* (Kronfol et al). Briefly, 20 ng of bisulfite converted DNA was amplified on Quantstudio 3 using MeltDoctor

reagents (Applied Biosystems), 0.2 μ M forward and 0.2 μ M reverse primer. For primer and product sequence refer to **Table 2.2** and **Table 3.2**. Samples were amplified by qPCR as follows 10min hold at 95°C followed by 45 cycles of: 15sec at 95°C, 60sec at 60°C or 57°C for *Sult1a1* or *Cyp2e1* respectively, followed by a melt curve stage. The High-Resolution Melt assays measured the methylation of 7 and 1 CpG levels for *Cyp2e1* and *Sult1a1* regions respectively. The Net Temperature Shift values (Newman et al. 2012) of the all samples were interpolated on the standard curve to yield their 5mC percentage. A standard consisting of 0, 5, 10, 25, 50, 75, and 100% methylated mouse genomic DNA was included on each plate (EpigenDx). Both the standard and the test samples were run in triplicates.

4.3.4. Statistics

Pearson correlation tests were conducted in R version 3.6.1 (www.r-project.org) with $\alpha=0.05$.

4.4. Results

4.4.1. *Cyp2e1* tissue-specific methylation and cross-tissue correlation

The mean 5-MethylCytosine (5mC) levels of *Cyp2e1* in descending order were as follows whole blood (93.5%), rest of brain after hippocampus and cortex were removed (66.3%), cortex (53.7%), hippocampus (43.5%), and liver (9.3%) (**Figure 4.1 a**). 5mC typically exerts a repressive influence on gene expression; therefore, we should expect the inverse of this pattern of descending order for expression in these tissues. This is broadly the case, with *Cyp2e1* tissue-dependent gene expression being highest in liver and lowest in blood, with the brain as an intermediate (**Figure 4.2 a**). *Cyp2e1* 5mC levels derived from whole blood were negatively correlated with those from the liver ($r = -0.35$, $p = 0.03$) but not with 5mC levels of any of other tissues ($p > 0.05$) (**Figure 4.1 a**). This indicates that an inverse relationship exists between *Cyp2e1* 5mC levels in the liver and those of whole blood.

4.4.2. *Sult1a1* tissue-specific methylation and cross-tissue correlation

The mean 5mC levels of *Sult1a1* in descending order were as follows whole blood (75%), rest of brain regions (50.3%), liver (39.6%), hippocampus (23.3%), and cortex (22.4%) (**Figure 4.1 b**). This pattern, however, does not resemble that of *Sult1a1* tissue-dependent gene expression indicating that additional factors regulate tissue-specific gene expression of *Sult1a1* than 5mC alone (**Figure 4.2 b**). 5mC levels derived from liver *Sult1a1* were positively correlated with those in the rest of brain ($r = 0.71$, $p = 0.03$), negatively with blood ($r = -0.16$, $p = 0.04$), but not with the 5mC levels of the other brain regions tested ($p > 0.05$) (**Figure 4.1 b**). In addition, blood 5mC levels were negatively correlated with the rest of brain ($r = -0.35$, $p = 0.02$) (**Figure 4.1 b**). Overall, these results indicate an inverse relationship exists between 5mC levels in the liver and whole blood for *Sult1a1*. However, the relationship between blood and liver seems weaker than

that of blood and brain. Therefore, blood *Sult1a1* 5mC measurements are most accurate predictors of that of brain regions, excluding the cortex and hippocampus, followed by the liver.

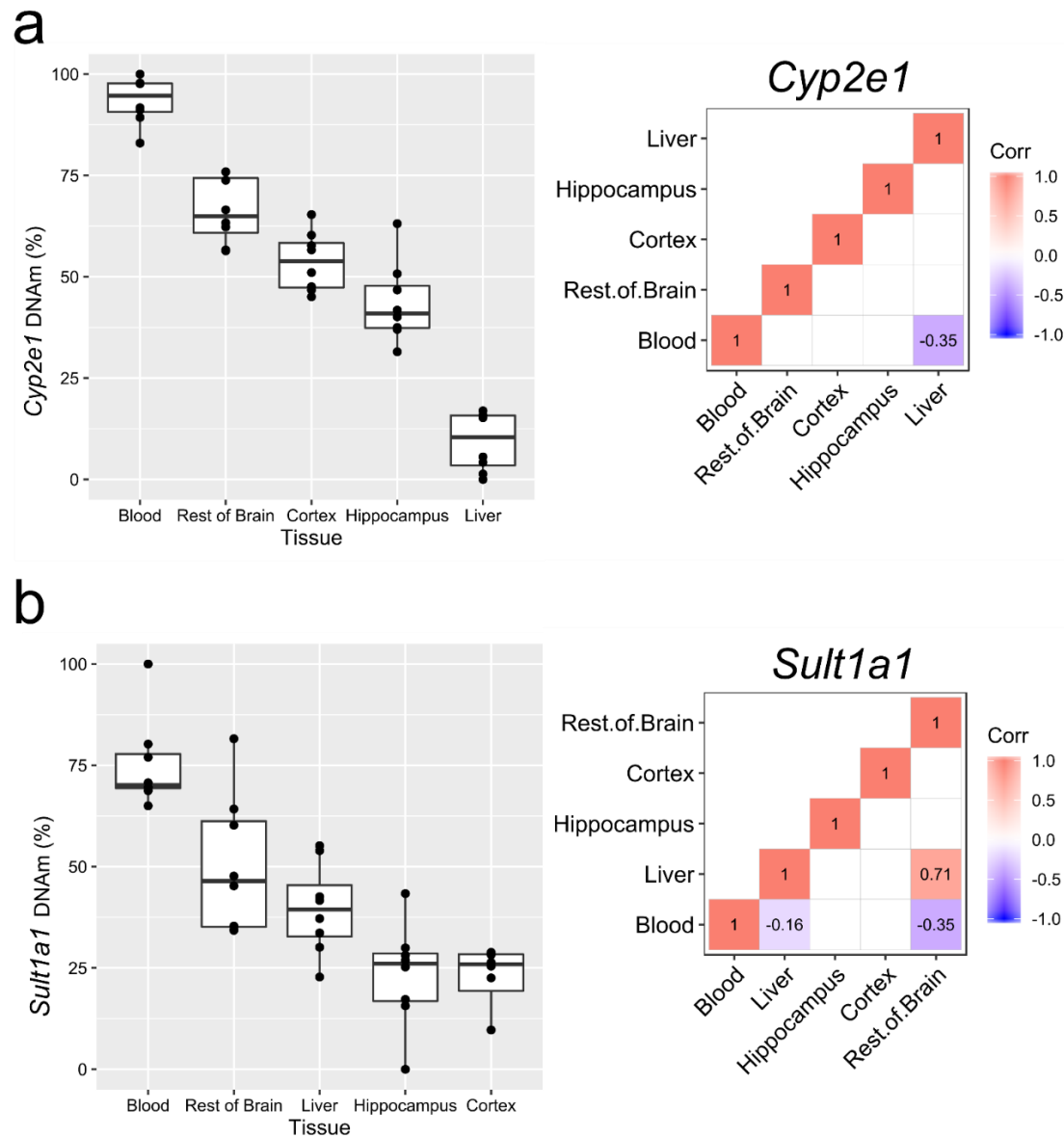


Figure 4.1. Boxplot of DNA methylation percent (DNAm) across the liver, rest of brain, cortex, hippocampus, and whole blood arranged in descending order and Correlation matrix reporting Pearson correlation statistical test result (r) for either (a) *Cyp2e1* (N=40, n=8) or (b) *Sult1a1* (N=40, n=8). White blank cells indicate non-significant association ($p>0.05$). Refer to **Table 4.1** and **4.2** for individual p-values of each Pearson correlation test of a given pair. Color gradient

indicates the direction of effect of the association with dark red representing the strongest positive association of 1 while dark blue representing the strongest negative association of -1. Only lower half of the plot is shown to prevent redundancy in reporting the results.

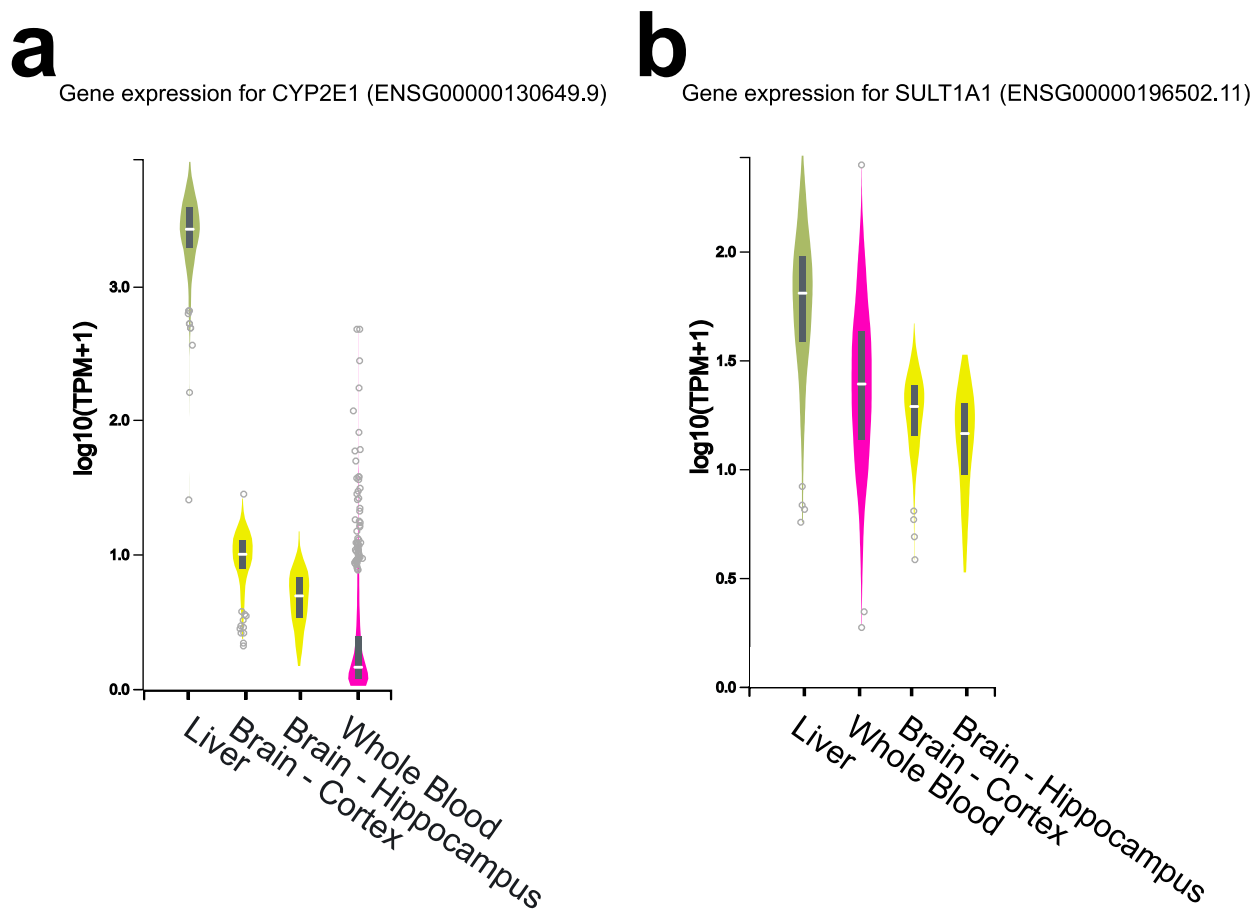


Figure 4.2. Violin plot showing average expression of either (a) CYP2E1 or (b) SULT1A1 across liver, whole blood, hippocampus, and cortex. Data obtained and plotted from GTEx Analysis Release V8 (dbGaP Accession phs000424.v8.p2). TPM: Transcripts Per Million.

	Blood	Rest of Brain	Cortex	Hippocampus	Liver
Blood	0				
Rest of Brain	0.1027	0			
Cortex	0.5319	0.9417	0		
Hippocampus	0.1405	0.2067	0.2323	0	
Liver	0.0301	0.1374	0.9634	0.4397	0

Table 4.1 *Cyp2e1* P-values for each pair of tissue types

	Blood	Liver	Hippocampus	Cortex	Rest of Brain
Blood	0				
Liver	0.0423	0			
Hippocampus	0.2947	0.1223	0		
Cortex	0.9754	0.7008	0.1884	0	
Rest of Brain	0.0258	0.0399	0.0899	0.5042	0

Table 4.2 *Sult1a1* P-values for each pair of tissue types

Significant p-values ($p < 0.05$) are highlighted in **red**

4.5. Discussion

We previously determined the extent and direction of effect of age-related changes to 5mC levels at *Cyp2e1* in the liver (Kronfol et al 2020). Here, we expanded our understanding of tissue-specific variation to 5mC in not only peripheral tissue (whole blood), but also the different regions of the brain that have significant expression of *Cyp2e1* and *Sult1a1*. Furthermore, we showed that variation in 5mC levels of *Cyp2e1* and *Sult1a1* in the liver are inversely reflected in 5mC levels at these genes in whole blood. The size of the inverse correlations was relatively large (approximately -0.3). This work confirms a relationship between 5mC levels at these two genes in different tissues of the same subject and could pave the way for similar studies in humans.

Considering our findings in terms with previous work, we found equivalent levels of 5mC as previously reported in mouse liver (Kronfol et al 2020) and blood (Peters et al 2015). In addition, for *Cyp2e1*, our data suggest that only 5mC levels in the liver are correlated with 5mC levels in blood. 5mC from other specimens (DNA from buccal or nasal swab, etc) should be investigated for correlation with that of different brain regions. For *Sult1a1*, the data suggest blood-derived 5mC is more correlated with 5mC of the brain, excluding the hippocampus and the cortex, than with the liver. In addition, tissue-specific gene expression of *Sult1a1* might be influenced by other factors than 5mC alone. Histone post translational modifications could also play a role, but these do not function well as biomarkers because they must be assayed from fixed chromatin, not DNA that is more readily available.

A limitation of our study, in the context of the broader substantive focus of this dissertation, is that we did not study how cross-tissue 5mC correlations change with age. Given the negative correlation between 5mC levels in blood and liver on *Cyp2e1* in young age, we can

predict that any age-related change may also be negatively correlated. Such that if we see age-related hypermethylation in the liver, we will see hypomethylation in blood. In addition, we typically see regions that are constitutively methylated at young age, like blood 5mC in this case, become hypomethylated due to epigenetic drift and attrition with age (Issa 2014; Jones et al. 2015; Zhu et al. 2018). Nonetheless, this study explicitly looked at the lower end of the mouse adulthood of an age of 5 months and the data should serve as a reference for future investigations of the relative baseline levels of 5mC in the brain, liver, and blood at older ages.

Limitations of this study include the exclusion of female mice. However, we anticipate that this should be included in future, larger studies. Studies intended to examine a wider range of the adult life of mice could be performed, or similar studies could be attempted for humans if DNA from multiple tissues (e.g. blood, liver) can be obtained from the same individuals. This may be possible from some biobanks. Finally, more work is needed to establish whether the extent of the relationship between 5mC on drug metabolism genes in blood and liver can be clinically useful as a proxy to guide drug dosing decisions.

Chapter 5: Method optimization of Reduced Representation Bisulfite Sequencing (RRBS) for genome-wide analysis of mouse liver DNA methylation

5.1. Abstract

DNA methylation is the most widely studied epigenetic mark to date. Several methods have been proposed to aid the accurate measurement of DNA methylation in the context of Cytosine-Phosphate-Guanine (CpG) positions in mammalian genomes. However, few have been adopted and implemented for different applications as much as reduced representation bisulfite sequencing (RRBS). RRBS has been widely used to optimize DNA methylation detection from tissues and cells, yet few methodologies expand the sequencing library preparation portion of RRBS. We proposed to augment the RRBS protocol using a commercially available Adaptase library technology to create optimized library complexity intended for the detection of CpG DNA methylation from mouse liver tissue belonging to young (4 months) and old ages (32 months). We report that this optimization produced high yields of RRBS libraries with consistent DNA fragment distributions between both ages and high proportions of shared number and positions of Cytosines assayed per age. We first start with the same procedure of column-based DNA extraction that is then enzymatically cut by Msp I, a methylation indifferent restriction enzyme. However, we perform DNA fragment size-selection of 100-220 bp followed by bisulfite conversion to this cut DNA before initiating the Adaptase library preparation protocol.

5.2. Introduction

Reduced Representation Bisulfite Sequencing (RRBS) is a robust method for detecting methylation and has been carried out by researchers for more than a decade and cited over 800 times (Meissner et al. 2005). We propose to optimize the current technique by coupling it with the Adaptase advanced library amplification technology for the detection of CpG DNA methylation obtained from mouse liver tissue. This method optimization effort will serve as the primary assay for a larger aging epigenome-wide association study by our group. We focus on DNA methylation because it is the best-characterized epigenetic mark, both overall and in the context of aging.

Our method of choice, RRBS, is robust and cost-effective, providing good coverage of CpGs in genes and regulatory regions (Gu et al. 2011). RRBS is not new, however, its application to aging and drug metabolism is highly innovative, because future findings may shed light on mechanisms of aging and open new avenues of research into novel biomarker strategies. We propose to use RRBS specifically for several reasons. Genome-wide DNA methylation analysis is typically carried out using microarrays or next generation sequencing (NGS) (Rakyan et al. 2011). Methylation arrays for humans are excellent, with the Illumina Infinium capable of measuring 5mC at ~850,000 loci. However, there are no equivalent arrays for mice. The best option we are aware of is the Mouse CpG Island Microarray from Agilent, which can assay ~90,000 loci, much less than the human arrays. However, the extent of genome-wide coverage offered by arrays of any kind is poor relative to Next Generation Sequencing (NGS). The gold-standard for genome-wide DNA methylation analysis is whole genome bisulfite sequencing (WGBS) (Lister et al. 2009; Rakyan et al. 2011). Here, the entire genome is subjected to bisulfite treatment and sequenced to high depth of coverage, providing single base resolution of

methylation. This makes it very attractive, but it is still too costly for the large numbers of samples required for association studies. RRBS, on the other hand, is an excellent compromise. Using enzymatic digestion at CpG sites followed by fragment size selection, the sequencing libraries are enriched for regions of the genome with high CpG density, which are often important regulatory regions. By trading full genome-wide coverage for high-resolution at these important loci, RRBS requires just ~20 million reads per sample, thereby enabling sufficient numbers to be assayed for an association study (Gu et al. 2011).

We focused on 5-methylCytosine (5mC) instead of other DNA modifications for various reasons. Although other DNA modifications have been discovered, 5-hydroxymethylcytosine (5hmC) (Kriaucionis and Heintz 2009; Pastor et al. 2011) or 5-formylcytosine (5fC) (Bachman et al. 2015), the role of 5mC in cell differentiation and regulation is the best-characterized, meaning that 5mC results are more readily interpretable. Furthermore, the bisulfite sequencing approach (RRBS) (Meissner et al. 2005; Gu et al. 2011) that we intend to optimize works by converting unmethylated cytosines to uracils via sodium bisulfite treatment (which then convert to thymines in PCR) (Frommer et al. 1992).

Previous epigenome-wide association studies of liver tissue have used RRBS methods that prepare sequencing libraries in a conventional way (Hahn et al. 2017; Stubbs et al. 2017). However, a recent systematic evaluation of library preparation methods by Li et al. ((Zhou et al. 2019) shows that the new Adaptase technology outperforms traditional library techniques. The authors conclude that libraries prepared by Adaptase achieve the highest proportion of CpGs assayed, most effective sequencing coverage, and lowest proportion of low-quality reads. No published reports utilize this new technology for liver RRBS. Therefore, we wanted to implement the Adaptase method in the RRBS protocol for liver DNA. We took this novel

method to see how it performs in test samples and obtain quality control information. Briefly, the Adaptase enzyme maximizes the recovery of low concentrations of single stranded DNA by ubiquitous ligation and priming by universal tags. This ensures successful subsequent amplification of all DNA fragments. Thus, preserving DNA information and library complexity.

We subjected 600 ng of genomic DNA from mouse liver to DNA methylation analysis by RRBS using the commercially available Adaptase technology in the ACCEL NGS Methyl-Seq Kit (Swift Bioscience). This involved Msp I digestion of DNA, size-selection, bisulfite conversion, simultaneous tailing and ligation by Adaptase of all single stranded DNA fragments, 3' extension, bottom strand ligation, and finally unique sequencing adapter ligation through PCR amplification to produce the final sequencing library (**Figure 5.1**). Library size distribution and integrity was validated using the high-sensitivity DNA chip on an Agilent BioAnalyzer. Multiplexed pair end 150bp sequencing was carried out on an Illumina HiSeq 4000 at the GeneWiz service provider sequencing facilities. We carried out NGS on 4 test samples. We aimed to exceed the recommended 20-25 million reads needed to obtain enough coverage depth for accurate methylation measurement.

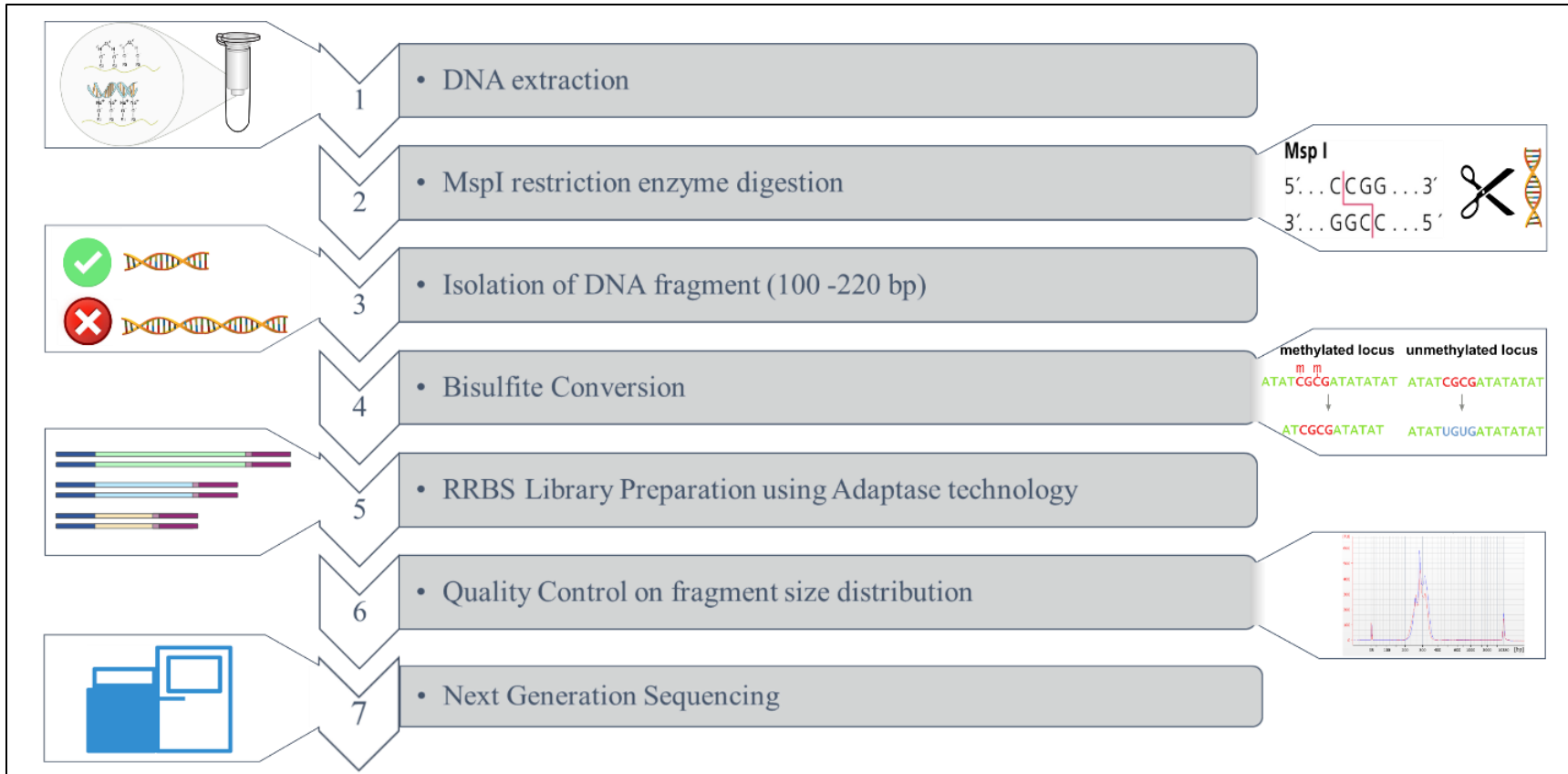


Figure 5.1. Schematic representation of the seven steps of the optimized RRBS protocol.

5.3. Method

5.3.1. Sample

Genomic DNA was obtained from 20 mg liver tissue of 4 months old sample and a 32 months old sample using the AllPrep DNA/RNA kit (Qiagen). DNA quality and quantity were measured on Nanodrop spectrophotometer (ThermoFisher) and Qubit 4.0 (ThermoFisher) respectively.

5.3.2. Reduced Representation Bisulfite Sequencing (RRBS)

RRBS libraries were prepared as previously described (Gu et al. 2011) with slight modifications. 600 ng genomic DNA was cut enzymatically by Msp I (R0106T, New England Biolabs, Ipswich, MA) overnight (16hrs) at 37 °C, then purified the next day by QIAquick PCR purification kit (Qiagen). The purified Msp I digested DNA was run on a 2% ethidium bromide agarose gel adjacent to a paired lane of genomic DNA of the same sample to check for successful Msp I digest. Unsuccessful digests were repeated. The sample was size selected for fragments between 100-220 base pair (bp) long using the 2% ethidium-free agarose gel cassette (CEF2010, Sage Science, Beverly, MA) on a Pippin Prep machine. The Pippin Prep protocol was set to the “Range” collection mode and reference lane 3 was used for the provided marker E. Samples were collected from the elution module using 40µL of provided electrophoresis buffer. The size selected Msp I digested DNA was bisulfite converted by the EZ DNA methylation kit (D5001, Zymo Research, Irvine, CA) according to manufacturer’s recommendation. Briefly, samples were incubated at 37 °C for 15 min followed by overnight (16hrs) incubation with 100µL of provided CT conversion reagent at 50 °C to allow the deamination process of unmethylated cytosines into uracils to occur. Samples were eluted in a final 10µL elution buffer. 2 µL was used to measure the concentration of the samples using the ssDNA Qubit assay

(Q10212, ThermoFisher). Samples with concentration below detection range were repeated. Finally, about 3 ng of Msp I digested, size-selected, and bisulfite converted DNA was used as input for the ACCEL-NGS Methyl-Seq DNA Library kit (30024, Swift Bioscience) to create the RRBS libraries.

Briefly, 8 μ L of sample was mixed with provided low EDTA TE buffer q.s 15 μ L and incubated at 95 °C for 2min and then placed on ice, spun down and added to 25 μ L of Adaptase reaction mixture. The Adaptase reaction mixture components are 11.5 μ L of low EDTA TE, 4 μ L each of provided Buffer G1 and Reagent G2, 2.5 μ L Reagent G3, and 1 μ L each of Enzyme G4, 5, and 6. The mixture was incubated at 37 °C for 15 min, then at 95 °C for 2 min. The samples were kept on ice followed by the addition of 44 μ L of Extension Reaction mixture containing the following, 2 μ L Reagent Y1, 42 μ L Enzyme Y2. The samples were mixed and incubated at 98°C for 1 min, followed by 62 °C for 2 min and 65 °C for 5 min and a 4°C hold. The samples were then cleaned up from reaction components using 134 μ L of SpriSelect beads (Beckman-Coulter). The samples were eluted in 15 μ L low EDTA TE and added to 15 μ L of the Ligation mixture. The Ligation mixture contained 3 μ L Buffer B1, 10 μ L Reagent B2, 2 μ L Enzyme B3. The samples were incubated at 25 °C for 15min. The samples were cleaned up from reaction components with 42 μ L beads. The samples were eluted in 20 μ L low EDTA TE buffer. 5 μ L of unique index from Methyl-Seq Set A indexing kit was used per sample (36024, Swift Bioscience). Each of the young and old sample was run twice with different indices. 25 μ L of PCR reaction mixture was added that contained the following 10 μ L low EDTA TE buffer, 10 μ L Buffer R1, 4 μ L Reagent R2, 1 μ L Enzyme R3 and allowed to amplify on Proflex thermal cycler (Applied Biosystems). PCR conditions were as follows 98 °C for 30 sec followed by 10 cycles of 98°C for 10sec, 60°C for 30sec, 68°C for 60sec, and a final hold at 4°C. PCR reaction was cleaned up twice with 50 μ L

of SpriSelect beads following manufacturer's recommendation for libraries intended for sequencing on patterned flow cells such as HiSeq4000. Final libraries were eluted in 22 μ L low EDTA TE and 1 μ L was used to measure concentration using the DS DNA Qubit assay (ThermoFisher). 1 μ L was used to trace the size-distribution and average library size on the HS DNA chip on Agilent 2100 Bioanalyzer. Libraries were sequenced pair ended 150 bp on Illumina HiSeq4000 using 5% Phi-X spike-in (as positive control for successful sequencing run) by GeneWiz service provider. Each RRBS sample yielded a single Fastq file. The reverse reads were discarded.

5.3.3. Data processing

Sequencing reads (FASTQ files) were mapped to the mouse genome (mm10) and methylation calls are made using Bismark (Krueger and Andrews 2011), which is based on Bowtie (Langmead and Salzberg 2012). Bismark yielded for each RRBS sample a quality control file and one coverage file per sample with CpG position and methylation information, expressed as unmethylated and methylated reads at each CpG.

5.4 Results

5.4.1. DNA extraction, MspI digestion, and fragment isolation

DNA extraction from the mouse liver samples was successful with mean DNA concentration of 120 ng/ μ L with an average 260/280 value of 2.0 [1.93-2.06]. 600 ng of genomic DNA was enzymatically cut with MspI and was size selected for fragment between 100-220 bp, which gave the highest resulting yield of 0.5-1% w/w, which was within expected range (Meissner et al. 2005).

5.4.2. RRBS library preparation and Quality control

3ng was used as input for library preparation. Library amplification was successful with a final library concentration of 12.9 ng/ μ L for an average of 258 ng per sample. Average library size and molarity was 301 bp and 63.6 nMol respectively. Our RRBS library distribution shows a unique pattern of three distinct peaks similar to those previously reported. Three unique peaks at 259, 282, and 316 bp were present in the BioAnalyzer trace of the RRBS libraries (**Figure 5.2**). Each peak represents high abundance of fragments of similar fragment sizes. This peak profile is a characteristic of enzymatically digest DNA fragment by MSP I.

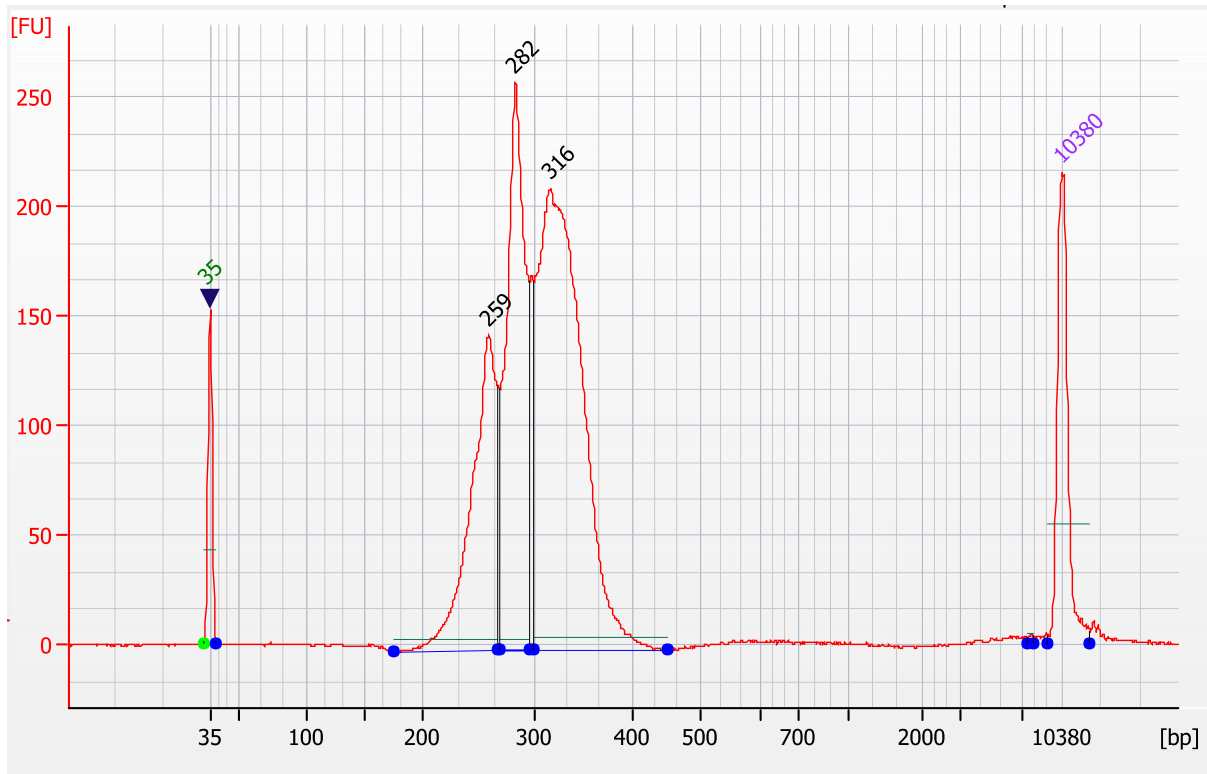


Figure 5.2. Representative RRBS library trace. Showing peaks distinct to RRBS libraries at 259, 282, 316 bp. X-axis is Arbitrary fluorescence units [FU], y-axis is fragment size in base pair [bp]. A peak at 35 and 10380 bp indicate the lower and upper ladder marks for the High sensitivity 2100 BioAnalyzer assay.

Age (months)	Sample ID	Index	Index sequence
4	4-11 replicate 1	I4	TGACCA(AT)
4	4-11 replicate 2	I2	CGATGT(AT)
32	32-15 replicate 1	I5	ACAGTG(AT)
32	32-15 replicate 2	I16	CCGTCC(CG)

Table 5.1. Summary table reporting chronological age (months) and ID of each sample, index and index sequence used.

Age (months)	Total number of reads	Total number of Unique Alignments	Proportion of Unique Alignments
4m rep1	37,014,015	19,576,596	0.549
4m rep2	54,032,672	27,520,231	0.509
32m rep1	57,122,708	28,007,798	0.490
32m rep2	41,196,659	16,898,265	0.410

Table 5.2. Summary table reporting average total number of reads and total number of Unique Alignments per age (months)

Age (months)	Number of Cytosines assayed post-QC	Cytosines in common across 2 replicates	Proportion in common across 2 replicates
4m rep1	1,048,263	1,029,626	0.982
4m rep2	1,171,890		
32m rep1	1,176,430	1,026,686	0.978
32m rep2	1,050,249		

Table 5.3. Summary table reporting number of unique cytosines captured per replicate after quality control (n reads per cytosine: $10 < C > 300$)

5.4.3. Next Generation Sequencing (NGS) data

Bismark was run according to default settings for RRBS fastq files (Krueger and Andrews 2011). Reference mouse genome used was mm10. Bismark output included a summary file and a methylation coverage file per sample. Total sequences analyzed for each replicate of

the 4 and 32 months samples respectively are shown in **Table 5.2**. Reads with unique alignments per sample ranged from 16.9M to 28M per sample/replicate (**Table 5.2**). The percentage of unique alignment to total sequence analyzed was approximately 50% for 3 of the 4 samples. These values improve upon previously reported results from traditional RRBS (Chatterjee et al. 2012). while replicate 2 of the 32 month sample was somewhat lower at 41% and this made the average percentage alignment for the 32 month samples somewhat lower (**Figure 5.3 a**). Quality control (QC) of cytosine position coverage was set at the levels used by Stubbs et al. whereby sites with 10 or fewer reads and those with 300 or more reads are discarded. Despite replicate 2 of the 32 month sample having least aligned reads (**Table 5.2**), the number of Cytosine positions with good data, i.e. 1,050,249 after QC, was still slightly more than for replicate 1 of the 4 month sample (**Table 5.3**). Overall, despite the number of uniquely aligned read numbers differing by a factor of 1.6 across the samples, the number of Cytosine positions passing QC was remarkably similar. Most importantly, replicates returned high quality quantitative information for almost the same sets of approximately 1 million Cytosine positions (98% the same) despite there being approximately 20 million CpGs in the mouse genome. This showed that the replicates were highly consistent in the regions of the genome they captured.

The percentage 5mC (in CpG context) was 37.25 and 33.85 % for the 4 and 32 months respectively (**Figure 5.3 b**). The percentage of non CpG methylation detected was about less than 1.5 % for both ages. This data suggests that the sequencing of the RRBS libraries was successful with equivalent numbers of total cytosine detected for both ages. However, a clear decrease in the CpG methylation calls was present in the 32 months (old) age compared to the 4 months (young) age. This effect direction mirrors that observed using ELISA global assay in previous section of this dissertation (see Chapter 2 **Figure 2.6**)

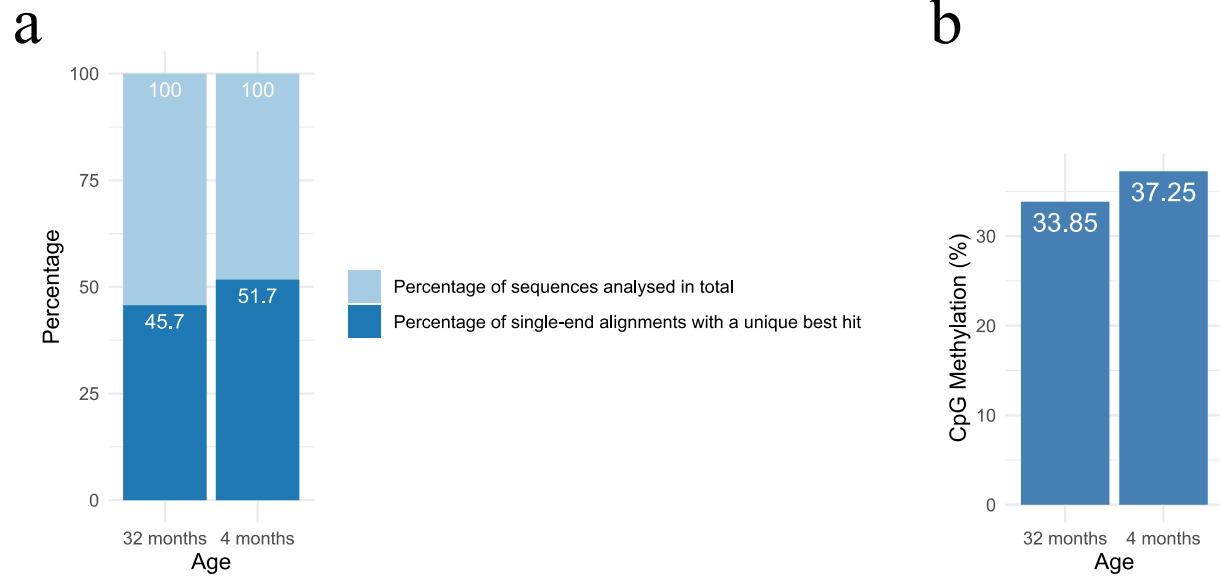


Figure 5.3. Bar plot of data from Bismark quality report showing (a) Percentage of total and unique alignments per age and (b) CpG methylation percent per age.

5.5. Discussion

We previously initiated a set of studies investigating liver specific methylation changes with age at candidate genes involved in phase I and II metabolism. Our studies were based on a gene selection approach identified from large epigenome-wide association studies in human blood. Indeed, these studies demonstrated, to the best of our knowledge, the first evidence of the influence of age-related epigenetics changes on the pharmacokinetics of drug metabolizing enzymes. However, several other genes from these human studies showed varying degree of evidence of change with age. An estimated one third of all genes involved in ADME processes show various levels of association with age (Dozmorov 2015). Therefore, optimization of a highly reproducible method for the genome-wide quantitation of epigenetic marks at regions of regulatory importance was warranted. We demonstrated in this study the feasibility of using RRBS to quantify 5mC from mouse liver DNA of old and young age that can be leveraged to larger epigenome-wide aging studies. This is an ongoing effort in our lab, where we will attempt to elucidate the degree of age-related variation of 5mC on genes controlling the attributes of mouse hepatic metabolism on a genome-wide basis.

Chapter 6: Overall Conclusions and Future Directions

Through this work we have demonstrated a novel approach for answering an overarching question of what additional determinants of biological variability are affecting drug metabolism in advanced age. Our hypothesis that epigenetic mechanisms such as DNA methylation and histone modifications influence drug metabolism with age was warranted in order to set the stage for new technologies to overcome the limitations of current tools used in the clinic that guide drug dosing decisions in the older adult population. We aimed to elucidate the nature of the relationship between epigenetic dysregulation and the function of drug metabolizing enzymes in advanced age. In fact, we were able to define the continuity of the relationship from DNA to function in a unique set of experiments that, to the best of our knowledge, have not been pursued before. In addition, this work described the influence of epigenetics on genes encoding both phase I and II metabolizing enzymes. We show that both phases are under the influence of age-related epigenetic change with varying degrees and through shared and distinctive mechanisms. For phase I, we showed that the *Cyp2e1* gene is under the influence of age-related changes to 5mC and histone acetylation (H3K9ac). The degree of effect on the downstream function of CYP2E1 is substantial for both epigenetic marks. On the other hand, while 5mC and H3K9ac levels at the *Sult1a1* phase II metabolism gene changed with age, only H3K9ac was shown to influence expression.

Epigenetic modifications have demonstrated clinical usefulness through successful examples, such as the use of DNA methylation as a clinical biomarker to guide drug selection. For example, *MGMT* methylation status is now being used clinically to guide treatment selection for glioma multiforme patients. We believe DNA methylation could be utilized in the clinic as a clinical biomarker to guide drug dosing decisions for older adults. Although H3K9ac was a

better predictor of function for both *Cyp2e1* and *Sult1a1*, it is difficult to conceive of histone modifications being used as clinical biomarkers using the methods we employed here (chromatin immunoprecipitation). Alternative, novel methods that are more rapid and robust will be needed before histone acetylation can see widespread use as a clinical biomarker.

DNA methylation is easy to obtain from peripheral tissue such as blood. Here, we demonstrated correlations between levels of 5mC in the liver for *Cyp2e1* and *Sult1a1* and those in whole blood. These relationships suggest that blood-based biomarkers may reflect hepatic 5mC levels and these may be useful to guide drug dosing in the future. However, significant additional work in humans will be necessary to demonstrate the feasibility of this innovation.

The work as presented here serves as a first step towards future research aimed at evaluating the utility of epigenetics in the clinic. Our group is in the process of pursuing a larger ageing study that examines the degree of genome-wide 5mC change with age in a mouse model. We believe that similar efforts might be underway and along with ours will serve the aging community to alleviate one of the major problems currently facing the older adult population, adverse events in pharmacological therapy.

References

- Abdel-Hameed EA, Ji H, Shata MT (2016) HIV-Induced Epigenetic Alterations in Host Cells. *Adv Exp Med Biol* 879:27–38. https://doi.org/10.1007/978-3-319-24738-0_2
- Aberg KA, McClay JL, Nerella S, et al (2014) Methylome-Wide Association Study of Schizophrenia: Identifying Blood Biomarker Signatures of Environmental Insults. *JAMA Psychiatry* 71:255–264. <https://doi.org/10.1001/jamapsychiatry.2013.3730>
- Absher DM, Li X, Waite LL, et al (2013) Genome-wide DNA methylation analysis of systemic lupus erythematosus reveals persistent hypomethylation of interferon genes and compositional changes to CD4+ T-cell populations. *PLoS Genet* 9:e1003678. <https://doi.org/10.1371/journal.pgen.1003678>
- Aguet F, Brown AA, Castel SE, et al (2017) Genetic effects on gene expression across human tissues. *Nature* 550:204–213. <https://doi.org/10.1038/nature24277>
- Amacher DE (2016) A 2015 survey of established or potential epigenetic biomarkers for the accurate detection of human cancers. *Biomarkers* 21:387–403. <https://doi.org/10.3109/1354750X.2016.1153724>
- Anjum S, Fourkala E-O, Zikan M, et al (2014) A BRCA1-mutation associated DNA methylation signature in blood cells predicts sporadic breast cancer incidence and survival. *Genome Med* 6:47. <https://doi.org/10.1186/gm567>
- Babenko VN, Chadaeva IV, Orlov YL (2017) Genomic landscape of CpG rich elements in human. *BMC Evol Biol* 17:. <https://doi.org/10.1186/s12862-016-0864-0>
- Bachman M, Uribe-Lewis S, Yang X, et al (2015) 5-Formylcytosine can be a stable DNA modification in mammals. *Nat Chem Biol* 11:555–557. <https://doi.org/10.1038/nchembio.1848>
- Bannister AJ, Kouzarides T (2011) Regulation of chromatin by histone modifications. *Cell Res* 21:381–395. <https://doi.org/10.1038/cr.2011.22>
- Barrera LO, Li Z, Smith AD, et al (2008) Genome-wide mapping and analysis of active promoters in mouse embryonic stem cells and adult organs. *Genome Res* 18:46–59. <https://doi.org/10.1101/gr.6654808>
- Barzilai N, Huffman DM, Muzumdar RH, Bartke A (2012) The critical role of metabolic pathways in aging. *Diabetes* 61:1315–1322. <https://doi.org/10.2337/db11-1300>
- Benayoun BA, Pollina EA, Brunet A (2015) Epigenetic regulation of ageing: linking environmental inputs to genomic stability. *Nat Rev Mol Cell Biol* 16:593–610. <https://doi.org/10.1038/nrm4048>
- Bird A (2002) DNA methylation patterns and epigenetic memory. *Genes Dev* 16:6–21. <https://doi.org/10.1101/gad.947102>

- Bjornsson HT, Sigurdsson MI, Fallin MD, et al (2008) Intra-individual change in DNA methylation over time with familial clustering. *JAMA* 299:2877–2883. <https://doi.org/10.1001/jama.299.24.2877>
- Bock C (2009) Epigenetic biomarker development. *Epigenomics* 1:99–110. <https://doi.org/10.2217/epi.09.6>
- Bocklandt S, Lin W, Sehl ME, et al (2011) Epigenetic predictor of age. *PLoS ONE* 6:e14821. <https://doi.org/10.1371/journal.pone.0014821>
- Bonder MJ, Kasela S, Kals M, et al (2014) Genetic and epigenetic regulation of gene expression in fetal and adult human livers. *BMC Genomics* 15:860. <https://doi.org/10.1186/1471-2164-15-860>
- Booth LN, Brunet A (2016) The Aging Epigenome. *Mol Cell* 62:728–744. <https://doi.org/10.1016/j.molcel.2016.05.013>
- Bowers EM, Yan G, Mukherjee C, et al (2010) Virtual ligand screening of the p300/CBP histone acetyltransferase: identification of a selective small molecule inhibitor. *Chem Biol* 17:471–482. <https://doi.org/10.1016/j.chembiol.2010.03.006>
- Brauch H, Mürdter TE, Eichelbaum M, Schwab M (2009) Pharmacogenomics of Tamoxifen Therapy. *Clinical Chemistry* 55:1770–1782. <https://doi.org/10.1373/clinchem.2008.121756>
- Brunet A, Berger SL (2014) Epigenetics of aging and aging-related disease. *J Gerontol A Biol Sci Med Sci* 69 Suppl 1:S17-20. <https://doi.org/10.1093/gerona/glu042>
- Budnitz DS, Lovegrove MC, Shehab N, Richards CL (2011) Emergency hospitalizations for adverse drug events in older Americans. *N Engl J Med* 365:2002–2012. <https://doi.org/10.1056/NEJMsa1103053>
- Budnitz DS, Pollock DA, Weidenbach KN, et al (2006) National surveillance of emergency department visits for outpatient adverse drug events. *JAMA* 296:1858–1866. <https://doi.org/10.1001/jama.296.15.1858>
- Butkus B Hopkins Lab, Cepheid Developing Methylated DNA Panel for Breast Cancer Dx, Monitoring. In: *GenomeWeb*. <https://www.genomeweb.com/molecular-diagnostics/hopkins-lab-cepheid-developing-methylated-dna-panel-breast-cancer-dx>. Accessed 28 Feb 2020
- Butler JM, Begg EJ (2008) Free Drug Metabolic Clearance in Elderly People. *Clin Pharmacokinet* 47:297–321. <https://doi.org/10.2165/00003088-200847050-00002>
- Cancer Genome Atlas Research Network (2011) Integrated genomic analyses of ovarian carcinoma. *Nature* 474:609–615. <https://doi.org/10.1038/nature10166>
- Cardon LR, Harris T (2016) Precision medicine, genomics and drug discovery. *Hum Mol Genet* 25:R166–R172. <https://doi.org/10.1093/hmg/ddw246>
- Caro AA, Cederbaum AI (2004) Oxidative Stress, Toxicology, and Pharmacology of CYP2E1. *Annual Review of Pharmacology and Toxicology* 44:27–42. <https://doi.org/10.1146/annurev.pharmtox.44.101802.121704>

- Cazaly E, Charlesworth J, Dickinson JL, Holloway AF (2015) Genetic Determinants of Epigenetic Patterns: Providing Insight into Disease. *Mol Med* 21:400–409. <https://doi.org/10.2119/molmed.2015.00001>
- Chang S, Wang R-H, Akagi K, et al (2011) Tumor suppressor BRCA1 epigenetically controls oncogenic microRNA-155. *Nat Med* 17:1275–1282. <https://doi.org/10.1038/nm.2459>
- Chatterjee A, Stockwell PA, Rodger EJ, Morison IM (2012) Comparison of alignment software for genome-wide bisulphite sequence data. *Nucleic Acids Research* 40:e79–e79. <https://doi.org/10.1093/nar/gks150>
- Cheishvili D, Boureau L, Szyf M (2015) DNA demethylation and invasive cancer: implications for therapeutics. *Br J Pharmacol* 172:2705–2715. <https://doi.org/10.1111/bph.12885>
- Chiam K, Centenera MM, Butler LM, et al (2011) GSTP1 DNA Methylation and Expression Status Is Indicative of 5-aza-2'-Deoxycytidine Efficacy in Human Prostate Cancer Cells. *PLOS ONE* 6:e25634. <https://doi.org/10.1371/journal.pone.0025634>
- Christensen BC, Houseman EA, Marsit CJ, et al (2009) Aging and Environmental Exposures Alter Tissue-Specific DNA Methylation Dependent upon CpG Island Context. *PLOS Genetics* 5:e1000602. <https://doi.org/10.1371/journal.pgen.1000602>
- Chung C-W, Coste H, White JH, et al (2011) Discovery and characterization of small molecule inhibitors of the BET family bromodomains. *J Med Chem* 54:3827–3838. <https://doi.org/10.1021/jm200108t>
- Consortium TGte (2015) The Genotype-Tissue Expression (GTEx) pilot analysis: Multitissue gene regulation in humans. *Science* 348:648–660. <https://doi.org/10.1126/science.1262110>
- Daigle SR, Olhava EJ, Therkelsen CA, et al (2013) Potent inhibition of DOT1L as treatment of MLL-fusion leukemia. *Blood* 122:1017–1025. <https://doi.org/10.1182/blood-2013-04-497644>
- De Jager PL, Srivastava G, Lunnon K, et al (2014) Alzheimer's disease: early alterations in brain DNA methylation at ANK1, BIN1, RHBDF2 and other loci. *Nat Neurosci* 17:1156–1163. <https://doi.org/10.1038/nn.3786>
- Dejeux E, Rønneberg JA, Solvang H, et al (2010) DNA methylation profiling in doxorubicin treated primary locally advanced breast tumours identifies novel genes associated with survival and treatment response. *Mol Cancer* 9:68. <https://doi.org/10.1186/1476-4598-9-68>
- DeWoskin VA, Million RP (2013) The epigenetics pipeline. *Nat Rev Drug Discov* 12:661–662. <https://doi.org/10.1038/nrd4091>
- Dietrich D, Kneip C, Raji O, et al (2012) Performance evaluation of the DNA methylation biomarker SHOX2 for the aid in diagnosis of lung cancer based on the analysis of bronchial aspirates. *Int J Oncol* 40:825–832. <https://doi.org/10.3892/ijo.2011.1264>

- Dmitrijeva M, Ossowski S, Serrano L, Schaefer MH (2018) Tissue-specific DNA methylation loss during ageing and carcinogenesis is linked to chromosome structure, replication timing and cell division rates. *Nucleic Acids Research* 46:7022–7039. <https://doi.org/10.1093/nar/gky498>
- Dozmorov MG (2015) Polycomb repressive complex 2 epigenomic signature defines age-associated hypermethylation and gene expression changes. *Epigenetics* 10:484–495. <https://doi.org/10.1080/15592294.2015.1040619>
- Duron E, Hanon O (2008) Hypertension, cognitive decline and dementia. *Arch Cardiovasc Dis* 101:181–189. [https://doi.org/10.1016/s1875-2136\(08\)71801-1](https://doi.org/10.1016/s1875-2136(08)71801-1)
- EIDesoky ES (2007) Pharmacokinetic-pharmacodynamic crisis in the elderly. *Am J Ther* 14:488–498. <https://doi.org/10.1097/01.mjt.0000183719.84390.4d>
- ENCODE Project Consortium (2012) An integrated encyclopedia of DNA elements in the human genome. *Nature* 489:57–74. <https://doi.org/10.1038/nature11247>
- Entrevan M, Schuettengruber B, Cavalli G (2016) Regulation of Genome Architecture and Function by Polycomb Proteins. *Trends Cell Biol* 26:511–525. <https://doi.org/10.1016/j.tcb.2016.04.009>
- Ernst J, Kheradpour P, Mikkelson TS, et al (2011) Mapping and analysis of chromatin state dynamics in nine human cell types. *Nature* 473:43–49. <https://doi.org/10.1038/nature09906>
- Esteller M, Garcia-Foncillas J, Andion E, et al (2000) Inactivation of the DNA-Repair Gene MGMT and the Clinical Response of Gliomas to Alkylating Agents. *New England Journal of Medicine* 343:1350–1354. <https://doi.org/10.1056/NEJM200011093431901>
- Fackler MJ, Lopez Bujanda Z, Umbricht C, et al (2014) Novel methylated biomarkers and a robust assay to detect circulating tumor DNA in metastatic breast cancer. *Cancer Res* 74:2160–2170. <https://doi.org/10.1158/0008-5472.CAN-13-3392>
- Feil R, Fraga MF (2012) Epigenetics and the environment: emerging patterns and implications. *Nat Rev Genet* 13:97–109. <https://doi.org/10.1038/nrg3142>
- Feinberg AP (2007) Phenotypic plasticity and the epigenetics of human disease. *Nature* 447:433–440. <https://doi.org/10.1038/nature05919>
- Feinberg AP, Koldobskiy MA, Göndör A (2016) Epigenetic modulators, modifiers and mediators in cancer aetiology and progression. *Nat Rev Genet* 17:284–299. <https://doi.org/10.1038/nrg.2016.13>
- Filippakopoulos P, Knapp S (2014) Targeting bromodomains: epigenetic readers of lysine acetylation. *Nat Rev Drug Discov* 13:337–356. <https://doi.org/10.1038/nrd4286>
- Fillit H, Rockwood K, Young J (eds) (2017) *Brocklehurst's textbook of geriatric medicine and gerontology* Chapter 26, Eighth edition. Elsevier, Inc, Philadelphia, PA
- Fisel P, Schaeffeler E, Schwab M (2016) DNA Methylation of ADME Genes. *Clin Pharmacol Ther* 99:512–527. <https://doi.org/10.1002/cpt.343>

- Fishilevich S, Nudel R, Rappaport N, et al (2017) GeneHancer: genome-wide integration of enhancers and target genes in GeneCards. Database (Oxford) 2017:.
<https://doi.org/10.1093/database/bax028>
- Fornaro L, Vivaldi C, Caparello C, et al (2016) Pharmacoepigenetics in gastrointestinal tumors: MGMT methylation and beyond. *Front Biosci (Elite Ed)* 8:170–180
- Fraga MF (2009) Genetic and epigenetic regulation of aging. *Curr Opin Immunol* 21:446–453.
<https://doi.org/10.1016/j.coi.2009.04.003>
- Fraga MF, Ballestar E, Paz MF, et al (2005) Epigenetic differences arise during the lifetime of monozygotic twins. *Proc Natl Acad Sci USA* 102:10604–10609.
<https://doi.org/10.1073/pnas.0500398102>
- Fraga MF, Esteller M (2007) Epigenetics and aging: the targets and the marks. *Trends in Genetics* 23:413–418. <https://doi.org/10.1016/j.tig.2007.05.008>
- French SW (2013) The importance of CYP2E1 in the pathogenesis of alcoholic liver disease and drug toxicity and the role of the proteasome. *Subcell Biochem* 67:145–164.
https://doi.org/10.1007/978-94-007-5881-0_4
- Frommer M, McDonald LE, Millar DS, et al (1992) A genomic sequencing protocol that yields a positive display of 5-methylcytosine residues in individual DNA strands. *Proc Natl Acad Sci USA* 89:1827–1831
- Fu ZD, Csanaky IL, Klaassen CD (2012) Effects of Aging on mRNA Profiles for Drug-Metabolizing Enzymes and Transporters in Livers of Male and Female Mice. *Drug Metab Dispos* 40:1216–1225.
<https://doi.org/10.1124/dmd.111.044461>
- Gajer JM, Furdas SD, Gründer A, et al (2015) Histone acetyltransferase inhibitors block neuroblastoma cell growth in vivo. *Oncogenesis* 4:e137. <https://doi.org/10.1038/oncsis.2014.51>
- García-Giménez JL (2015) Epigenetic biomarkers and diagnostics. Academic Press
- Glatt H, Boeing H, Engelke CEH, et al (2001) Human cytosolic sulphotransferases: genetics, characteristics, toxicological aspects. *Mutation Research/Fundamental and Molecular Mechanisms of Mutagenesis* 482:27–40. [https://doi.org/10.1016/S0027-5107\(01\)00207-X](https://doi.org/10.1016/S0027-5107(01)00207-X)
- Goldberg AD, Allis CD, Bernstein E (2007) Epigenetics: a landscape takes shape. *Cell* 128:635–638.
<https://doi.org/10.1016/j.cell.2007.02.006>
- Gomez A, Karlgren M, Edler D, et al (2007) Expression of CYP2W1 in colon tumors: regulation by gene methylation. *Pharmacogenomics* 8:1315–1325. <https://doi.org/10.2217/14622416.8.10.1315>
- Gonzalo S (2010) Epigenetic alterations in aging. *Journal of Applied Physiology* 109:586–597.
<https://doi.org/10.1152/jappphysiol.00238.2010>

- Gu H, Smith ZD, Bock C, et al (2011) Preparation of reduced representation bisulfite sequencing libraries for genome-scale DNA methylation profiling. *Nat Protoc* 6:468–481. <https://doi.org/10.1038/nprot.2010.190>
- Hahn O, Grönke S, Stubbs TM, et al (2017) Dietary restriction protects from age-associated DNA methylation and induces epigenetic reprogramming of lipid metabolism. *Genome Biology* 18:56. <https://doi.org/10.1186/s13059-017-1187-1>
- Hannum G, Guinney J, Zhao L, et al (2013) Genome-wide Methylation Profiles Reveal Quantitative Views of Human Aging Rates. *Molecular Cell* 49:359–367. <https://doi.org/10.1016/j.molcel.2012.10.016>
- Hansen KH, Helin K (2009) Epigenetic inheritance through self-recruitment of the polycomb repressive complex 2. *Epigenetics* 4:133–138. <https://doi.org/10.4161/epi.4.3.8483>
- He Z-X, Chen X-W, Zhou Z-W, Zhou S-F (2015) Impact of physiological, pathological and environmental factors on the expression and activity of human cytochrome P450 2D6 and implications in precision medicine. *Drug Metab Rev* 47:470–519. <https://doi.org/10.3109/03602532.2015.1101131>
- Hegi ME, Diserens A-C, Gorlia T, et al (2005) MGMT Gene Silencing and Benefit from Temozolomide in Glioblastoma. *New England Journal of Medicine* 352:997–1003. <https://doi.org/10.1056/NEJMoa043331>
- Heyn H, Esteller M (2012) DNA methylation profiling in the clinic: applications and challenges. *Nat Rev Genet* 13:679–692. <https://doi.org/10.1038/nrg3270>
- Heyn H, Li N, Ferreira HJ, et al (2012) Distinct DNA methylomes of newborns and centenarians. *Proc Natl Acad Sci U S A* 109:10522–10527. <https://doi.org/10.1073/pnas.1120658109>
- Hildebrandt M, Adjei A, Weinshilboum R, et al (2009) Very important pharmacogene summary: sulfotransferase 1A1. *Pharmacogenet Genomics* 19:404–406. <https://doi.org/10.1097/FPC.0b013e32832e042e>
- Horvath S (2013) DNA methylation age of human tissues and cell types. *Genome Biology* 14:3156. <https://doi.org/10.1186/gb-2013-14-10-r115>
- Horvath S, Raj K (2018) DNA methylation-based biomarkers and the epigenetic clock theory of ageing. *Nature Reviews Genetics* 19:371–384. <https://doi.org/10.1038/s41576-018-0004-3>
- Human Ageing Genomic Resources Longevity Map. <http://genomics.senescence.info/>. Accessed 21 Nov 2019
- Hunt CM, Strater S, Stave GM (1990) Effect of normal aging on the activity of human hepatic cytochrome P450IIE1. *Biochemical Pharmacology* 40:1666–1669. [https://doi.org/10.1016/0006-2952\(90\)90470-6](https://doi.org/10.1016/0006-2952(90)90470-6)

- Hunter P (2015) The second coming of epigenetic drugs: a more strategic and broader research framework could boost the development of new drugs to modify epigenetic factors and gene expression. *EMBO Rep* 16:276–279. <https://doi.org/10.15252/embr.201540121>
- Imperiale TF, Ransohoff DF, Itzkowitz SH, et al (2014) Multitarget stool DNA testing for colorectal-cancer screening. *N Engl J Med* 370:1287–1297. <https://doi.org/10.1056/NEJMoa1311194>
- Ingelman-Sundberg M (2004a) Pharmacogenetics of cytochrome P450 and its applications in drug therapy: the past, present and future. *Trends Pharmacol Sci* 25:193–200. <https://doi.org/10.1016/j.tips.2004.02.007>
- Ingelman-Sundberg M (2004b) Human drug metabolising cytochrome P450 enzymes: properties and polymorphisms. *Naunyn-Schmiedeberg's Arch Pharmacol* 369:89–104. <https://doi.org/10.1007/s00210-003-0819-z>
- Irizarry RA, Ladd-Acosta C, Wen B, et al (2009) The human colon cancer methylome shows similar hypo- and hypermethylation at conserved tissue-specific CpG island shores. *Nat Genet* 41:178–186. <https://doi.org/10.1038/ng.298>
- Issa J-P (2002) Epigenetic variation and human disease. *J Nutr* 132:2388S-2392S. <https://doi.org/10.1093/jn/132.8.2388S>
- Issa J-P (2014) Aging and epigenetic drift: a vicious cycle. *J Clin Invest* 124:24–29. <https://doi.org/10.1172/JCI69735>
- Ito S, Shen L, Dai Q, et al (2011) Tet proteins can convert 5-methylcytosine to 5-formylcytosine and 5-carboxylcytosine. *Science* 333:1300–1303. <https://doi.org/10.1126/science.1210597>
- Ivanov M, Barragan I, Ingelman-Sundberg M (2014) Epigenetic mechanisms of importance for drug treatment. *Trends Pharmacol Sci* 35:384–396. <https://doi.org/10.1016/j.tips.2014.05.004>
- Ivanov M, Kacevska M, Ingelman-Sundberg M (2012) Epigenomics and interindividual differences in drug response. *Clin Pharmacol Ther* 92:727–736. <https://doi.org/10.1038/clpt.2012.152>
- Jabbari K, Bernardi G (2004) Cytosine methylation and CpG, TpG (CpA) and TpA frequencies. *Gene* 333:143–149. <https://doi.org/10.1016/j.gene.2004.02.043>
- Jaenisch R, Bird A (2003) Epigenetic regulation of gene expression: how the genome integrates intrinsic and environmental signals. *Nature Genetics* 33:245. <https://doi.org/10.1038/ng1089>
- Jenuwein T, Allis CD (2001) Translating the histone code. *Science* 293:1074–1080. <https://doi.org/10.1126/science.1063127>
- Jia L, Chang X, Qian S, et al (2018) Hepatocyte toll-like receptor 4 deficiency protects against alcohol-induced fatty liver disease. *Mol Metab* 14:121–129. <https://doi.org/10.1016/j.molmet.2018.05.015>
- Jones MJ, Goodman SJ, Kobor MS (2015) DNA methylation and healthy human aging. *Aging Cell* 14:924–932. <https://doi.org/10.1111/acel.12349>

- Jowaed A, Schmitt I, Kaut O, Wüllner U (2010) Methylation regulates alpha-synuclein expression and is decreased in Parkinson's disease patients' brains. *J Neurosci* 30:6355–6359. <https://doi.org/10.1523/JNEUROSCI.6119-09.2010>
- Kaut O, Schmitt I, Wüllner U (2012) Genome-scale methylation analysis of Parkinson's disease patients' brains reveals DNA hypomethylation and increased mRNA expression of cytochrome P450 2E1. *Neurogenetics* 13:87–91. <https://doi.org/10.1007/s10048-011-0308-3>
- Kent WJ, Sugnet CW, Furey TS, et al (2002) The Human Genome Browser at UCSC. *Genome Res* 12:996–1006. <https://doi.org/10.1101/gr.229102>
- Khan SN, Khan AU (2010) Role of histone acetylation in cell physiology and diseases: An update. *Clin Chim Acta* 411:1401–1411. <https://doi.org/10.1016/j.cca.2010.06.020>
- Kloten V, Becker B, Winner K, et al (2013) Promoter hypermethylation of the tumor-suppressor genes ITIH5, DKK3, and RASSF1A as novel biomarkers for blood-based breast cancer screening. *Breast Cancer Res* 15:R4. <https://doi.org/10.1186/bcr3375>
- Knights KM, Stresser DM, Miners JO, Crespi CL (2016) In Vitro Drug Metabolism Using Liver Microsomes. *Curr Protoc Pharmacol* 74:7.8.1-7.8.24. <https://doi.org/10.1002/cpph.9>
- Koh KH, Xie H, Yu A-M, Jeong H (2011) Altered cytochrome P450 expression in mice during pregnancy. *Drug Metab Dispos* 39:165–169. <https://doi.org/10.1124/dmd.110.035790>
- Kriaucionis S, Heintz N (2009) The nuclear DNA base 5-hydroxymethylcytosine is present in Purkinje neurons and the brain. *Science* 324:929–930. <https://doi.org/10.1126/science.1169786>
- Kronfol MM, Dozmorov MG, Huang R, et al (2017) The role of epigenomics in personalized medicine. *Expert Review of Precision Medicine and Drug Development* 2:33–45. <https://doi.org/10.1080/23808993.2017.1284557>
- Kronfol MM, Jahr FM, Dozmorov MG, et al (2020) DNA methylation and histone acetylation changes to cytochrome P450 2E1 regulation in normal aging and impact on rates of drug metabolism in the liver. *GeroScience*. <https://doi.org/10.1007/s11357-020-00181-5>
- Kronfol MM, McClay JL (2019) Chapter 14 - Epigenetic biomarkers in personalized medicine. In: Sharma S (ed) *Prognostic Epigenetics*. Academic Press, pp 375–395
- Krueger F, Andrews SR (2011) Bismark: a flexible aligner and methylation caller for Bisulfite-Seq applications. *Bioinformatics* 27:1571–1572. <https://doi.org/10.1093/bioinformatics/btr167>
- Krueger F, Kreck B, Franke A, Andrews SR (2012) DNA methylome analysis using short bisulfite sequencing data. *Nat Methods* 9:145–151. <https://doi.org/10.1038/nmeth.1828>
- Kurita M, Holloway T, García-Bea A, et al (2012) HDAC2 regulates atypical antipsychotic responses through the modulation of mGlu2 promoter activity. *Nat Neurosci* 15:1245–1254. <https://doi.org/10.1038/nn.3181>

- Kurmasheva RT, Sammons M, Favours E, et al (2017) Initial testing (stage 1) of tazemetostat (EPZ-6438), a novel EZH2 inhibitor, by the Pediatric Preclinical Testing Program. *Pediatr Blood Cancer* 64:. <https://doi.org/10.1002/pbc.26218>
- Ladabaum U, Mannalithara A (2016) Comparative Effectiveness and Cost Effectiveness of a Multitarget Stool DNA Test to Screen for Colorectal Neoplasia. *Gastroenterology* 151:427-439.e6. <https://doi.org/10.1053/j.gastro.2016.06.003>
- Ladd-Acosta C (2015) Epigenetic Signatures as Biomarkers of Exposure. *Curr Environ Health Rep* 2:117–125. <https://doi.org/10.1007/s40572-015-0051-2>
- Laird PW (2010) Principles and challenges of genome-wide DNA methylation analysis. *Nature Reviews Genetics* 11:191. <https://doi.org/10.1038/nrg2732>
- Lane AA, Chabner BA (2009) Histone deacetylase inhibitors in cancer therapy. *J Clin Oncol* 27:5459–5468. <https://doi.org/10.1200/JCO.2009.22.1291>
- Langmead B, Salzberg SL (2012) Fast gapped-read alignment with Bowtie 2. *Nat Methods* 9:357–359. <https://doi.org/10.1038/nmeth.1923>
- Lazarou J, Pomeranz BH, Corey PN (1998) Incidence of adverse drug reactions in hospitalized patients: a meta-analysis of prospective studies. *JAMA* 279:1200–1205. <https://doi.org/10.1001/jama.279.15.1200>
- Ledford H (2015) Epigenetics: The genome unwrapped. *Nature* 528:S12-13. <https://doi.org/10.1038/528S12a>
- Lee WH, Morton RA, Epstein JI, et al (1994) Cytidine methylation of regulatory sequences near the p1-class glutathione S-transferase gene accompanies human prostatic carcinogenesis. *Proc Natl Acad Sci USA* 91:11733–11737. <https://doi.org/10.1073/pnas.91.24.11733>
- Lee WM (2017) Public Health: Acetaminophen (APAP) Hepatotoxicity—Isn't It Time for APAP to Go Away? *J Hepatol* 67:1324–1331. <https://doi.org/10.1016/j.jhep.2017.07.005>
- Liang G, Gonzales FA, Jones PA, et al (2002) Analysis of gene induction in human fibroblasts and bladder cancer cells exposed to the methylation inhibitor 5-aza-2'-deoxycytidine. *Cancer Res* 62:961–966
- Lieber CS (1997) Cytochrome P-450E1: its physiological and pathological role. *Physiological Reviews* 77:517–544. <https://doi.org/10.1152/physrev.1997.77.2.517>
- Lister R, Pelizzola M, Downen RH, et al (2009) Human DNA methylomes at base resolution show widespread epigenomic differences. *Nature* 462:315–322. <https://doi.org/10.1038/nature08514>
- Liu Y, Zheng X, Yu Q, et al (2016) Epigenetic activation of the drug transporter OCT2 sensitizes renal cell carcinoma to oxaliplatin. *Sci Transl Med* 8:348ra97. <https://doi.org/10.1126/scitranslmed.aaf3124>
- Lucas D, Ferrara R, Gonzalez E, et al (1999) Chlorzoxazone, a selective probe for phenotyping CYP2E1 in humans. *Pharmacogenetics* 9:377–388. <https://doi.org/10.1097/00008571-199906000-00013>

- Luger K, Mäder AW, Richmond RK, et al (1997) Crystal structure of the nucleosome core particle at 2.8 Å resolution. *Nature* 389:251–260. <https://doi.org/10.1038/38444>
- Lunnon K, Smith R, Hannon E, et al (2014) Methylomic profiling implicates cortical deregulation of ANK1 in Alzheimer's disease. *Nat Neurosci* 17:1164–1170. <https://doi.org/10.1038/nn.3782>
- Mach J, Huizer-Pajkos A, Mitchell SJ, et al (2016) The effect of ageing on isoniazid pharmacokinetics and hepatotoxicity in Fischer 344 rats. *Fundam Clin Pharmacol* 30:23–34. <https://doi.org/10.1111/fcp.12157>
- Manolio TA, Collins FS, Cox NJ, et al (2009) Finding the missing heritability of complex diseases. *Nature* 461:747–753. <https://doi.org/10.1038/nature08494>
- Marques M, Laflamme L, Gervais AL, Gaudreau L (2010) Reconciling the positive and negative roles of histone H2A.Z in gene transcription. *Epigenetics* 5:267–272. <https://doi.org/10.4161/epi.5.4.11520>
- Martinez SM, Bradford BU, Soldatow VY, et al (2010) Evaluation of an in vitro toxicogenetic mouse model for hepatotoxicity. *Toxicol Appl Pharmacol* 249:208–216. <https://doi.org/10.1016/j.taap.2010.09.012>
- Marttila S, Kananen L, Häyrynen S, et al (2015) Ageing-associated changes in the human DNA methylome: genomic locations and effects on gene expression. *BMC Genomics* 16:179. <https://doi.org/10.1186/s12864-015-1381-z>
- McCarroll SA, Murphy CT, Zou S, et al (2004) Comparing genomic expression patterns across species identifies shared transcriptional profile in aging. *Nat Genet* 36:197–204. <https://doi.org/10.1038/ng1291>
- McCarthy JJ, McLeod HL, Ginsburg GS (2013) Genomic medicine: a decade of successes, challenges, and opportunities. *Sci Transl Med* 5:189sr4. <https://doi.org/10.1126/scitranslmed.3005785>
- McClay JL, Aberg KA, Clark SL, et al (2014) A methylome-wide study of aging using massively parallel sequencing of the methyl-CpG-enriched genomic fraction from blood in over 700 subjects. *Hum Mol Genet* 23:1175–1185. <https://doi.org/10.1093/hmg/ddt511>
- McClay JL, Shabalín AA, Dozmorov MG, et al (2015) High density methylation QTL analysis in human blood via next-generation sequencing of the methylated genomic DNA fraction. *Genome Biol* 16:291. <https://doi.org/10.1186/s13059-015-0842-7>
- McLachlan A, Hilmer S, Le Couteur D (2009) Variability in Response to Medicines in Older People: Phenotypic and Genotypic Factors. *Clinical Pharmacology & Therapeutics* 85:431–433. <https://doi.org/10.1038/clpt.2009.1>
- McLachlan AJ, Pont LG (2012) Drug Metabolism in Older People—A Key Consideration in Achieving Optimal Outcomes With Medicines. *J Gerontol A Biol Sci Med Sci* 67A:175–180. <https://doi.org/10.1093/gerona/qlr118>

- McLean AJ, Le Couteur DG (2004) Aging biology and geriatric clinical pharmacology. *Pharmacol Rev* 56:163–184. <https://doi.org/10.1124/pr.56.2.4>
- Meissner A, Gnirke A, Bell GW, et al (2005) Reduced representation bisulfite sequencing for comparative high-resolution DNA methylation analysis. *Nucleic Acids Res* 33:5868–5877. <https://doi.org/10.1093/nar/gki901>
- Newman M, Blyth BJ, Hussey DJ, et al (2012) Sensitive quantitative analysis of murine LINE1 DNA methylation using high resolution melt analysis. *Epigenetics* 7:92–105. <https://doi.org/10.4161/epi.7.1.18815>
- Noble D (2015) Conrad Waddington and the origin of epigenetics. *J Exp Biol* 218:816–818. <https://doi.org/10.1242/jeb.120071>
- Okino ST, Pookot D, Li L-C, et al (2006) Epigenetic inactivation of the dioxin-responsive cytochrome P4501A1 gene in human prostate cancer. *Cancer Res* 66:7420–7428. <https://doi.org/10.1158/0008-5472.CAN-06-0504>
- Ouni M, Belot MP, Castell AL, et al (2016) The P2 promoter of the IGF1 gene is a major epigenetic locus for GH responsiveness. *Pharmacogenomics J* 16:102–106. <https://doi.org/10.1038/tpj.2015.26>
- Pace L, Goudot C, Zueva E, et al (2018) The epigenetic control of stemness in CD8+ T cell fate commitment. *Science* 359:177–186. <https://doi.org/10.1126/science.aah6499>
- Pal S, Tyler JK (2016) Epigenetics and aging. *Sci Adv* 2:UNSP e1600584. <https://doi.org/10.1126/sciadv.1600584>
- Park H-J, Choi Y-J, Kim JW, et al (2015) Differences in the Epigenetic Regulation of Cytochrome P450 Genes between Human Embryonic Stem Cell-Derived Hepatocytes and Primary Hepatocytes. *PLoS ONE* 10:e0132992. <https://doi.org/10.1371/journal.pone.0132992>
- Partin AW, Van Neste L, Klein EA, et al (2014) Clinical validation of an epigenetic assay to predict negative histopathological results in repeat prostate biopsies. *J Urol* 192:1081–1087. <https://doi.org/10.1016/j.juro.2014.04.013>
- Pastor WA, Pape UJ, Huang Y, et al (2011) Genome-wide mapping of 5-hydroxymethylcytosine in embryonic stem cells. *Nature* 473:394–397. <https://doi.org/10.1038/nature10102>
- Peedicayil J (2016) Epigenetic Drugs for Multiple Sclerosis. *Curr Neuropharmacol* 14:3–9. <https://doi.org/10.2174/1570159x13666150211001600>
- Peters MJ, Joehanes R, Pilling LC, et al (2015) The transcriptional landscape of age in human peripheral blood. *Nat Commun* 6:. <https://doi.org/10.1038/ncomms9570>
- Pidsley R, Viana J, Hannon E, et al (2014) Methylomic profiling of human brain tissue supports a neurodevelopmental origin for schizophrenia. *Genome Biol* 15:483. <https://doi.org/10.1186/s13059-014-0483-2>

- Porubsky PR, Meneely KM, Scott EE (2008) Structures of Human Cytochrome P-450 2E1. *J Biol Chem* 283:33698–33707. <https://doi.org/10.1074/jbc.M805999200>
- Rajasethupathy P, Antonov I, Sheridan R, et al (2012) A role for neuronal piRNAs in the epigenetic control of memory-related synaptic plasticity. *Cell* 149:693–707. <https://doi.org/10.1016/j.cell.2012.02.057>
- Rakyan VK, Down TA, Balding DJ, Beck S (2011) Epigenome-wide association studies for common human diseases. *Nat Rev Genet* 12:529–541. <https://doi.org/10.1038/nrg3000>
- Rebeck TR, Troxel AB, Wang Y, et al (2006) Estrogen Sulfation Genes, Hormone Replacement Therapy, and Endometrial Cancer Risk. *JNCI: Journal of the National Cancer Institute* 98:1311–1320. <https://doi.org/10.1093/jnci/djj360>
- Reid GK, Besterman JM, MacLeod AR (2002) Selective inhibition of DNA methyltransferase enzymes as a novel strategy for cancer treatment. *Curr Opin Mol Ther* 4:130–137
- Reik W, Dean W, Walter J (2001) Epigenetic Reprogramming in Mammalian Development. *Science* 293:1089–1093. <https://doi.org/10.1126/science.1063443>
- Reynolds LM, Taylor JR, Ding J, et al (2014) Age-related variations in the methylome associated with gene expression in human monocytes and T cells. *Nature Communications* 5:5366. <https://doi.org/10.1038/ncomms6366>
- Riches Z, Stanley EL, Bloomer JC, Coughtrie MWH (2009) Quantitative evaluation of the expression and activity of five major sulfotransferases (SULTs) in human tissues: the SULT “pie.” *Drug Metab Dispos* 37:2255–2261. <https://doi.org/10.1124/dmd.109.028399>
- Ritchie MD (2012) The success of pharmacogenomics in moving genetic association studies from bench to bedside: study design and implementation of precision medicine in the post-GWAS era. *Hum Genet* 131:1615–1626. <https://doi.org/10.1007/s00439-012-1221-z>
- Roadmap Epigenomics Consortium, Kundaje A, Meuleman W, et al (2015) Integrative analysis of 111 reference human epigenomes. *Nature* 518:317–330. <https://doi.org/10.1038/nature14248>
- Roses AD (2000) Pharmacogenetics and the practice of medicine. *Nature* 405:857–865. <https://doi.org/10.1038/35015728>
- Routledge PA, O’Mahony MS, Woodhouse KW (2004) Adverse drug reactions in elderly patients. *Br J Clin Pharmacol* 57:121–126. <https://doi.org/10.1046/j.1365-2125.2003.01875.x>
- Royo JL, Hidalgo M, Ruiz A (2007) Pyrosequencing protocol using a universal biotinylated primer for mutation detection and SNP genotyping. *Nat Protoc* 2:1734–1739. <https://doi.org/10.1038/nprot.2007.244>
- Ruoß M, Damm G, Vosough M, et al (2019) Epigenetic Modifications of the Liver Tumor Cell Line HepG2 Increase Their Drug Metabolic Capacity. *International Journal of Molecular Sciences* 20:347. <https://doi.org/10.3390/ijms20020347>

- Russo VE, Martienssen RA, Riggs AD (1996) Epigenetic mechanisms of gene regulation. Cold Spring Harbor Laboratory Press
- Rutter M (2016) Why is the topic of the biological embedding of experiences important for translation? *Dev Psychopathol* 28:1245–1258. <https://doi.org/10.1017/S0954579416000821>
- Scarzello AJ, Jiang Q, Back T, et al (2016) LT β R signalling preferentially accelerates oncogenic AKT-initiated liver tumours. *Gut* 65:1765–1775. <https://doi.org/10.1136/gutjnl-2014-308810>
- Schaeffeler E, Hellerbrand C, Nies AT, et al (2011) DNA methylation is associated with downregulation of the organic cation transporter OCT1 (SLC22A1) in human hepatocellular carcinoma. *Genome Med* 3:82. <https://doi.org/10.1186/gm298>
- Schmidt B, Liebenberg V, Dietrich D, et al (2010) SHOX2 DNA methylation is a biomarker for the diagnosis of lung cancer based on bronchial aspirates. *BMC Cancer* 10:600. <https://doi.org/10.1186/1471-2407-10-600>
- Schmucker DL, Woodhouse KW, Wang RK, et al (1990) Effects of age and gender on in vitro properties of human liver microsomal monooxygenases. *Clin Pharmacol Ther* 48:365–374. <https://doi.org/10.1038/clpt.1990.164>
- Schroeder FA, Lewis MC, Fass DM, et al (2013) A Selective HDAC 1/2 Inhibitor Modulates Chromatin and Gene Expression in Brain and Alters Mouse Behavior in Two Mood-Related Tests. *PLOS ONE* 8:e71323. <https://doi.org/10.1371/journal.pone.0071323>
- Seripa D, Panza F, Daragjati J, et al (2015) Measuring pharmacogenetics in special groups: geriatrics. *Expert Opinion on Drug Metabolism & Toxicology* 11:1073–1088. <https://doi.org/10.1517/17425255.2015.1041919>
- Sharma S, Taliyan R (2016) Histone deacetylase inhibitors: Future therapeutics for insulin resistance and type 2 diabetes. *Pharmacol Res* 113:320–326. <https://doi.org/10.1016/j.phrs.2016.09.009>
- Singh P, Konar A, Kumar A, et al (2015) Hippocampal chromatin-modifying enzymes are pivotal for scopolamine-induced synaptic plasticity gene expression changes and memory impairment. *J Neurochem* 134:642–651. <https://doi.org/10.1111/jnc.13171>
- Slone Epidemiology Center (2006) Patterns of medication use in the United States - A report from the Slone Survey. Boston University
- Stamatoyannopoulos JA, Snyder M, Hardison R, et al (2012) An encyclopedia of mouse DNA elements (Mouse ENCODE). *Genome Biology* 13:418. <https://doi.org/10.1186/gb-2012-13-8-418>
- Steegenga WT, Boekschoten MV, Lute C, et al (2014) Genome-wide age-related changes in DNA methylation and gene expression in human PBMCs. *AGE* 36:9648. <https://doi.org/10.1007/s11357-014-9648-x>
- Stefansson OA, Esteller M (2013) Epigenetic modifications in breast cancer and their role in personalized medicine. *Am J Pathol* 183:1052–1063. <https://doi.org/10.1016/j.ajpath.2013.04.033>

- Stefansson OA, Villanueva A, Vidal A, et al (2012) BRCA1 epigenetic inactivation predicts sensitivity to platinum-based chemotherapy in breast and ovarian cancer. *Epigenetics* 7:1225–1229. <https://doi.org/10.4161/epi.22561>
- Stricker SH, Köferle A, Beck S (2017) From profiles to function in epigenomics. *Nat Rev Genet* 18:51–66. <https://doi.org/10.1038/nrg.2016.138>
- Stubbs TM, Bonder MJ, Stark A-K, et al (2017) Multi-tissue DNA methylation age predictor in mouse. *Genome Biology* 18:68. <https://doi.org/10.1186/s13059-017-1203-5>
- Sultana J, Cutroneo P, Trifirò G (2013) Clinical and economic burden of adverse drug reactions. *J Pharmacol Pharmacother* 4:S73–S77. <https://doi.org/10.4103/0976-500X.120957>
- Sun Y, Sahbaie P, Liang D, et al (2015) DNA Methylation Modulates Nociceptive Sensitization after Incision. *PLoS ONE* 10:e0142046. <https://doi.org/10.1371/journal.pone.0142046>
- Suvà ML, Riggi N, Bernstein BE (2013) Epigenetic reprogramming in cancer. *Science* 339:1567–1570. <https://doi.org/10.1126/science.1230184>
- Sykiotis GP, Kalliolias GD, Papavassiliou AG (2005) Pharmacogenetic principles in the Hippocratic writings. *J Clin Pharmacol* 45:1218–1220. <https://doi.org/10.1177/0091270005281091>
- Szyf M (2009) Epigenetics, DNA methylation, and chromatin modifying drugs. *Annu Rev Pharmacol Toxicol* 49:243–263. <https://doi.org/10.1146/annurev-pharmtox-061008-103102>
- Tammen SA, Dolnikowski GG, Ausman LM, et al (2014) Aging and alcohol interact to alter hepatic DNA hydroxymethylation. *Alcohol Clin Exp Res* 38:2178–2185. <https://doi.org/10.1111/acer.12477>
- Tan JL, Eastment JG, Poudel A, Hubbard RE (2015) Age-Related Changes in Hepatic Function: An Update on Implications for Drug Therapy. *Drugs Aging* 32:999–1008. <https://doi.org/10.1007/s40266-015-0318-1>
- Teschendorff AE, Menon U, Gentry-Maharaj A, et al (2010) Age-dependent DNA methylation of genes that are suppressed in stem cells is a hallmark of cancer. *Genome Res* 20:440–446. <https://doi.org/10.1101/gr.103606.109>
- Thakore PI, Black JB, Hilton IB, Gersbach CA (2016) Editing the epigenome: technologies for programmable transcription and epigenetic modulation. *Nat Methods* 13:127–137. <https://doi.org/10.1038/nmeth.3733>
- Tokizane T, Shiina H, Igawa M, et al (2005) Cytochrome P450 1B1 is overexpressed and regulated by hypomethylation in prostate cancer. *Clin Cancer Res* 11:5793–5801. <https://doi.org/10.1158/1078-0432.CCR-04-2545>
- Tost J, Dunker J, Gut IG (2003) Analysis and quantification of multiple methylation variable positions in CpG islands by Pyrosequencing. *BioTechniques* 35:152–156. <https://doi.org/10.2144/03351md02>

- Tracy TS, Chaudhry AS, Prasad B, et al (2016) Interindividual Variability in Cytochrome P450-Mediated Drug Metabolism. *Drug Metab Dispos* 44:343–351. <https://doi.org/10.1124/dmd.115.067900>
- Unnikrishnan A, Freeman WM, Jackson J, et al (2018) The role of DNA methylation in epigenetics of aging. *Pharmacology & Therapeutics*. <https://doi.org/10.1016/j.pharmthera.2018.11.001>
- Unnikrishnan A, Hadad N, Masser DR, et al Revisiting the genomic hypomethylation hypothesis of aging. *Annals of the New York Academy of Sciences* 1418:69–79. <https://doi.org/10.1111/nyas.13533>
- van Kessel KEM, Van Neste L, Lurkin I, et al (2016) Evaluation of an Epigenetic Profile for the Detection of Bladder Cancer in Patients with Hematuria. *J Urol* 195:601–607. <https://doi.org/10.1016/j.juro.2015.08.085>
- Wang Y, Krishnan HR, Ghezzi A, et al (2007) Drug-induced epigenetic changes produce drug tolerance. *PLoS Biol* 5:e265. <https://doi.org/10.1371/journal.pbio.0050265>
- Weber CM, Henikoff S (2014) Histone variants: dynamic punctuation in transcription. *Genes Dev* 28:672–682. <https://doi.org/10.1101/gad.238873.114>
- White RR, Milholland B, MacRae SL, et al (2015) Comprehensive transcriptional landscape of aging mouse liver. *BMC Genomics* 16:899. <https://doi.org/10.1186/s12864-015-2061-8>
- Wilhelm A, Aldridge V, Haldar D, et al (2016) CD248/endothelial cell critically regulates hepatic stellate cell proliferation during chronic liver injury via a PDGF-regulated mechanism. *Gut* 65:1175–1185. <https://doi.org/10.1136/gutjnl-2014-308325>
- Wilson VL, Smith RA, Ma S, Cutler RG (1987) Genomic 5-methyldeoxycytidine decreases with age. *J Biol Chem* 262:9948–9951
- Zanger UM, Schwab M (2013) Cytochrome P450 enzymes in drug metabolism: Regulation of gene expression, enzyme activities, and impact of genetic variation. *Pharmacology & Therapeutics* 138:103–141. <https://doi.org/10.1016/j.pharmthera.2012.12.007>
- Zhang B, Zhou Y, Lin N, et al (2013) Functional DNA methylation differences between tissues, cell types, and across individuals discovered using the M&M algorithm. *Genome Research* 23:1522–1540. <https://doi.org/10.1101/gr.156539.113>
- Zhi D, Aslibekyan S, Irvin MR, et al (2013) SNPs located at CpG sites modulate genome-epigenome interaction. *Epigenetics* 8:802–806. <https://doi.org/10.4161/epi.25501>
- Zhou D, Li Z, Yu D, et al (2015) Polymorphisms involving gain or loss of CpG sites are significantly enriched in trait-associated SNPs. *Oncotarget* 6:39995–40004. <https://doi.org/10.18632/oncotarget.5650>
- Zhou L, Ng HK, Drautz-Moses DI, et al (2019) Systematic evaluation of library preparation methods and sequencing platforms for high-throughput whole genome bisulfite sequencing. *Sci Rep* 9:10383. <https://doi.org/10.1038/s41598-019-46875-5>

Zhu T, Zheng SC, Paul DS, et al (2018) Cell and tissue type independent age-associated DNA methylation changes are not rare but common. *Aging (Albany NY)* 10:3541–3557.
<https://doi.org/10.18632/aging.101666>

VITA

Mohamad Maher Kronfol was born on November 20, 1990, in Beirut, Lebanon. He received his bachelor's degree in Pharmacy with honors from Beirut Arab University in 2013. He practiced as a clinical pharmacist in his native Beirut and decided to pursue his interest in pharmacogenetics by studying for a Ph.D. at the Department of Pharmacotherapy and Outcomes Science at Virginia Commonwealth University School of Pharmacy. He joined Dr. Joseph McClay's lab in Fall 2016.